COMPUTER MODELING AND EXPERIMENTAL VALIDATION
OF LOSSES IN A STRIP GEOMETRY EXPLOSIVE
MAGNETIC FLUX COMPRESSION GENERATOR

THESIS

Mary P. Jeffrey   James L. Hebert
First Lieutenant, USAF   Second Lieutenant, USAF

AFIT/GE/EE/83D-28

DTIC
ELECTE
FEB 2 2 1984

B

DEPARTMENT OF THE AIR FORCE
AIR UNIVERSITY

AIR FORCE INSTITUTE OF TECHNOLOGY

Wright-Patterson Air Force Base, Ohio

84 02 21 191

COMPUTER MODELING AND EXPERIMENTAL VALIDATION
OF LOSSES IN A STRIP GEOMETRY EXPLOSIVE
MAGNETIC FLUX COMPRESSION GENERATOR

THESIS

Mary P. Jeffrey   James L. Hebert
First Lieutenant, USAF Second Lieutenant, USAF

AFIT/GE/EE/83D-28

DTIC
ELECTE
S FEB 2 2 1984 D
B

COMPUTER MODELING AND EXPERIMENTAL VALIDATION

OF LOSSES IN A STRIP GEOMETRY EXPLOSIVE

MAGNETIC FLUX COMPRESSION GENERATOR

THESIS

Presented to the Faculty of the School of Engineering

of the Air Force Institute of Technology

Air University

In Partial Fulfillment of the

Requirements for the Degree of

Master of Science in Electrical Engineering

Mary P. Jeffrey, B.S.   James L. Hebert, B.S.

First Lieutenant, USAF   Second Lieutenant, USAF

December 1983

Preface

The purpose of this thesis was to develop and validate a computer model of strip geometry explosive flux compression generator. The Air Force Weapons Laboratory had designed a strip generator and conducted preliminary familiarization experiments with it. A computer program to predict generator output was developed. This computer model was then validated using the AFWL strip generator.

Accession For

NTIS GRA&I
DTIC TAB
Unannounced
Justification

By
Distribution/
Availability Codes
Dist | Avail and/or Special
A-1

DTIC
COPY
INSPECTED

Table of Contents

List of Figures

Figure		Page

List of Tables

Abstract

A computer program to predict the performance of a strip geometry explosive magnetic flux compression generator (MCG) was developed and validated.

The program contains five separate models of the MCG, two theoretical and three empirically based. The first model is a theoretical lossless flux conserved model. The second model accounts for resistive losses due to plate resistance and a flux diffusion equivalent resistance. The first empirical model models the remaining losses as a slipping loss. The second empirical model adjusts the flux conserved model with an additional time varying inductance. The final empirical model is a simple flux trapping efficiency model.

Actual MCG experiments were conducted using the Air Force Weapons Laboratory's strip MCG. The data from these experiments was used to validate the computer program. Input currents varied from 294.0 KA to 1100.0 KA with resulting output currents of 2210.0 KA to 10261.0 KA and current amplification factors between 6.29 and 15.75.

COMPUTER MODELING AND EXPERIMENTAL VALIDATION OF LOSSES IN A STRIP GEOMETRY EXPLOSIVE MAGNETIC FLUX COMPRESSION GENERATOR

I. Introduction

Magnetic flux compression generators (MCGs) are devices which create ultrahigh magnetic fields by compressing magnetic fields between two metal surfaces to achieve field multiplication. This field multiplication is achieved by converting chemical energy into electrical energy.

Background

MCGs have been under investigation since the early 1950s (1:10). Initial experiments were done in strip geometries, explosively driving two plates together. Because experiments in coaxial geometry proved more efficient, attention soon focused on coaxial geometry (2:5191). For many years, the focus remained on the coaxial flux compression generators.

Recently, attention has returned to the strip geometry MCG. Because of their higher current densities and relatively simple construction, the military is now considering strip geometry MCGs as a possible power supply for some of its advanced weapons and experiments (3).

By their nature, explosive MCGs are one shot devices. For this reason, computer models predicting the MCG's output characteristics are beneficial in terms of cost and time of development.

Problem

The purpose of this thesis was to develop and validate a simple computer model of a strip geometry MCG's operation. The computer model accounts for the major physical processes involved in the MCG's operation. Model validation was done using the Air Force Weapons Laboratory's (AFWL) MCG shown in Figure 1-1.

Trough

Top Plate

Cutting Wedge

Bottom Plate

Jet Catcher

Jet Wedge

Load
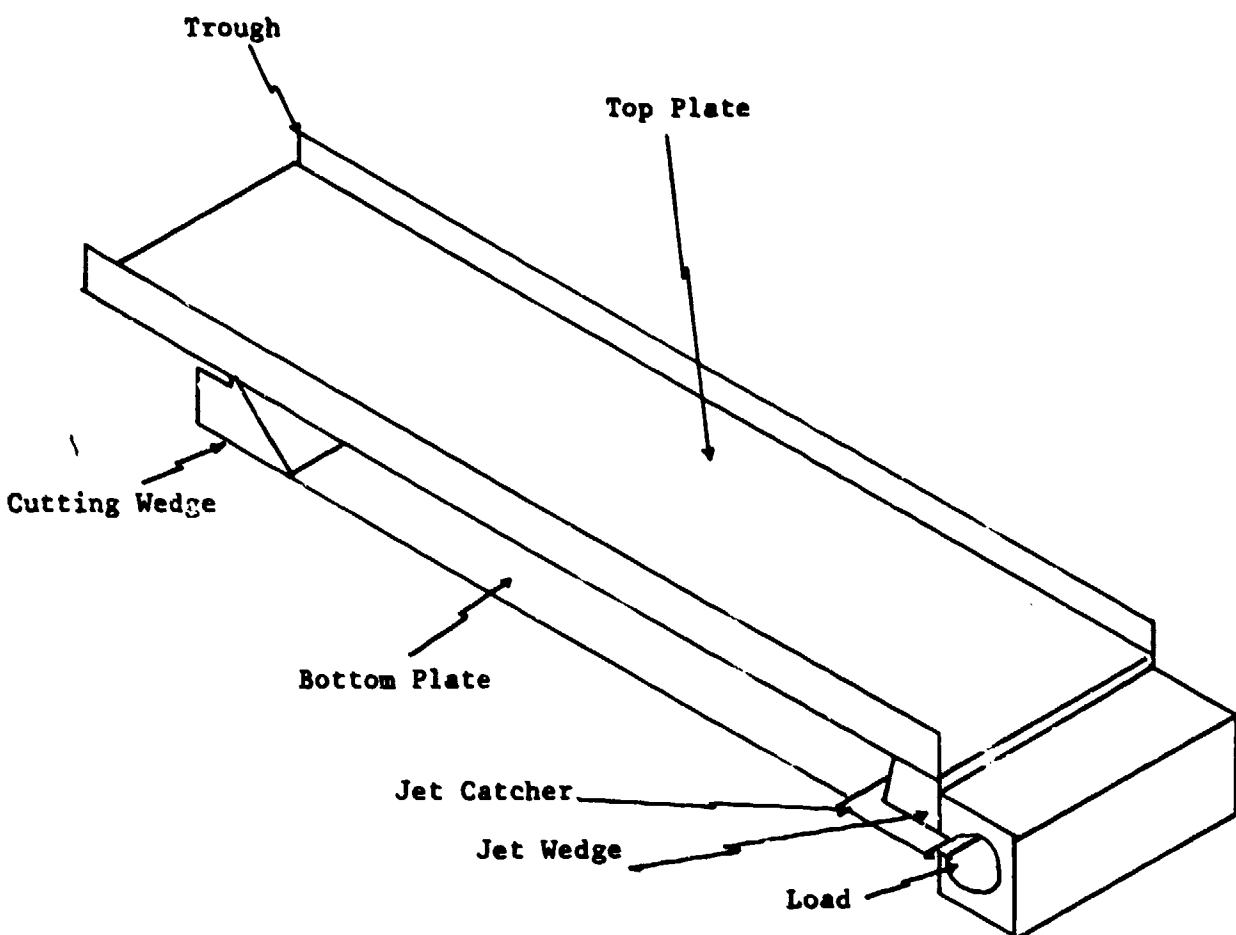
Figure 1-1. Air Force Weapons Laboratory's MCG

Scope

The study done for this thesis was limited to the design and validation of a computer model of a strip geometry MCG. The loss mechanisms considered were flux diffusion, plate resistance, sliding contact, and incomplete compression.

The criteria used to evaluate the model were the ability to predict the output current as a function of time and the time to peak current amplification.

Assumptions

In order to model the MCG's operation several basic assumptions were made. These assumptions include:

1) The electrical circuit used in the experiments can be modeled by the lumped parameter elements of inductance, capacitance, and resistance (4:327); (This allows the MCG's operation to be described by RLC circuit analysis.);

2) The magnetic fields are spatially uniform within the MCG;

3) The load and throat inductance of the MCG are constant with time;

4) The metal plates are incompressible (5:364);

5) The explosive process brings the two plates together in a uniform motion so that the compression can be considered linear (6:7);

6) During the compression process, the metal plates offer no resistance to plate motion (6:3); and

7) Specific heat remains constant (5:362).

3

General Approach

Computer Model. In order to model the generator's operation with an equivalent electrical circuit, basic relationships which describe the physical processes involved had to be developed. The first problem was to determine how the explosive energy was transferred to the metal plates. The detonation of the explosive accelerated the metal plate converting the chemical energy of the explosive to kinetic energy or changing velocity. Although complex computer codes exist to describe this energy conversion, the Gurney method provides a quick, simple approximation for the changing metal velocity (6:3).

The second physical process to be accounted for was the time varying inductance. The changing metal velocity predicts the motion of the metal plates which, in turn, is used to calculate the changing area enclosed by the MCG. From this changing area, a time varying inductance was calculated. Combined with the lumped element parameters determined from the experimental circuit, a totally flux conserved (lossless) model was developed. As the plates are driven together, the inductance decreases, converting kinetic energy to electric energy.

Using this flux conserved model, the flux diffusion losses were calculated. These losses were modeled by a time varying effective resistance. Losses due to the copper's resistance were also computed. This resistance, combined with the effective resistance which accounts for flux diffusion losses, was used to produce a total resistance model of the MCG.

During experimental validation, it was discovered that other physical loss mechanisms were present. These losses had to be

4

accounted for in order to completely describe the MCG's operation. Three empirical models were developed. The first model which accounts for slipping losses was developed in a manner similar to that of Knoepfel (1:189-191). A second model which allows for compression at rates faster or slower than predicted by the Gurney velocity was also developed. A final model which is based totally on empirical measurements accounts for a flux compression efficiency.

A detailed description of the computer models can be found in Chapter III.

Experimental Validation. Validation of the computer program consisted of performing actual strip MCG experiments. The experimental circuit was set up as shown in Figure 1-2. Constant ircuit parameters such as line inductance and resistance were determined by discharging the capacitor bank through a shorted line as well as through the AFWL MCG. Current measurements were used to determine these values.

Several parameters were varied to check the validity of the computer model. These included changing the load impedance, the tamping, the amount of explosive, a..d the input voltage to the capacitor bank.

Five MCG experiments were successfully performed. Test measurements included voltages across the switch and load, and current derivatives through the switch, line, and load. Currents were obtained by actively integrating the current derivatives. Data was displayed on oscilloscopes photographed with polaroid cameras.
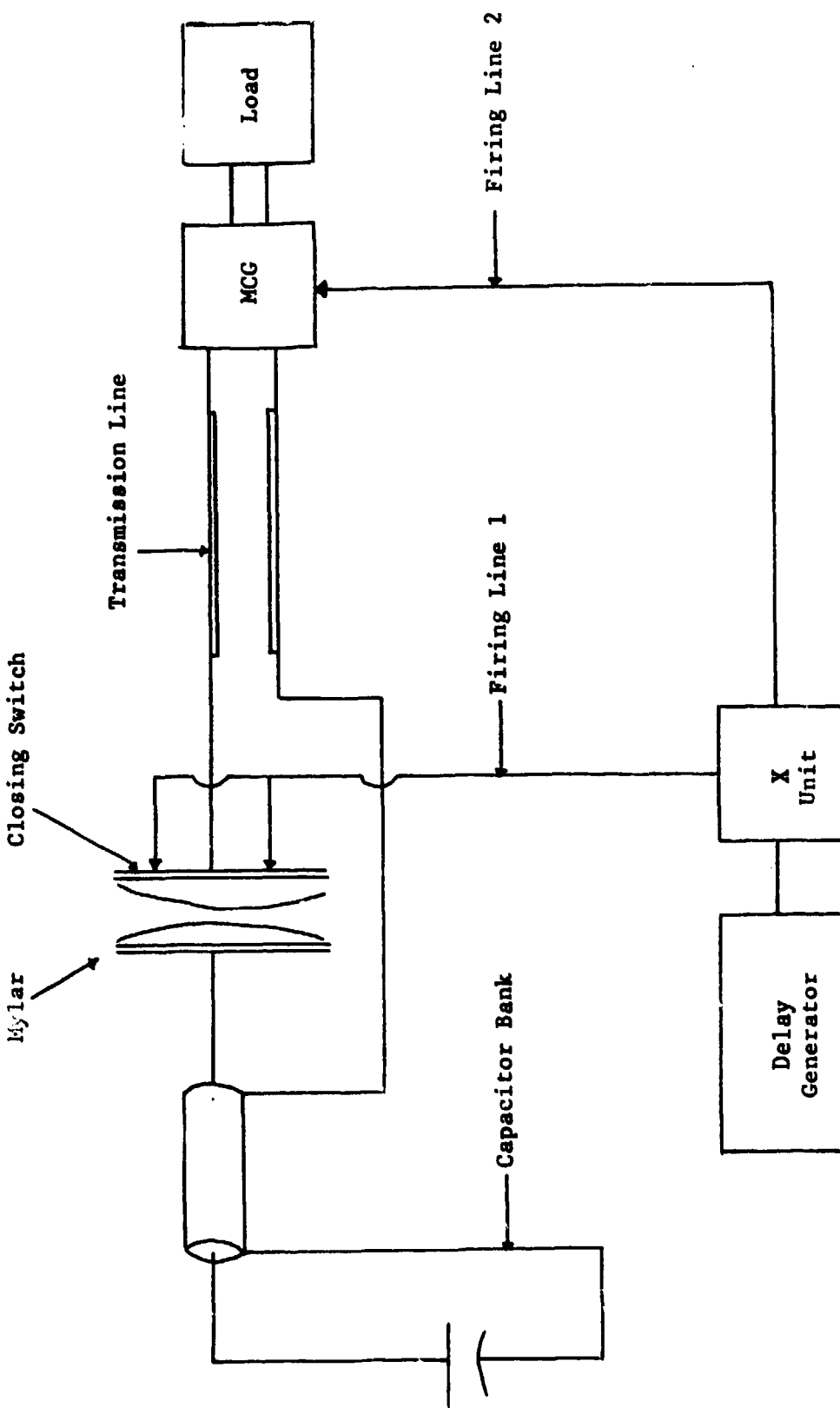
Figure 1-2. Experimental Set Up

6

A detailed description of the experimental apparatus can be found in Chapter IV. Chapter V describes the experimental procedures used. Finally, the results comparing the experimental data with the computer models, conclusions, and recommendations can be found in Chapter VI.

II. Basic Theory

Numerous models have been developed to describe MCG operation. The models can be broken down into two major categories, equivalent electrical circuit modeling and empirical modeling.

Equivalent Circuit Modeling

Many models used to describe MCG operation use an equivalent electrical circuit approach. Each of these models describe MCG operation as having four major components: an input power supply, an inductance, a resistance, and a load inductance. The equivalent circuit is shown below.
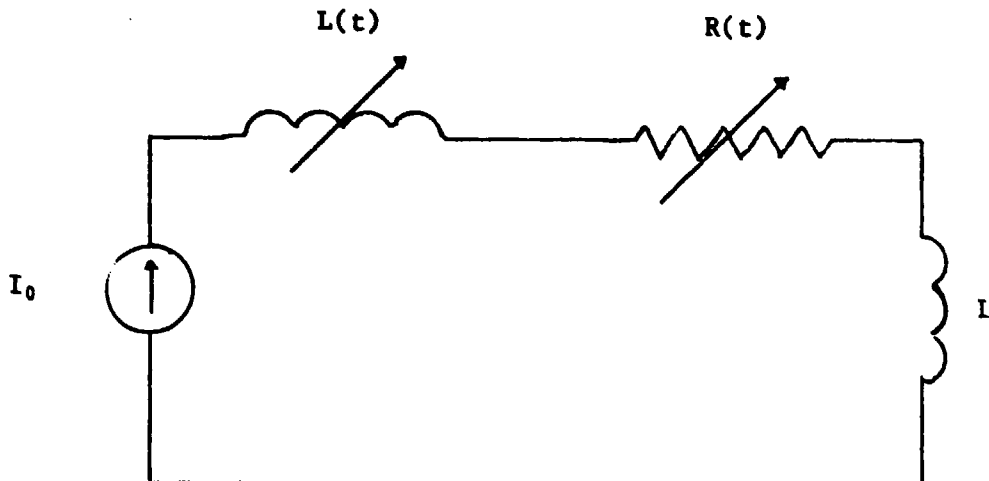
Figure 2-1. Equivalent Electrical Circuit

The input power is generally described as an input current whose value is determined by the input circuitry. The load inductance is

determined by the particular use of the generator. The models all describe the generator inductance as a time varying inductance. They differ in their description of the resistance; some describe it as a time varying resistance while others describe it as a constant.

Time Varying Inductance. Inductance varies as a function of the dimensions of the system. During the compression process, the metal plates are explosively driven together. This drastically alters the dimensions of the system and hence the system inductance. Through a change of variables, this dimensionally changing inductance can be modeled as a time varying inductance (7:147;8:334).

Time Varying Resistance. Experts generally agree that, as a minimum, resistance is a function of resistivity, temperature, and path length (8:334;9:554). Resistivity and temperature are interrelated. As long as the metal plates do not liquify, resistivity can be described as a linear function of temperature (10:393).

$$\rho = \rho_0(1 + k\theta) \qquad (2\text{-}1)$$

where

ρ_0 is the resistivity of the plate at room temperature

k is a constant equal to $10^{-3}/{}^0C$

θ is the temperature in ${}^0C$

A method must then be determined to describe how temperature changes with a known variable. Because the thermal diffusion process is much slower than the magnetic diffusion process, temperature can be described strictly as a function of the magnetic flux density (1:74).

$$\theta = \chi B^2 \qquad (2\text{-}2)$$

where

χ is a constant equal to $1170^\circ C/(MG)^2$

B is the magnetic flux density in megagauss (10:392)

As MCG operation progresses, the magnetic flux is compressed. (A detailed discussion of how the magnetic flux is compressed is contained in Chapter III.) This means that the magnetic flux density and hence the resistivity can be made a function of time through a change of variables. Additionally, the path through which the current flows changes during MCG operation. By using the familiar expression

$$R = \frac{\rho \, \ell}{A} \qquad (2\text{-}3)$$

where

ρ is resistivity

ℓ is path length

A is cross sectional area

The resistance of the plates, R_p, can be defined as a function of time.

The process of magnetic flux diffusion is modeled in the equivalent electrical circuit approach as a time varying resistance (1:185). By using a skin layer method, a time varying resistance modeling flux diffusion is defined as

$$R = \frac{1}{\sigma_0 \sqrt{\dfrac{\tau}{\sigma_0 \mu}}} \qquad (2\text{-}4)$$

10

where

σ_0 is conductivity

μ_0 is magnetic permeability

τ is a characteristic time defined by

$$\tau = \frac{H}{\frac{dH}{dt}}$$
(2-5)

Because τ is a function of time, magnetic flux diffusion can be modeled as a time varying resistance.

Constant Resistance Model. Experts who model the resistance as a constant during MCG operation realize that resistance does in fact change with time. These changes are small and linear. Thus, they can be modeled as an average resistance (1:83);11:DI-8-3). In this manner, resistance can be modeled as a constant.

Empirical Modeling

Empirical models are based on experimental data. Knoepfel suggests that a loss mechanism not modeled by previous methods is a slipping contact loss. Slipping losses occur when plate compression is incomplete and flux is trapped between the plates. For the AFWL generator, this slipping loss occurs on the surfaces shown as a dark line in Figure 2-2.
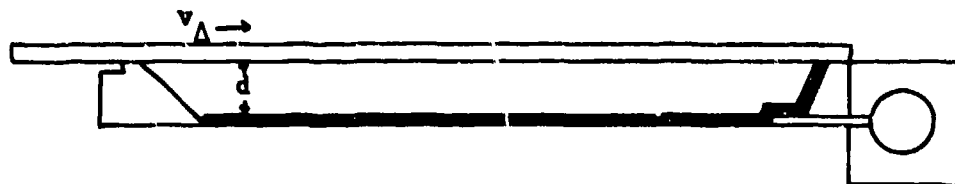
Figure 2-2. Slipping Loss Surfaces

11

Along these surfaces, the empirical model claims flux is lost at a rate of

$$\frac{d\phi}{dt} = -2sv_{\Delta}\mu_0 H \tag{2-6}$$

where

    s   is a mean depth of ripples in the slipping surfaces

    v_{Δ} is the detonation velocity shown in Figure 2-2

    μ_0 is the magnetic permeability

    H   is the magnetic field

In a manner similar to that of Knoepfel, it has been determined that

$$\frac{I}{I_0} = (C(t))^{1 - \frac{2s}{d}} \tag{2-7}$$

where

    I_0 is the initial current in the generator

    $C(t)$ is the flux compression factor determined in Chapter III

    s   is the mean depth of the ripples

    d   is the initial plate separation

In this manner, an output current can be determined.

A second empirical method to account for additional losses adjusts the time varying inductance of the generator predicted by the resistance model. This additional inductance L_{ex} is added to the total time varying generator inductance.

$$L_{Gen}(t) = L_G(t) + L_{ex}(t) \tag{2-8}$$

where $L_G(t)$ is the time varying inductance predicted by the Gurney method. $L_{ex}(t)$ can be either negative or positive in value. A

12

negative value indicates a faster flux compression and smaller time varying inductance. A positive value indicates a slower flux compression and larger time varying inductance.

Finally, the generator's performance can be empirically modeled by calculating a flux trapping efficiency.

$$E_{ff} = \frac{\text{Ideal Flux Present} - \text{Flux Lost}}{\text{Ideal Flux Present}} \times 100\% \qquad (2-9)$$

The ideal flux present is the initial flux present when generator operation begins. The flux lost is all flux lost regardless of the loss mechanism.

III. Computer Model

Five basic models were developed to described MCG operation. Two of these models, the flux conserved model and the time varying resistance model are theoretical equivalent circuit models. The remaining models, the sliding contact loss model, the changing area loss model, and the efficienc model are empirical models.

All models are derived from the flux conserved model. The models are capable of describing operation for both rectangular and trapezoidal geometry strip generators. A detailed description of the program inputs, outputs, and the program itself can be found in Appendix A.

Theoretical Models

Flux Conserved Model. The flux conserved model uses an equivalent electrical circuit approach to model the MCG's operation. This model assumes that there are no flux diffusion losses and that the metal plates are perfectly conducting so that the circuit has essentially no resistance. The circuit relationship is then

$$\frac{d}{dt}(LI) = 0 \qquad (3-1)$$

The current solution at any time, t, is then given by

$$I(t) = I_0 \frac{L(0)}{L(t)} \qquad (3-2)$$

14

where

L(0) and I_0 are initial conditions at t=0

L(t) is a time varying system inductance

With no losses, the MCG operation may be modeled completely by a time varying inductance. For this particular circuit, there are three inductances, the generator inductance, L_G, the load inductance, L_L, and the throat inductance, ℓ_0. The throat inductance is the inductance of the small transmission line connecting the generator to the load. Both L_L and ℓ_0 are assumed to be constant.

The generator inductance varies with time. The change in inductance results from the conversion and partial transfer of chemical energy of the explosive to the kinetic energy of the top metal plate. Rather than using a complex computer code to derive this energy transfer, this computer model uses the Gurney method which provides a quick, accurate approximation of the energy transfer.

The Gurney method is based on energy and momentum balances and can be used to describe a large variety of gemoetries. For the strip generators, the top plate, explosive, and tamper can be modeled as an asymmetric sandwich as shown in Figure 3-1.

| Tamper |
| Explosive |
| Top Plate |
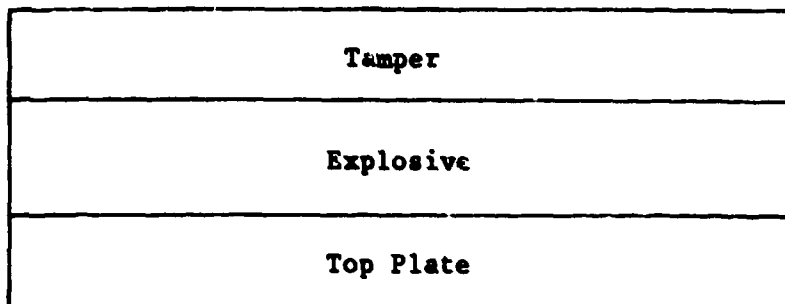
Figure 3-1. Asymmetric Sandwich

15

In this particular configuration, the velocity imparted to the metal is described as

$$v_m = \sqrt{2E} \left[\frac{1 + A^2}{3(1 + A)} + \frac{N}{C} A^2 + \frac{M}{C} \right]^{-1/2} \qquad (3\text{-}3)$$

where

$\sqrt{2E}$ is the Gurney energy for the particular explosive

$\frac{N}{C}$ is the tamper mass to explosive mass ratio

$\frac{M}{C}$ is the metal mass to explosive mass ratio

A is a constant defined by $\dfrac{1 + \frac{M}{C}}{1 + \frac{N}{C}}$ (6:8)

As the explosive burns, the top plate is driven to the bottom plate as shown in Figure 3-2.
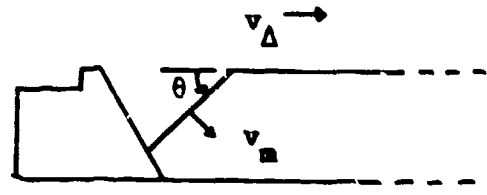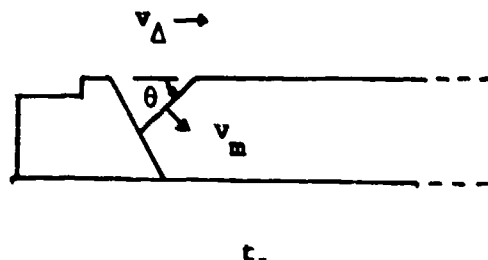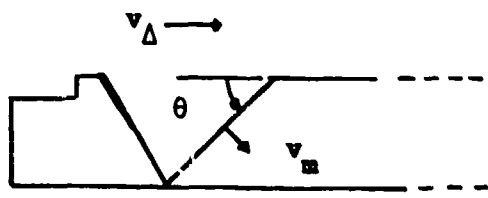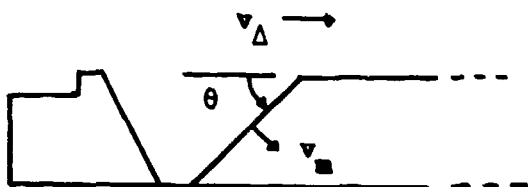
Figure 3-2. Compression of Generator

16

The angle, Δ, shown in Figure 3-2 is known as the Gurney angle. The Gurney angle is defined by the following equation

$$\theta = \sin^{-1}\left(\frac{v_m}{2v_\Delta}\right) \qquad (3-4)$$

where

v_m is the metal velocity from Eq (3-3)

v_Δ is the detonation velocity of the explosive (6:27)

Using the detonation velocity, the Gurney angle, and simple geometry, a time varying area can easily be calculated. Generation operation ceases when the top plate of the generator touches the jet catcher as shown in Figure 3-3.
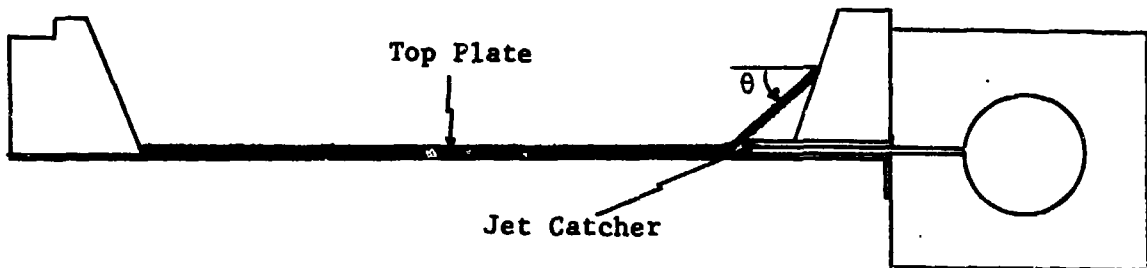
Figure 3-3. Generator Ceasation

Using this time varying area, the time varying inductance is easily calculated using

$$L(t) = \frac{1.2566371 \; A(t)}{W} \; \mu H \qquad (3\text{-}5)$$

where

$A(t)$ is the time varying area in m^2

W is the plate width in m

Because the program allows for the width of the plate to vary, $L(t)$ is calculated incrementally.

Once the time varying generator inductance is calculated, the system inductance can be defined as

$$L(t) = L_G(t) + \ell_0 + L_L \qquad (3\text{-}6)$$

The flux conserved solution to Eq (3-2) is then

$$I_{Ideal}(t) = I_0 \; \frac{L_G(0) + \ell_0 + L_L}{L_G(t) + \ell_0 + L_L} \qquad (3\text{-}7)$$

From this ideal current the magnetic field and magnetic flux density are easily found using

$$H(t) = \frac{I_{Ideal}(t)}{W} \qquad (3\text{-}8)$$

and

$$B(t) = \mu_0 H(t) \qquad (3\text{-}9)$$

Time Varying Resistance Model. The time varying resistance model also uses an equivalent electrical circuit approach. It assumes the

18

only resistive mechanisms are flux diffusion and plate resistivity. The circuit relationship is then

$$\frac{d}{dt}(LI) + IR = 0 \qquad (3-10)$$

The current solution at any time is then

$$I(t) = I_0 \frac{L(0)}{L(t)} e^{-\int_0^t \frac{R(t)}{L(t)} dt} \qquad (3-11)$$

where

L(0) and I_0 are initial conditions at t=0

L(t) is the time varying system inductance

R(t) is the time varying system resistance

L(t) has been described in the flux conserved model and the mechanism for its generation is identical in the time varying resistance model. In this particular model, it is assumed that all resistive mechanisms are described by the resistivity of the copper plates or as an equivalent resistance due to flux diffusion.

Plate resistance is described by the well-known relationship

$$R_p = \frac{\rho \ell}{A} \qquad (3-12)$$

where

ρ is resistivity

ℓ is path length

A is cross sectional area in which the current flows

As metal heats, its resistivity changes. As long as the plates remain solid, this change can be approximated by the linear function

$$\rho = \rho_0(1 + k\theta) \qquad (3-13)$$

19

where

ρ_0 is resistivity at room temperature

k   is a proportionality constant ($\sim 10^{-3}/^{0}$C)

θ is the temperature in ^{0}C (10:393)

A method must then be used for describing how the temperature changes with time. A reasonable approximation for temperature below melting point is

$$\theta = \chi B^2 \qquad (3-14)$$

where

$\chi = 1170^{0}$C/(MG)^2

B   is the magnetic flux density in megagauss (10:392)

χ is a function of the specific heat, C_p, and the magnetic permeability, μ_0. Resistivity can then be described as

$$\rho(t) = \rho_0(1 + k\chi B^2) \qquad (3-15)$$

The path length also varies with time. As the generator is compressed, the path length decreases. By using simple geometry and the Gurney angle, a time varying path length is calculated. The cross sectional area of the plate is defined as

$$A = Wd \qquad (3-16)$$

where

W   is the width of the generator

d   is the depth of penetration of the magnetic field

20

d is defined as

$$d = 2\sqrt{\kappa_0 t} \qquad (3-17)$$

where

$\kappa_0 = \dfrac{\rho}{\mu}$ and ρ is defined in Eq (3-13)

t is time

Coupling all these time varying functions together resu__s in a piece wise continuous time varying $R_p(t)$.

During generator operation, a portion of the flux diffuses into the conductor. By using the skin layer method described in Knoepfel (1:184-186), the flux resistance could be modeled as a time varying resistance by

$$R_d = \frac{\rho}{s_\psi} \qquad (3-18)$$

where

ρ is the resistivity described by Eq (3-13)

s_ψ is a magnetic skin depth

s_ψ is defined as

$$s_\psi = \sqrt{\kappa_0 \tau} \qquad (3-19)$$

where

$\kappa_0 = \dfrac{\rho}{\mu}$

$\tau = \dfrac{H}{\dfrac{dH}{dt}}$ based on the ideal magnetic fields

21

Coupling these time varying functions together results in a time varying $R_d(t)$. The total system time varying resistance is then described by

$$R(t) = R_p(t) + R_d(t) \qquad (3\text{-}20)$$

The resistance model solution to Eq (3-10) is then

$$I_{Res}(t) = \left\{ \frac{L_G(0) + \ell_0 + L_L}{L_G(t) + \ell_0 + L_L} \right\} I_0 \exp\left[-\int_0^t \frac{R_p(t) + R_d(t)}{L_G(t) + \ell_0 + L_L} \, dt \right] \qquad (3\text{-}21)$$

Integration is done using the trapezoidal approximation. The magnetic fields are found in a manner identical to that of the ideal case substituting I_{Res} for I_{Ideal}.

Empirical Models

Empirical models were developed when it was discovered that the resistive loss mechanisms were not the primary loss mechanism. Each of the following models uses a different approach to attempt to model the additional loss mechanisms occurring in the generator.

Sliding Contact Model. In a manner similar to that of Knoepfel (1:189-191), an empirical model for slipping contact losses was developed. Knoepfel accounts for all losses with his sliding contact loss. The sliding contact model developed herein assumes the loss mechanisms are resistive losses and sliding contact losses. The sliding contact loss mechanism is due to flux trapping when two plates are driven together and the plate surfaces do not come together smoothly.

22

It was assumed that the sliding contact current could be described by

$$I_{Slip}(t) = I_0 \left[\frac{I_{Res}(t)}{I_0}\right]^{1 - \frac{2s}{d}} \tag{3-22}$$

where

I_0 is the initial current

$I_{Res}(t)$ is the time varying current using the resistive model

s   is a mean ripple depth

d   is the initial plate separation

Solving Eq (3-21) for s yields

$$s = \frac{d}{2}\left(\log \frac{I_{Res}(t)}{I_0} - \log \frac{I_{Slip}(t)}{I_0} + 1\right) \tag{3-23}$$

Using experimental data, s(t) was calculated for each test using the actual current in place of $I_{Slip}(t)$. These curves were linearized using three times during generator operation. These times are shown in Figure 3-4. The first match point corresponds to when the top plate has completed its run down the cutting wedge and begins to compress against the bottom plate. The second match point corresponds to when the top plate of the generator is about to begin its run down the end wedge. The final match point occurs when the maximum experimental output current is reached.

The ripple depth at each match point is calculated from Eq (3-23), and the ripple depth at any point between the match points is found through linear interpolation. From the sets of data, best and worst case slipping losses were modeled. $I_{Slip}(t)$ is then calculated using Eq (3-21) and the experimentally derived, computer linearized ripple

23

depth, s(t). The magnetic fields are again found in a manner identical to that of the ideal case substituting I_{Ideal} with I_{Slip}.
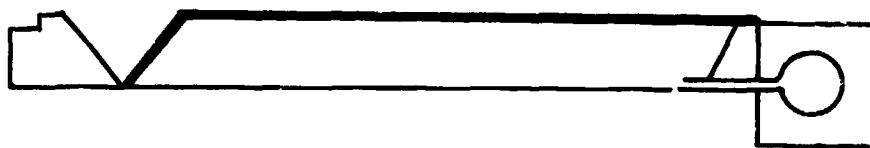
Point 1

Point 2

Point 3

Figure 3-4. Slipping Model Match Points

Changing Area Loss Model. Since the ripple depth, s, could not be tied to any known parameter, a changing area loss model was developed. This model assumes that the changing inductance derived from the

Gurney approximations may be incorrect. It assumes that the generator inductance can be defined as

$$L_{Gen}(t) = L_G(t) + L_{ex}(t) \tag{3-24}$$

where

$L_G(t)$ is the generator inductance calculated from the Gurney approximations

$L_{ex}(t)$ is an additional inductance caused by incomplete Gurney compression

If we replace $L_G(t)$ in Eq (3-21) with $L_{Gen}(t)$, the principal effect is to decrease the flux compression factor, $\gamma(t)$.

$$\gamma(t) = \frac{L_G(0) + \ell_0 + L_L}{L_{Gen}(t) + \ell_0 + L_L} \tag{3-25}$$

Because $L_G(t)$ is determined by a changing area, so too is $L_{Gen}(t)$. This model assumes that the changing area current can be described by

$$I_{Carea}(t) = I_0 \frac{L_G(0) + \ell_0 + L_L}{L_G(t) + L_{ex}(t) + \ell_0 + L_L}$$

$$\exp\left[-\int_0^t \frac{R_d(t) + R_p(t)}{L_{Gen} + \ell_0 + L_L} dt\right] \tag{3-26}$$

Solving Eq (3-26) for $L_{ex}(t)$ yields

$$L_{ex}(t) = I_0 \frac{L_G(0) + \ell_0 + L_L}{I_{Carea}(t)}$$

$$\exp\left[-\int_0^t \frac{R}{L} dt - (L_G(t) + \ell_0 + L_L)\right] \tag{3-27}$$

Using experimental data, $L_{ex}(t)$ was calculated for each test using the actual current in place of $I_{Carea}(t)$. Once calculated, a changing area was calculated using Eq (3-5).

$$A_{ex}(t) = \frac{L_{ex}(t)W}{\mu_0} \qquad (3\text{-}28)$$

This changing area was then graphed for analysis.

Efficiency Model. In a manner similar to that of Fowler, a flux trapping efficiency model was developed (12:26). Using the well-known relationship for flux of

$$\phi = LI \qquad (3\text{-}29)$$

a time varying ϕ was developed. In this model, it is assumed that $L_G(t)$ from the Gurney calculations is a valid representation of the time varying inductance. This model makes no attempt to physically explain where or why the flux loss occurs. It models all losses, whether due to slipping or due to inaccuracies in the Gurney derived inductance as a time varying flux trapping efficiency. This flux trapping efficiency is defined by

$$\epsilon = \frac{\phi_0 - \phi(t)}{\phi_0} \qquad (3\text{-}30)$$

where

ϕ_0 is the initial flux in the system

$\phi(t)$ is calculated from test data

This efficiency is smoothed out and linearized and a best and worst case efficiencies are determined. An efficiency current is then determined using

$$I_{Eff}(t) = cI_{Res}(t) \qquad (3-31)$$

The magnetic fields are found in a manner identical to that of the ideal case substituting I_{Ideal} with I_{Eff}.

IV. Experimental Apparatus

Experiments to validate the computer model were conducted at the Air Force Weapons Laboratory explosive test facility located on the McCormick Range at Kirtland AFB, New Mexico. The major components and diagnostic equipment used in the magnetocumulative generator tests are described in detail in this chapter. The major components consist of the capacitor bank, the solid dielectric explosive closing switch, the fire control system, the transmission line, and the MCG and load coil (See Figure 4-1). The primary diagnostic devices used in the experiments were Rogowski coils, voltage probes, and oscilloscopes.

Major Components

Capacitor Bank. The capacitor bank provided the initial feed current to the MCG. The bank consisted of fifty 6.1 μF 60 KV capacitors connected in parallel to yield a total nominal capacitance of 305 μF. Charge voltages between 15 KV and 45 KV were used. The bank was charged by a Maxwell Laboratory charging system and discharged into the transmission line and MCG through a solid dielectric closing switch.

Closing Switch. The closing switch used during the experiments was a solid dielectric explosive switch. The switch consisted of two 6 foot long by 8 inch wide by 0.5 inch thick steel plates. The connection of the closing switch to the transmission line and capacitor bank is shown in Figure 4-1.

One of the plates was connected via the solid inner conductors of numerous parallel coaxial cables to the capacitor bank. The other

28

Figure 4-1. MCG Experimental Set Up

Labels in figure: Load, MCG, Firing Line 2, Transmission Line, Closing Switch, Firing Line 1, Mylar, Firing Line 2, X Unit, Delay Generator, Capacitor Bank
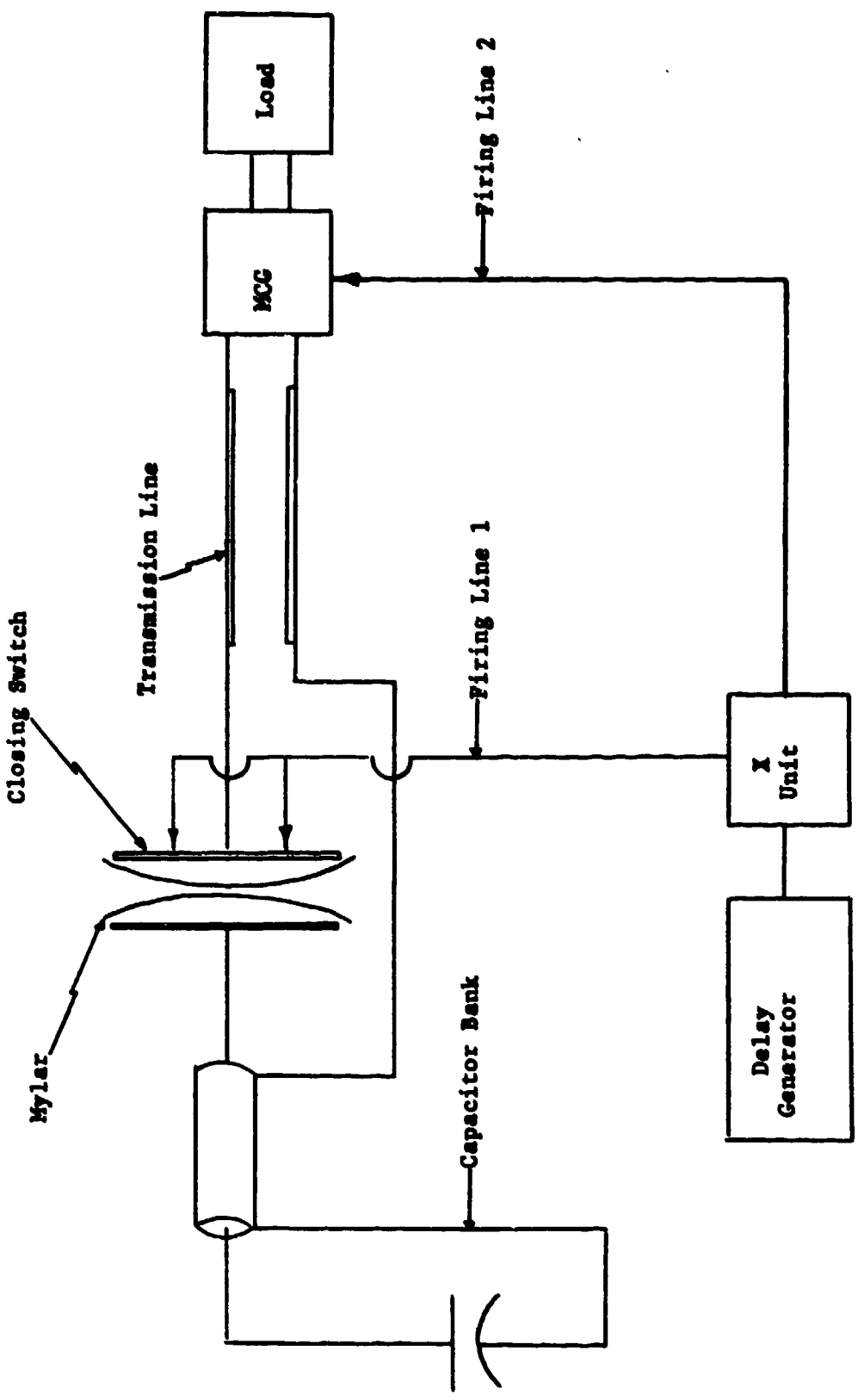
plate was attached to the top of the transmission line and could be pulled back to facilitate cleaning and rebuilding of the switch.

Sheets of mylar sandwiched between the two aligned plates acted as the solid dielectric insulation for the switch. A 1 mil thickness of mylar was used for each 1 KV of potential across the plates. Plate separation was determined by the number of sheets of mylar required for the test voltage applied.

Before each test, two RP2 PETN explosive shaped charge detonators were placed into 0.5 inch holes which were drilled along the top edge of the plate connected to the transmission line. Closing of the switch occurred when the two detonators were fired, rupturing the mylar insulation and allowing breakdown of the switch. The capacitor bank then discharged its energy through the switch into the transmission line and the MCG.

Because of its destructive nature, the switch required rebuilding after each shot. Rebuilding consisted of replacing the mylar sheets between the plates, replacing the detonators, and reconnecting the detonation lines to the X Units.

Firing System. The firing systems consisted of two TRW Model 64A Trigger Delay Generators and a Los Alamos National Laboratory X Unit. The trigger delay generators provided a variable time delayed output pulse to fire the X Unit and trigger the other diagnostic equipment. The X Unit provided the current pulse used to fire the detonators in both the switch bunker and the explosive on the MCG.

Transmission Line. The transmission line consisted of two parallel plates of 60 mil aluminum, 40 feet long and 4 feet wide.

30

This length allowed the feed current to be delivered to the MCG at a safe distance from the bunker and switch, avoiding damage to the switch during the MCG explosions.

The two aluminum sheets are separated by twelve sheets of 5 mil thick 6 foot wide mylar. This allows for a hold off voltage of 60 KV at 1 mil per kilovolt. The total insulation thickness of 60 mils results in a line capacitance of

$$C = \epsilon A/d$$
$$= 0.26 \ \mu F$$

(4-1)

Since $C_{Line} \ll C_{Bank}$, C_{Line} was neglected in all circuit calculations. The plate edges were further insulated against edge field enhancement effects by the placement of 0.5 inch diameter tygon tubing between the sixth and seventh sheets of mylar along the edge of the entire length of the line (3).

Because the end of the transmission line was connected directly to the MCG, it was destroyed with each test. To avoid replacing the entire transmission line, 6 foot long by 4 foot wide end pieces were bolted onto the end of the line using clamping bars to ensure good electrical contact. Sandbags protected the clamping bars during the explosions. Following each test, the end pieces and final sections of mylar were replaced.

Diagnostics

Rogowski Coils. Rogowski coils provide a means to measure the derivative of time varying high currents, responding only to the current passing through the coil loop (13:180).

Four Rogowski coils were used for each test, placed as shown in

Figure 4-2.
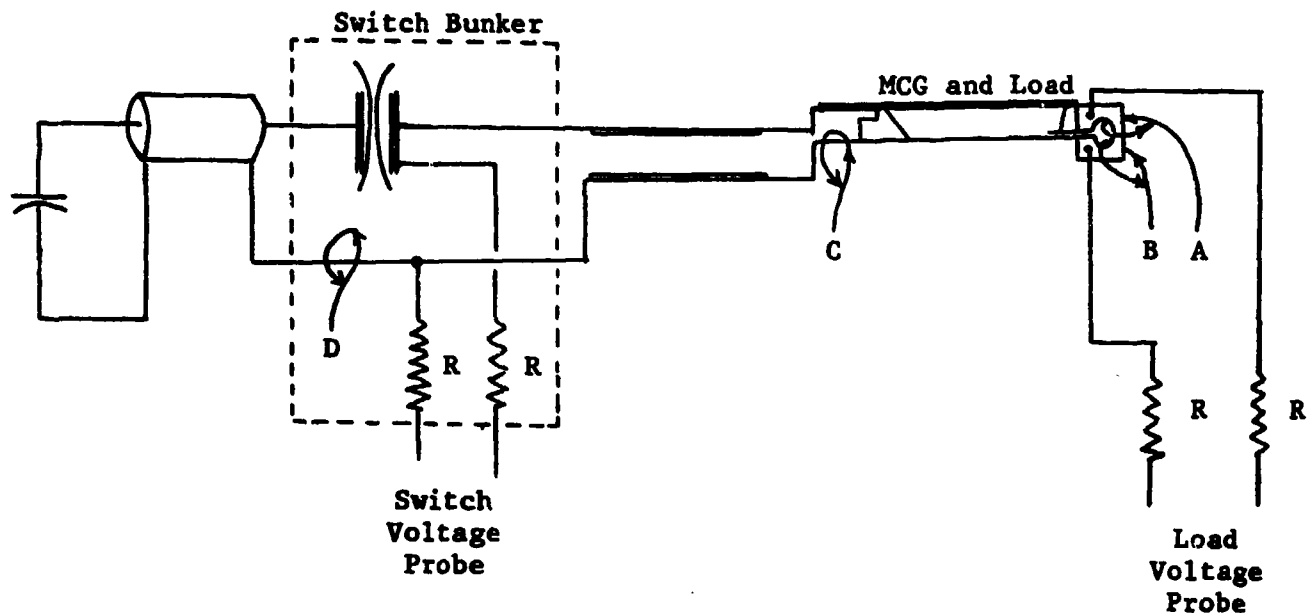
Figure 4-2. Placement of Test Diagnostic Devices

Coils A and B were used to measure the load current derivative.
Coil C was used to measure the feed current derivative until
crowbarring occurs and Coil D, located in the switch bunker, measured
the derivative of the return current of the transmission line.

Both handwound and etched Rogowski coils were used. The handwound
Rogowski coils provided a 1 volt signal for every 10^9 A/sec present
while the etched Rogowski coils provided a 1 volt signal for every 10^{10}
A/sec present. Coil A was etched, while coils B, C, and D were
handwound.

To enhance coil survivability during the explosion, all four Rogowski coils were placed inside through tygon tubing. Coils A, B, and C were destroyed during each test and had to be replaced prior to the next shot. Coil D remained undamaged throughout the explosion and thus provided a uniform means to compare the input parameters from test to test.

The current derivatives from coils A, B, and D were actively integrated using Textronixs Type O Operational Amplifier integrators. The output from these integrators was fed into oscilloscopes and recorded on film.

Voltage Probes. At least one voltage probe was used in each experiment; the one located in the switch bunker was used to measure the voltage across the switch. In the experiments where a MCG load coil of 10.31 nH was used, a second voltage probe was connected to the load coil to measure the voltage across the load during the operation of the MCG. The voltage probes consisted of resistive dividers to measure voltage and were connected as shown in Figure 4-2. In both voltage probes, the two resistors were filled with a copper sulfate solution with copper electrodes sealing each end. The copper sulfate solution was adjusted to give a nominal resistance of 20 KΩ. Coaxial diagnostic cables fed the signals to 50 Ω terminators across the oscilloscope inputs. Therefore, a 2.5 volt signal was measured at the oscilloscope for every 1 KV across the switch or load coil. The outer cable shields were shorted together at the resistors and at the oscilloscope inputs to balance any induced shield currents. The two signals from each probe were then connected to a differential amplifier which eliminated any common mode signals (13:182).

33

Oscilloscopes. Data from each test was recorded on fourteen Textronixs 7603 oscilloscopes. Four oscilloscopes recorded signals generated from each load Rogowski coil with two recording dI/dt and two recording the integrated current waveforms. Two oscilloscopes measured the differential voltage across the load when the 10.31 nH load was used. One oscilloscope was used to record the line dI/dt from coil C. Another oscilloscope recorded the line dI/dt from coil D. Two other oscilloscopes recorded the integrated current from coil D and the differential voltage across the switch. The data from each of the oscilloscopes was recorded by Polaroid cameras which were triggered by the delay generators.

V. Experimental Procedures

Five strip geometry magnetocumulative generator experiments, referred to as MCG shots, were performed in order to obtain data with which the computer model could be compared and validated. Prior to every MCG shot, two preliminary experiments were conducted. The first of these, referred to as a line short shot was required to obtain element values for the equivalent circuit of the capacitor bank and transmission line. The second, referred to as a MCG short shot, was conducted in order to calibrate the diagnostic Rogowski coils which would be used during the actual MCG shot. This chapter describes in detail the general procedures that are common to all three of these shots. It then describes the experimental procedures which are unique to the line short shot, the MCG short shot, and the MCG shot.

General Procedures

Prior to each shot several experimental procedures common to all shots were performed. These procedures include diagnostic line tests, X Unit and detonation line tests, and preparation of the oscilloscopes.

Diagnostic Line Tests. To preclude the loss of experimental data due to faulty diagnostic lines, these lines were tested prior to each shot. A repetitive train of pulses from the TRW Delay Generators was delivered to the MCG connection end of the transmission line via a test line. This test signal was connected to each diagnostic line in turn. The return signal was then monitored on an oscilloscope to insure that the line was operating reliably prior to being connected to a Rogowski coil or voltage probe.

X Unit and Detonation Line Test. Prior to each test, the X Units and detonation lines were tested for reliable operation and timing. Blown bridge wires were attached to the detonation lines to simulate detonators during the test. Using a pencil, a carbon path was marked between the two terminals where the bridge wire was originally connected, providing a path for breakdown when the X Units fired. The resulting flash and distinctive pop accompanying this breakdown gave clear indication that the X Units were operating correctly.

Preparation of the Oscilloscopes. Preparation of the oscilloscopes prior to each shot included calibration, setting of graticules, and setting of baselines. Once the scopes were calibrated, the graticules and baselines were adjusted to levels which would ensure clear data recording of measured signals with cameras.

Just prior to the shot, the shutters of the Polaroid cameras were opened to record the graticules. The graticules were then turned off to prevent them from being recorded again during the shot. As the capacitor bank was being charged, the shutters were opened one final time in order to record the data signals. The TRW Delay Generators were coordinated with the data signals from the various Rogowski coils and voltage probes.

Line Short Shots

A total of four line short shots were performed to determine circuit element values for the equivalent circuit model of the capacitor bank, switch, transmission line, and connections. This section describes the line short shot and the general procedures to obtain these circuit element values.

For line short shots the ends of the transmission line where the MCG would later be connected were shorted together giving rise to the name line short shot. The two load Rogowski coils and the end of the line current Rogowski coil were looped around the shorting bar at the end of the line.

The capacitor bank was charged and then discharged through the switch and the transmission line. This resulted in an exponentially damped sinusoidal waveform (See Figure 5-1).
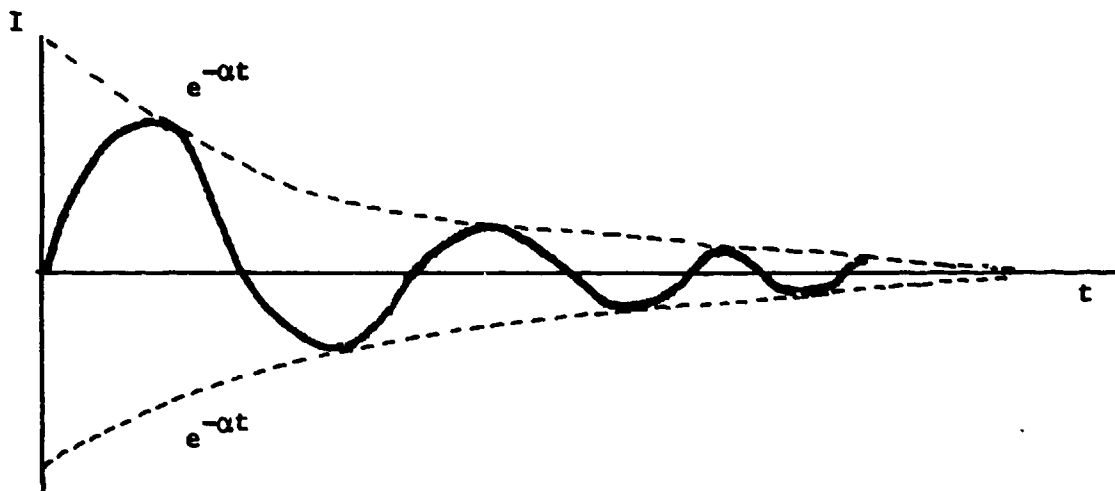
Figure 5-1. Typical Short Circuit Plot

The only known values in these experiments were the bank capacitance, C_{Bank}, and the charge voltage, V_0. All other capacitances were neglected because they were much less than C_{Bank}. The period, τ, was determined directly from the oscilloscope traces.

The solution to a time invarient RLC circuit is well-known (1:132).
A least squares fit was done to determine the exponential damping
factor, α, shown in Figure 5-1. Knowing τ, C, and α, the circuit
inductance was calculated using

$$\tau = 2\pi\omega_r$$
$$= 2\pi/\{(\omega_0)^2 - (\alpha)^2\}^{1/2} \qquad (5-1)$$

where $\omega_0 = \dfrac{1}{\sqrt{LC}}$
yielding

$$L = \tau^2/C(4\pi^2 + \tau\alpha^2) \qquad (5-2)$$

and the circuit resistance was determined by

$$R = 2\alpha L \qquad (5-3)$$

In MCG work, the input circuit is crowbarred away from the
generator after the first quarter cycle at I_{peak}. A comparison of the
values of I_{peak} and the quarter cycle time using the time invariant
RLC solution and an approximate LC solution showed that R could be
neglected without significant loss of accuracy.

MCG Short Shots

This section describes in detail the MCG short shot and the
general procedures for calculating the total system inductance and the
sensitivities of the Rogowski coils. A minimum of one MCG short shot
was performed prior to each MCG shot. For a successful MCG shot, the
entire system must operate reliably. When one part of the system was
found to have a problem, it was fixed or replaced and another MCG

short test was performed. For this reason, as many as four MCG short
shots were performed prior to one actual MCG shot. These shots provide
a final test of the entire system to ensure all components were
operating correctly.

These shots provided oscilloscope traces of the current outputs
from which the total system inductance would be determined. They also
provided dI/dt traces from each Rogowski coil so that their sensitivi-
ties could be experimentally determined prior to the actual MCG shot.

For the MCG short shot, the MCG was bolted to the end of the
transmission line in the same manner as for the actual shot. The only
differences were the lack of explosive on the generator and the place-
ment of the load voltage probe. The two load coil Rogowski coils were
placed through the load coil and the end of the line return Rogowski
coil was placed around the bottom return transmission line's plate at
the connection to the MCG. For the actual MCG shot, these were moved
to the load coil.

The capacitor bank was charged to 15 KV for each MCG short shot.
The capacitor bank was then discharged through the switch, transmission
line, and the MCG. This again resulted in a damped sinusoidal waveform.

The oscilloscope traces from the MCG short shot were used in order
to determine the total system inductance of the capacitor bank, the
switch, the transmission line, connections, and the MCG. The period,
τ, of the damped sinusoidal waveform was read directly from the traces.

With a known bank capacitance and neglecting system resistance,
the total system inductance could be determined using

$$\tau = 2\pi\sqrt{L_T C_{Bank}} \qquad (5-4)$$

39

which when solved for the inductance yields

$$L_T = \tau^2/4\pi^2 C_{Bank} \qquad (5\text{-}5)$$

Oscilloscope traces of dI/dt from each Rogowski coils were used to experimentally determine the sensitivity of the Rogowski coils which would be used during the succeeding MCG shot. Knowing the capacitor bank charge voltage, V_0, the total inductance, L_T, and neglecting system resistance, the maximum dI/dt is given by

$$\frac{dI}{dt}_{max} = \frac{V_0}{L_T} \qquad (5\text{-}6)$$

Measuring the maximum voltage of the dI/dt trace, the sensitivity of the Rogowski coil is given by

$$\text{Sensitivity} = \frac{dI}{dt}_{max}/V_{max} \qquad (5\text{-}7)$$

With the integrator time constant, TI, the sensitivity of the Rogowski coil and the voltage peak of the integrated dI/dt trace, V_p, I_{Peak} was calculated using

$$I_{Peak} = V_p \times \text{Sensitivity} \times TI \qquad (5\text{-}8)$$

This I_{Peak} was then compared with the value predicted by the time invariant RLC solution as a check of the integrators. This procedure was performed for each coil to be used during the actual MCG shot.

MCG Shots

A total of five MCG shots were performed to obtain data for validation of the computer model. This section details the set up, procedures, and input conditions for each of these shots.

40

The explosive used in all shots was DuPont Detasheet. As described earlier in this chapter, the total system inductance as well as the sensitivities of the Rogowski coils were determined during a MCG short shot just prior to the actual MCG shot. The total inductance varies with the length of the transmission line end pieces and the connection to the MCG. After the MCG short shot, the X Units and detonation lines were once again tested, the switch rebuilt, and the oscilloscopes prepared. During this period of time explosives are readied on the MCG by contractor personnel from the Civil Engineering Research Facility (CERF). Each generator is identical except for the size of the load coil. For three shots the load coil had an inductance of 10.31 nH. For two shots, a smaller load was used; one had an inductance of 0.2213 nH and the other had an inductance of 0.5701 nH. The MCG was placed on a plate of one inch steel which was separated from the MCG by several sheets of mylar. This steel plate is placed on a bed of cinder blocks. A smaller 40 inch long by 8 inch wide by 3/16 inch thick steel tamper is placed on top of the explosive for every shot. The amount of cement tamper placed on this steel sheet, as well as, the bank voltage varied from shot to shot. Shown in Table 5-1 is a summary of the input conditions for the five MCG shots.

Table 5-1

Summary of Input Conditions

Test	V(KA)	L (nH)	I (KA)	Explo-sive Weight (lbs)	Steel Weight (lbs)	Cement Weight (lbs)	L_{Load} (nH)
1	44.88	499.500	1100.00	1.85	4.911	5.0	10.31
2	25.00	437.700	294.00	8.16	4.911	20.0	10.31
3	25.40	487.693	630.00	5.90	4.911	10.0	10.31
4	27.70	540.380	652.00	7.37	4.911	20.0	0.5701
5	24.99	487.690	620.00	6.40	4.911	15.0	0.2213

VI. Results and Conclusions

This chapter presents the results of the computer models and compares them with the experimental data. In addition, it includes recommendations for further study.

Results

The goal of this study was to develop a computer model of the strip geometry MCG and to validate it through actual MCG shots. The primary criterion for evaluating the computer model was the model's ability to reproduce the current curves produced by actual MCG experiments. Accurate reproduction of these curves indicates that the computer program should be able to reliably predict the current curves for future rests. This section shows the results of the actual MCG shots and compares them with the results of the computer models.

A total of six experiments were conducted using the AFWL strip MCG. Five of these experiments were successful. The unsuccessful experiment was caused by a destructive failure of one of the capacitors in the capacitor bank. The results of the five successful shots are summarized in Table 6-1.

A plot of the actual current from the first experiment is shown in Figure 6-1. Actual currents from the remaining tests are contained in Appendix B. In four of the tests, crowbar occurred at or near I_{Peak} of the sinusoidal input current where dI/dt is equal to zero. In the second test, the generator crowbarred late resulting in an input current of 294.0 KA. Input currents varied from 294.0 to 1100.0 KA while output current peaks varied from 2210.0 to 10261.0 KA.

43
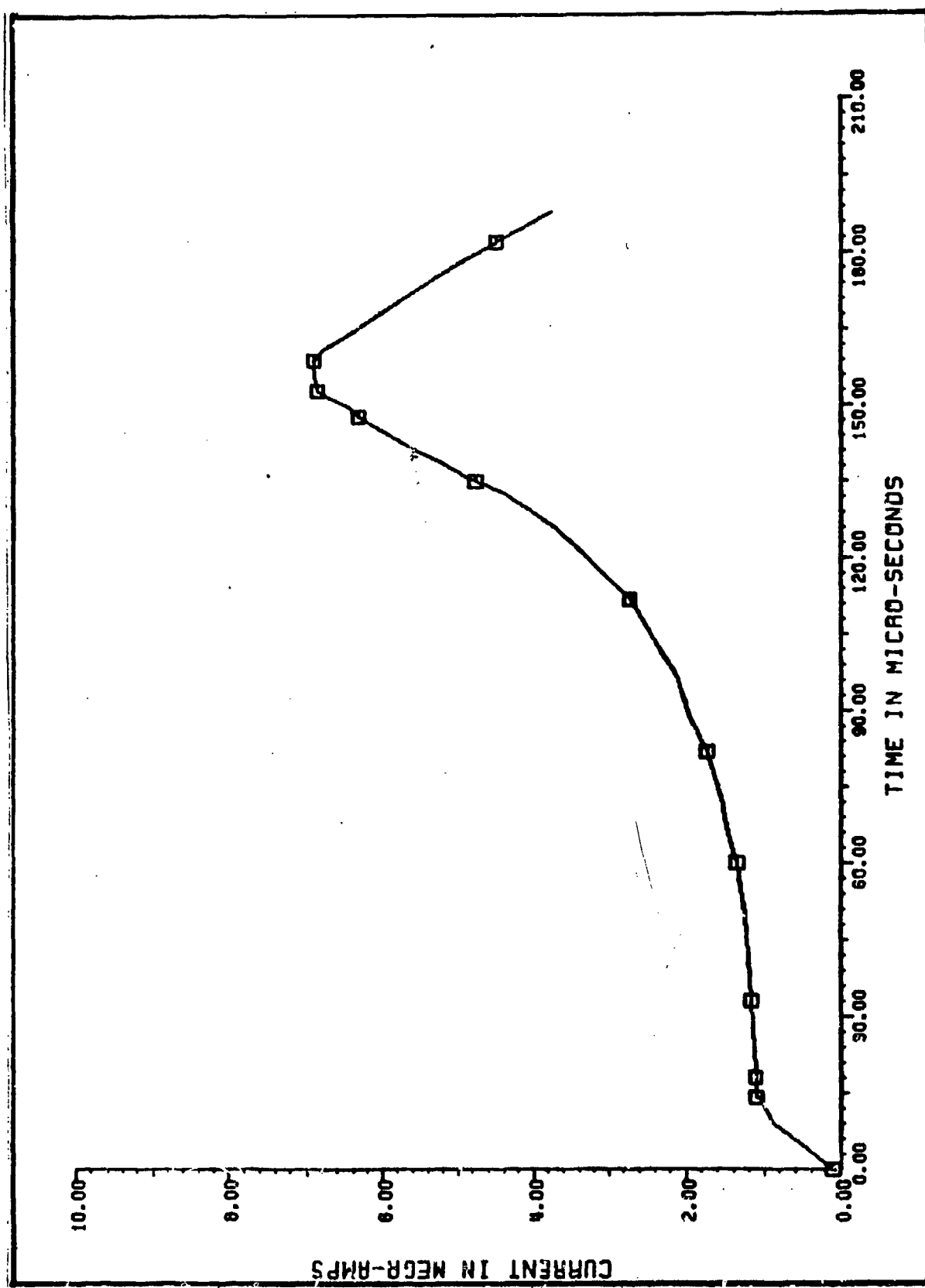
Figure 6-1. Experimental Current Test 1

44

Table 6-1

Summary of Results

Test	Input Current (KA)	Maximum Output Current (KA) Ideal/Actual	Current Amplification Factor Ideal/Actual
1	1100.00	15188.6/6928.0	13.81/6.29
2	294.0	4128.7/2210.0	14.04/7.50
3	630.78	8715.3/5355.0	13.82/8.50
4	652.66	35646.0/10261.0	54.62/15.75
5	620.05	29556.4/6031.0	47.68/9.73

Computer Model Results. Based on the input parameters the computer program calculates and prints the currents predicted by each of five models: the flux conserved model, the resistance model, the sliding contact loss model, the changing area model, and the efficiency model. The results of these models are best described in terms of how well they correspond to the actual experimental data. The results are considered individually.

Flux Conserved Model. The flux conserved model calculates the output current as if no losses occur. The current is a function of only the time varying inductance, which in turn is a function of the detonation velocity and the Gurney angle. The time varying inductance which corresponds to a Gurney angle of 5.6^0 from the first test is shown in Figure 6.2

The flux conserved current versus the test current for the first test is shown in Figure 6-3; the curves for the remaining tests are shown in Appendix B. Points 1, 2, and 3 from Figure 3-4, corresponding

45
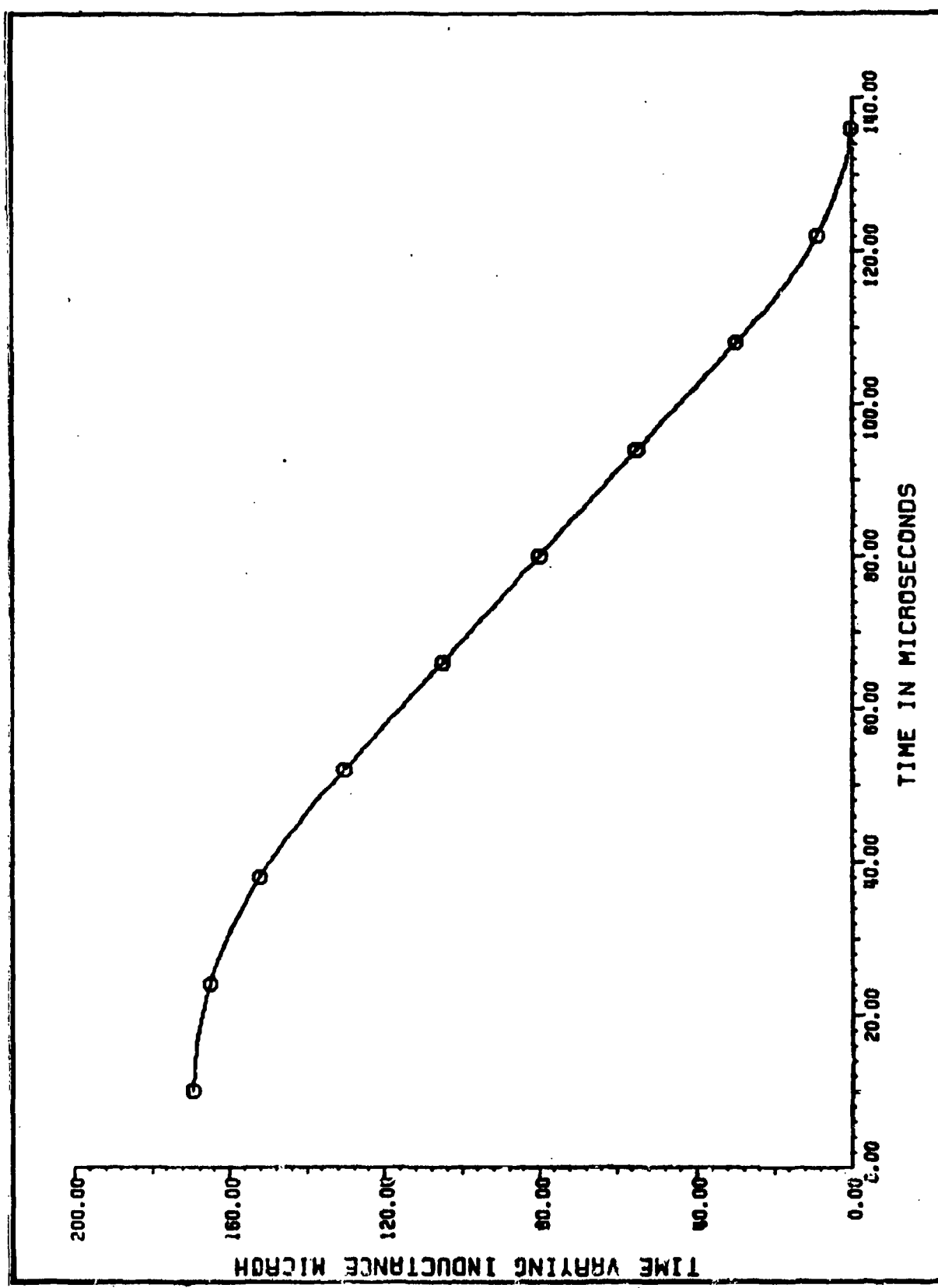
Figure 6-2. Time Varying Inductance

46
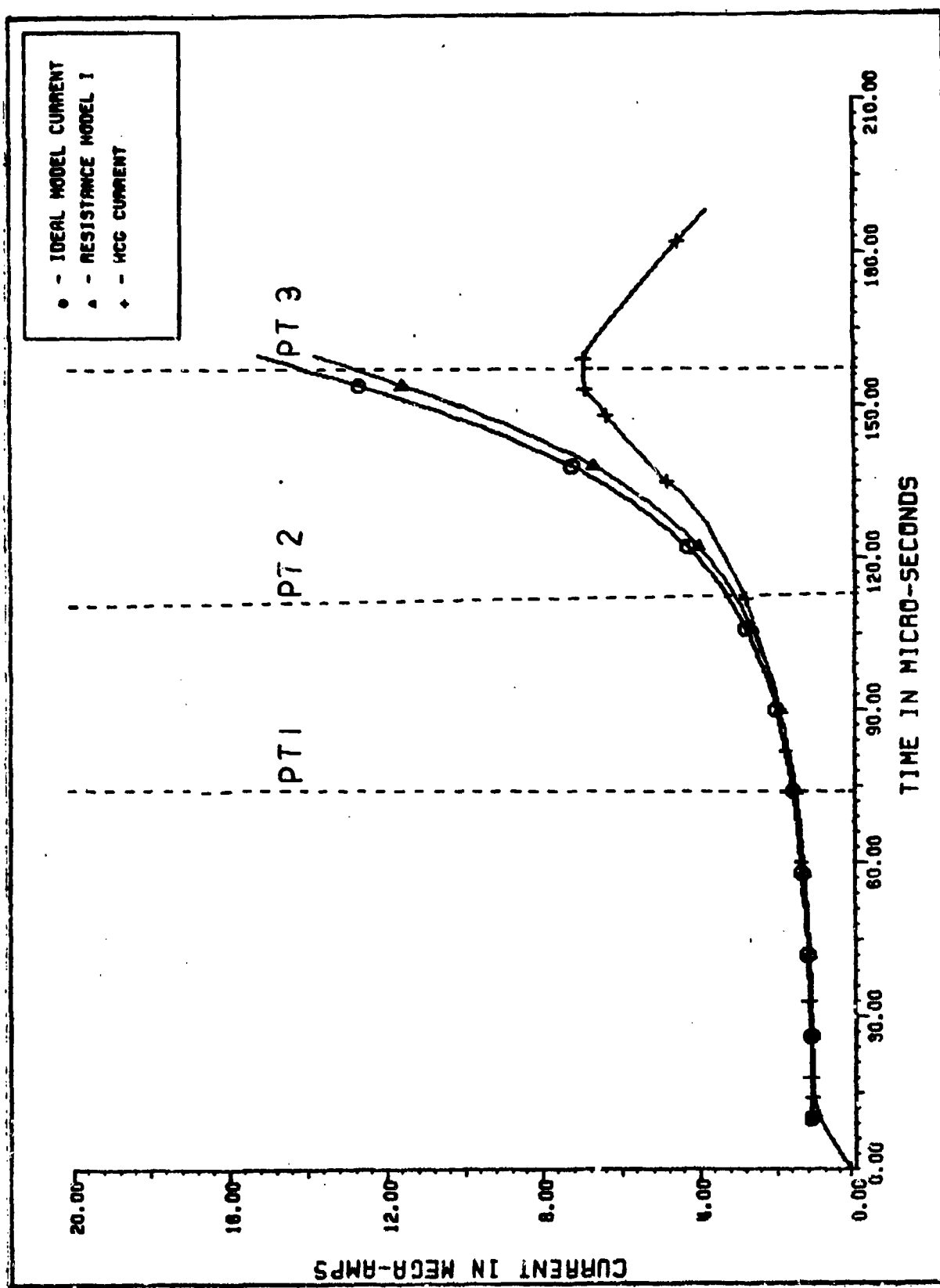
Figure 6-3. Equivalent Circuit Currents Test 1

47

to key generator operation points, are shown in this figure. A
comparison of these two curves show that the flux conserved model
provides a good approximation of the actual currents for the first 50%
of generation. Because the flux conserved model neglects all losses,
these plots show that for the first 50% of operation, the system is
basically lossless. During the last 50% of operation this model
predicts higher currents than those actually present. This indicates
the presence of loss mechanisms which must be accounted for to obtain a
complete model of the generator.

Resistance Model. The resistance model theoretically calculates
the losses due to the plate resistance and flux diffusion equivalent
resistance. A plot of the time varying resistance for the first test
is shown in Figure 6-4; curves for the other tests are shown in
Appendix B. A plot of the time varying resistance model's current
versus the test current for the first test is shown in Figure 6-3.

These plots clearly indicate that plate resistance and flux
diffusion resistance play only a limited role as loss mechanisms.
Resistance effects are negligible during the initial 50% of generator
operation, again indicating the system is essentially lossless during
this time period. During the final 50% of operation, the time varying
resistance predicts a current about 1% lower than that calculated by
the flux conserved model.

An examination of the resistance shows that the plate resistances
exceed the flux diffusion equivalent resistances by two orders of
magnitude throughout generator operation. This indicates that flux
diffusion plays only a minor role as a loss mechanism.

48
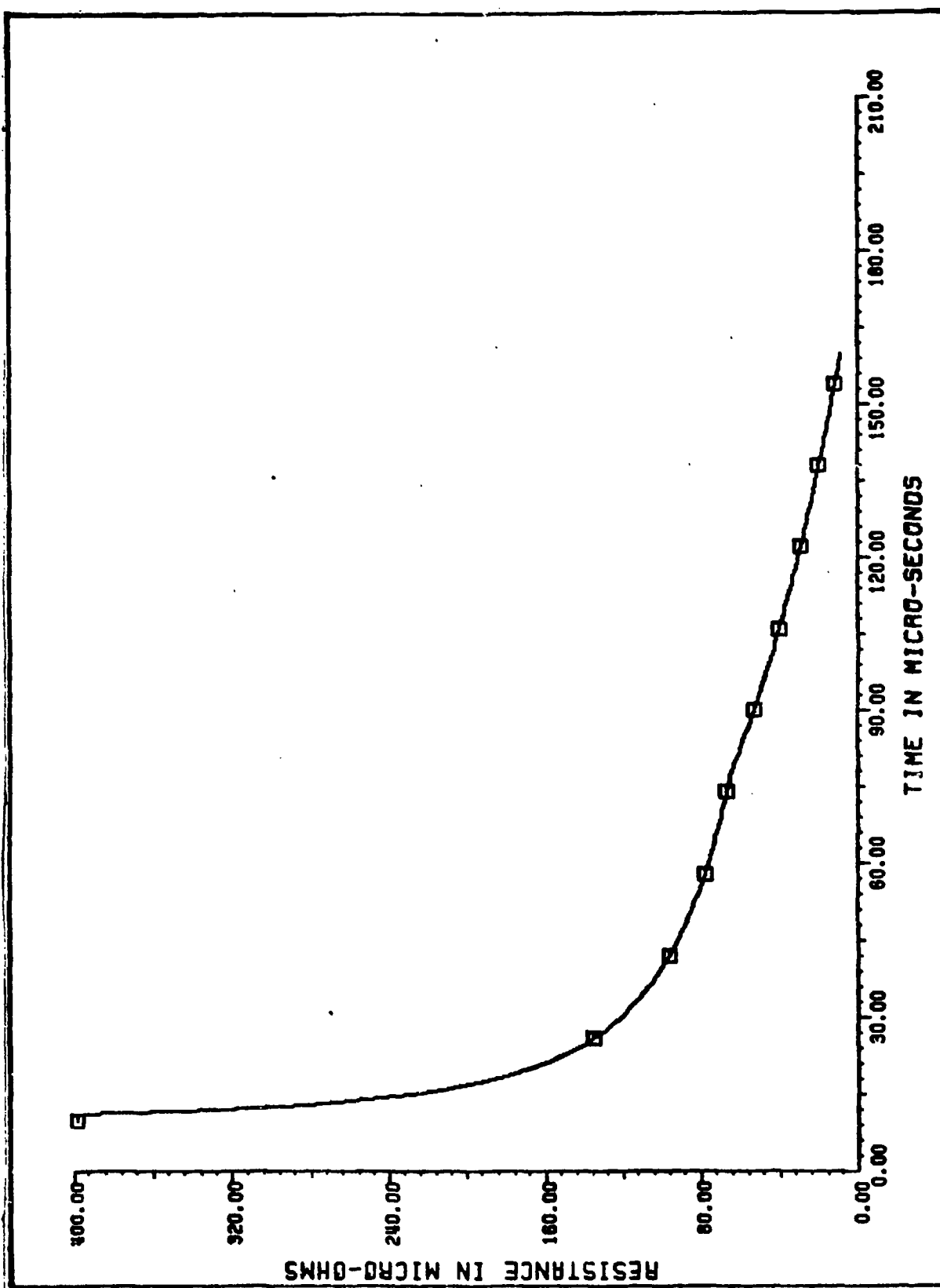
Figure 6-4. Time Varying Resistance Test 1

49

The resistivity which would be required were resistance alone to account for all losses in the generator's operation was calculated. This resistivity was found to be at least two orders of magnitude larger than the resistivity of vaporized copper. Since the magnitude of the ideal B fields was not sufficient to cause surface vaporization, a resistance this large was not reasonable. The resistance model's poor prediction during the final 50% of the generator's operation shows that additional loss mechanisms must be considered.

Sliding Contact Model. Unlike the flux conserved and resistance models, the sliding contact model is based on empirical data. A time varying mean ripple depth, s, was determined for the first three experiments with a load inductance of 10.31 nH. A plot of the s curve for the first experiment is shown in Figure 6-5, while the s curves for the second and third tests are presented in Appendix B. Points 1, 2, and 3 from Figure 3-4, corresponding to key generator operation points, are shown in this figure.

The bubble height gives a measure of how much flux is lost due to the sliding losses. Since s could not be linked to any parameter, a best and worst case sliding contact loss model was developed. Plots of the slipping loss model's best and worst case currents versus the test current for the first test are shown in Figure 6-6 with plots for later tests in Appendix B.

A comparison of these curves shows that the ranges described by the curves are reasonable. All test currents fall between the best and worst case curves of the slipping loss model.

Changing Area Loss Model. Instead of modeling the additional losses as the bubble height, this model assumes that the Gurney

50
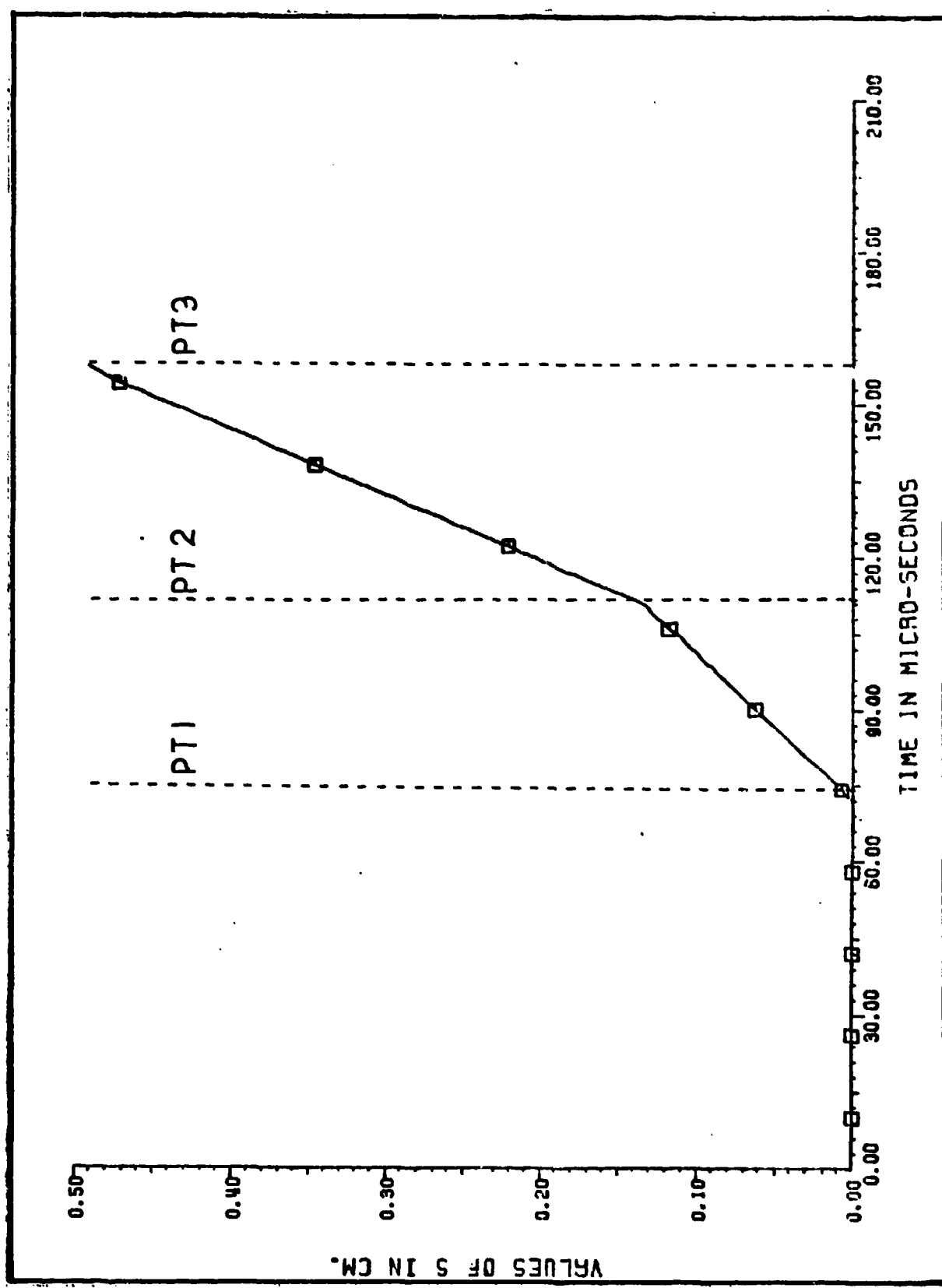
Figure 6-5. S Curve Test 1

51
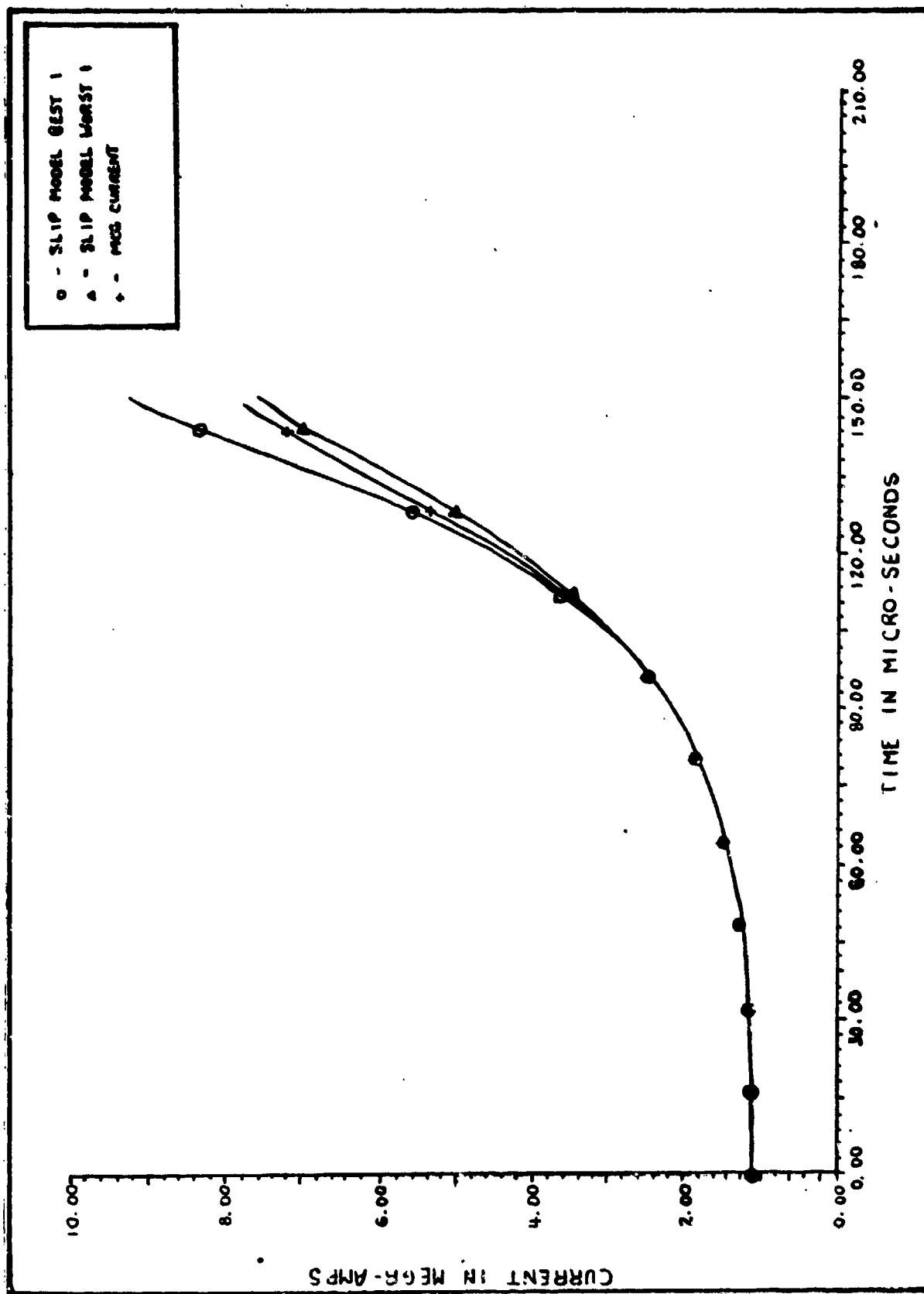
Figure 6-6. Slipping Currents Test 1

52

approximations for the changing inductance are not valid. Figure 6-7 shows a plot of the additional area which must be added for the model current to match the experimental current. Points 1, 2, and 3 from Figure 3-4 are shown on this figure. Figure 6-8 shows the Gurney based area, the additional area, and the sum of these areas; similar curves for the second and third test are contained in Appendix B.

Negative areas indicate that flux compression is occurring faster than that predicted by the Gurney approximations based time varying inductance. This occurs early during generator operation. Positive areas indicate that flux compression is occurring slower than that predicted by the Gurney approximations. This occurs late during MCG operation. A momentum balance during this time period shows that the momentum of the metal plate due to the explosive initially is orders of magnitude larger than the momentum of the metal plate due to magnetic pressure. By the time the top plate has started down the jet wedge, the two momentums are essentially equal with the explosive momentum always slightly larger. This means the Gurney approximations are probably not valid during the final microseconds of generator operation.

Best and worst case changing area models were developed. The best and worst case changing area model currents for the first test are shown in Figure 6-9 while similar curves for the remaining tests are contained in Appendix B. A comparison of these curves shows that the experimental currents fall between the best and worst case curves for the first and third tests. The two curves are a bit higher than the experimental current for the second test.
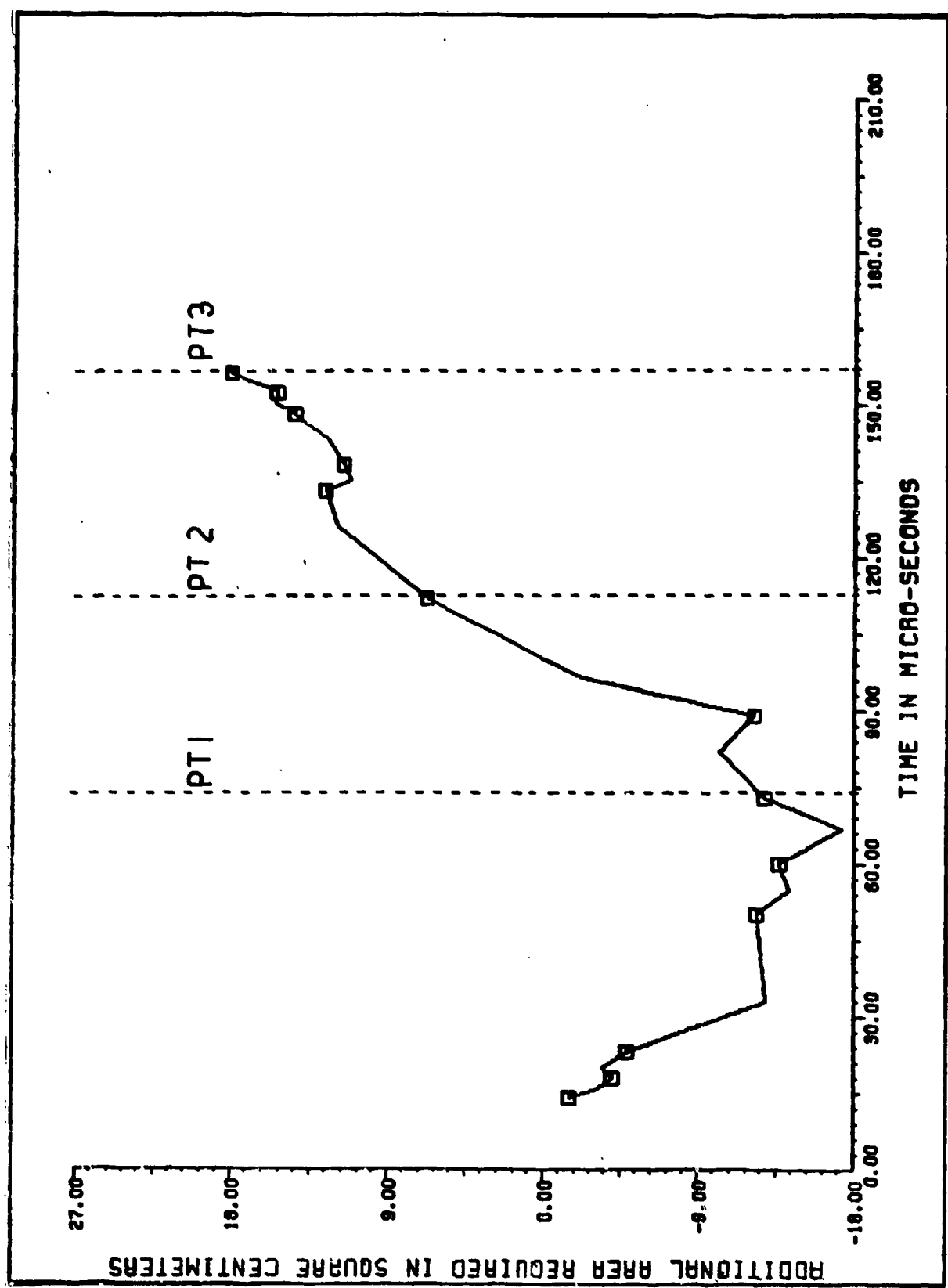
Figure 6-7. Additional Area Test 1
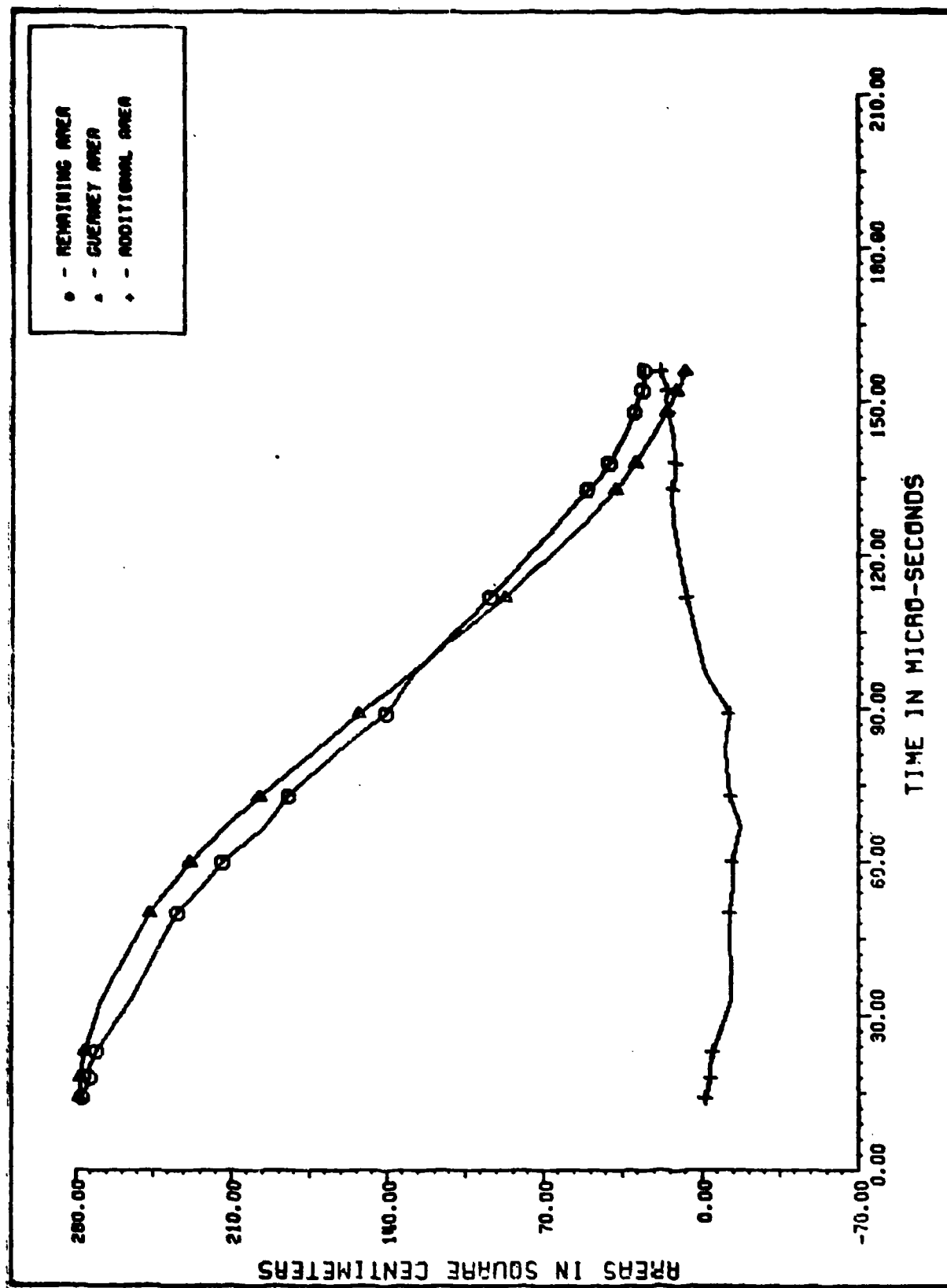
Figure 6-8. Changing Areas Test 1
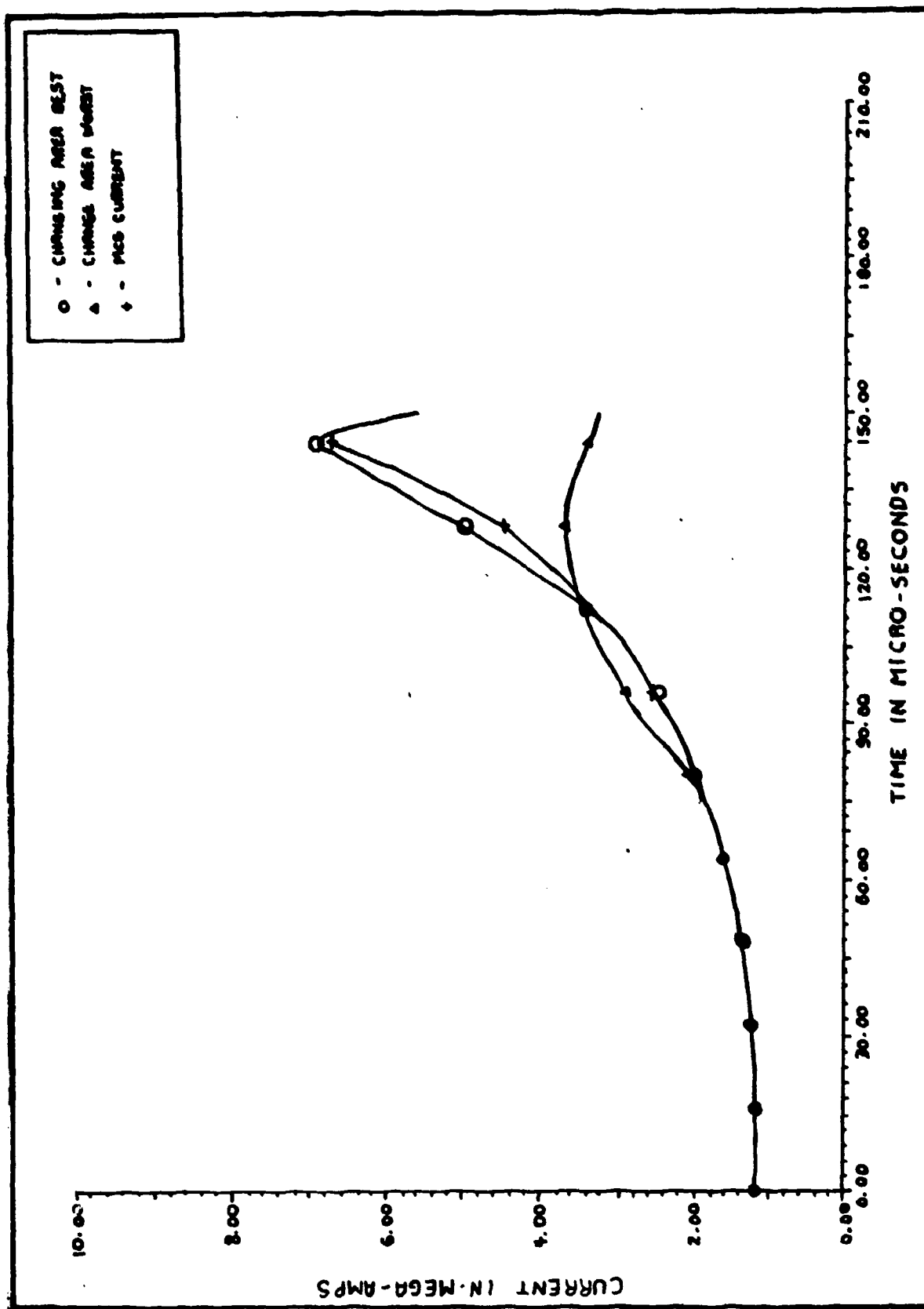
Figure 6-9. Changing Area Currents Test 1

56

Flux Trapping Efficiency Model. This model considers the flux trapping efficiency without regard to the flux loss mechanism. A plot of the efficiency for the first test is shown in Figure 6-10 and similar curves for the remaining tests are in Appendix B. Points 1, 2, and 3 from Figure 3-4, corresponding to key points in generator operation, are shown in this figure.

In each test, the efficiency remains better than 90% for the first half of generator operation. The values greater than 100% in the first experiment again indicate that flux compression is occurring faster than that predicted by the Gurney approximations. During the next 25% of generator operation the efficiency drops to approximately 80%. During the final 20 microseconds, severe losses occur. The final efficiency ranges between 50 and 60 percent.

The curves from the first three experiments were used to generate a best and worst case efficiency model. The plots for the best and worst case currents for the efficiency model for the first test are shown in Figure 6-11. Curves for the remaining experiments are presented in Appendix B. At the end of generation, the final currents in each test fall well within the predicted range indicating that the efficiency model is reliable.

General Results. All the models reliably predict the generator output for the first 50% of generator operation. Beyond that point only the empirical models can predict the current values. Based on the experimental data, the computer model can reliably predict the range of output currents.
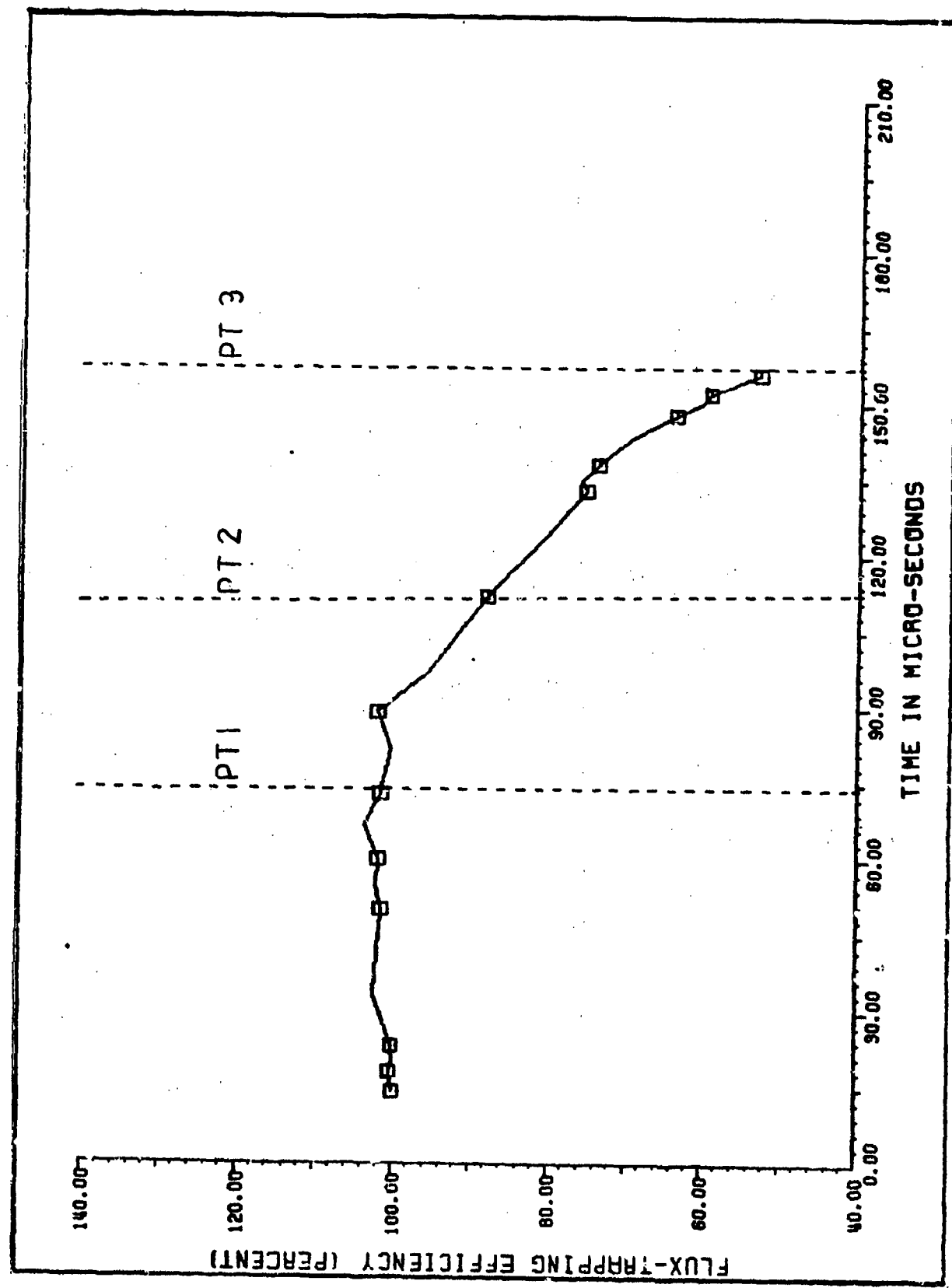
Figure 6-10. Efficiency Test 1
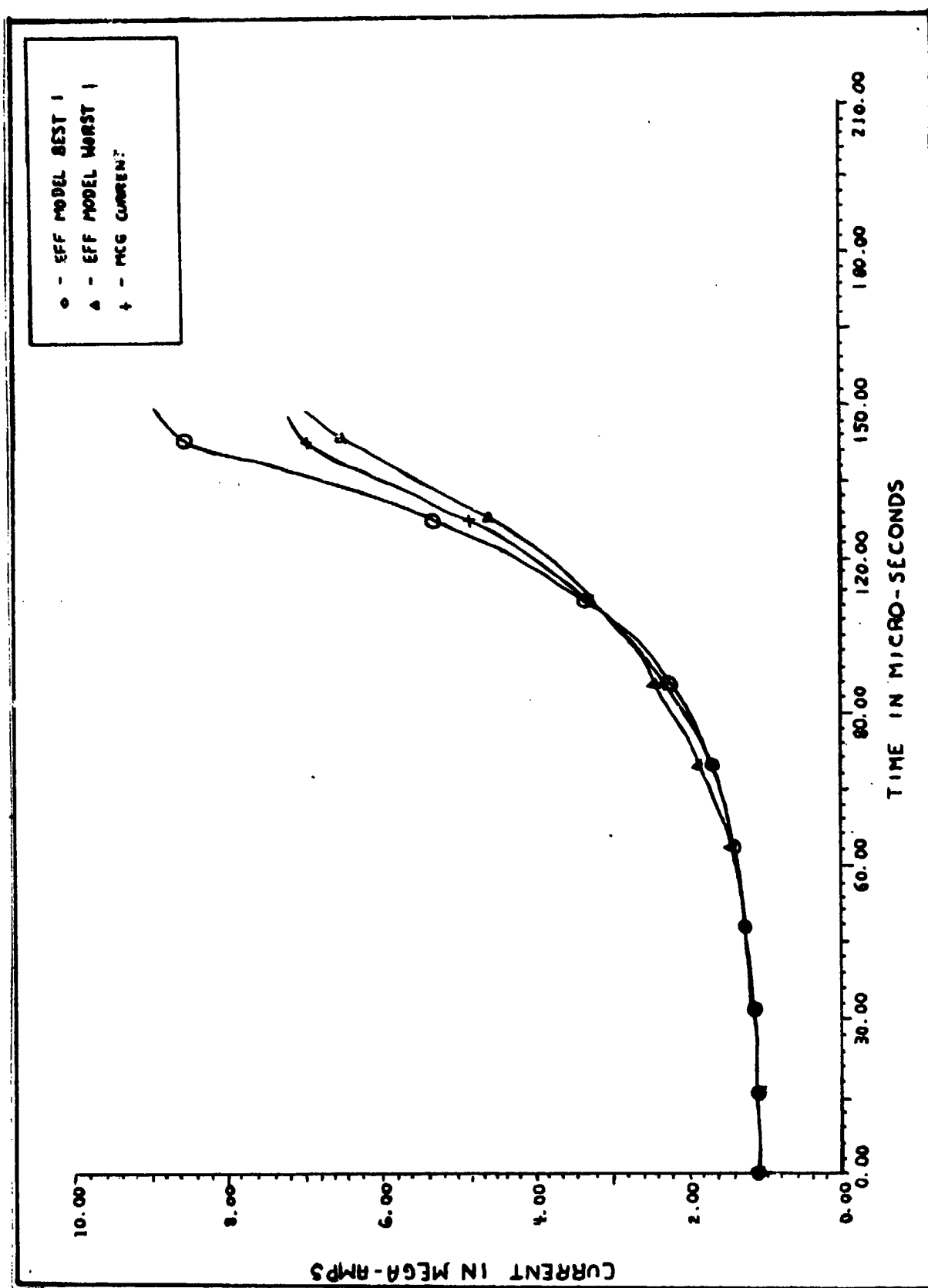
Figure 6-11. Efficiency Currents Test 1

Conclusions

Several conclusions can be drawn:

1) The computer model can predict the generator output current reliably during the first 50% of operation. It can also predict the ranges in which the final maximum output current will fall;

2) The losses during the initial 50% of generator operation can be neglected and the generator may be considered lossless for this period;

3) The plate resistance and flux diffusion resistance account for only a minor portion of the loss mechanisms in generator operation;

4) The empirical models show that the flux compression described by the Gurney approximations is not totally accurate;

5) Losses are severe during the final moments of generator operation; and

6) The validation experiments show that the strip MCG is capable of delivering large currents over a relatively long period of time.

Recommendations

Based on the work performed for this thesis several recommendations can be made. These include:

1) Computer validation of the trapezoidal portion of the computer program has never been accomplished. This portion of the program should be validated;

2) The empirical models are based on the results of only three tests. Further tests should be conducted to further validate them or to refine their accuracy;

60

3) Strip generators other than the AFWL MCG should be used to further validate the models (for example, different materials or dimensions);

4) Because the loss mechanisms in bellows generators are similar, the computer program should be expanded to include this geometry MCG;

5) Because the generator drives a low inductance load, the use of transformers to drive capacitive and resistive loads should be investigated and perhaps incorporated into the computer program;

6) Due to the momentum balances performed, tapered explosives should be considered to overcome the intense magnetic pressure as generator operation draws to an end;

7) When high magnetic fields and high currents were present, the load coil was visibly deformed; it opened up. This effect should be included in the computer program;

8) High speed photographs of generator operation should be done to gain a better understanding of how the inductance actually changes with time;

9) Explosive type and plate material should also be varied to further validate the computer model; and

10) Due to the intense magnetic pressures present near the end of generator operation, a momentum balance should be incorporated into the computer program.

Appendix A

This appendix describes the computer program. This program is written in FORTRAN V. The inputs to the program are best described by Figure A-1.
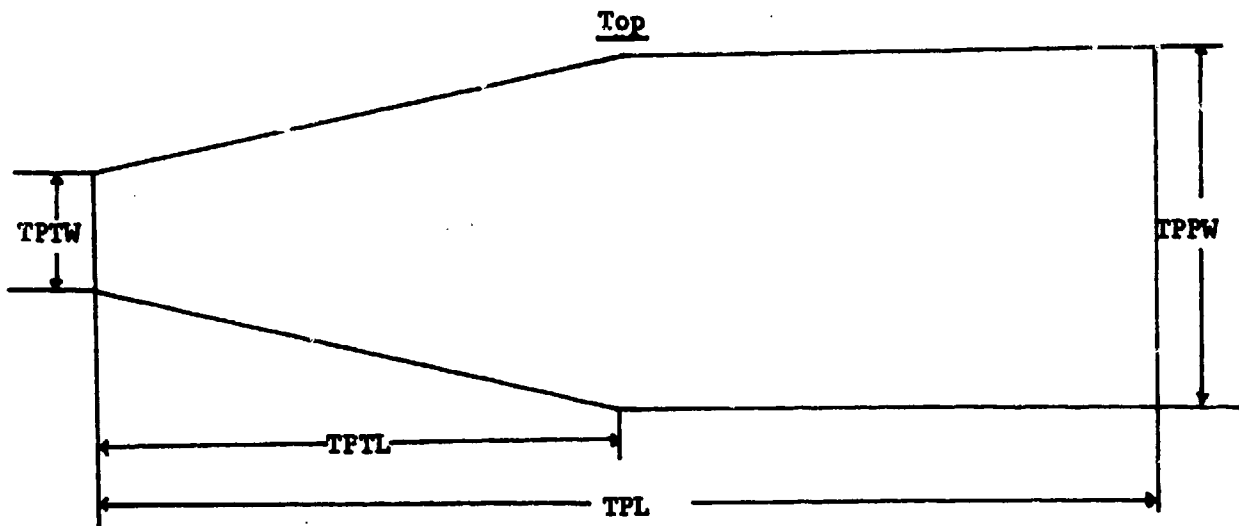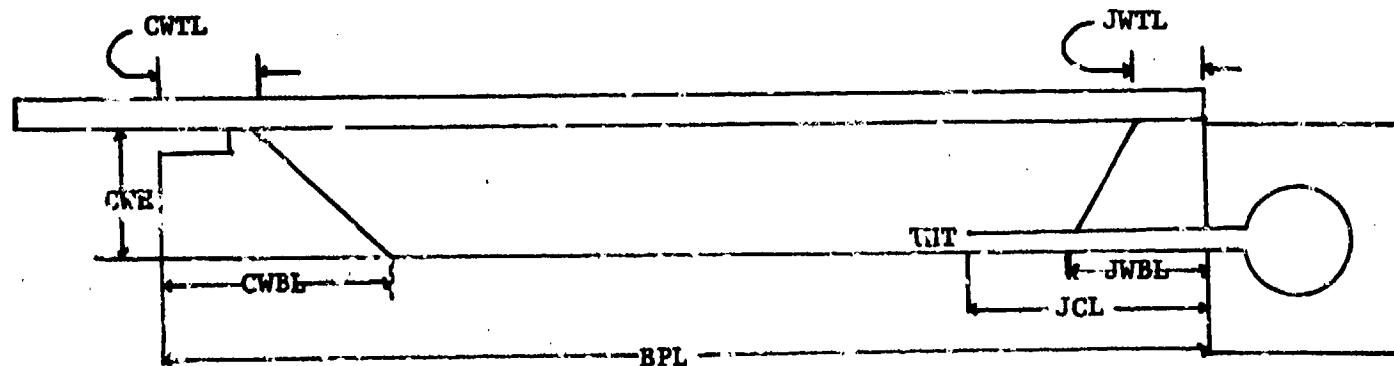
Figure A-1. Computer Inputs

Inputs

TPPW is the parallel width of the top plate. TPTW is the trapezoidal width of the top plate at the edge. TPT is the plate thickness. TPTL is the trapezoidal length of the top plate. TPL is the total length of the top plate. TTH is the height of the trough of the top plate. BPL is the length of the bottom plate. CWH is the height of the cutting wedge. CWTL is the length of the top of the cutting wedge. CWBL is the length of the bottom of the cutting wedge. JWTL is the length of the top of the jet wedge. JWBL is the length of the bottom of the jet wedge. JCL is the length of the jet catcher. THT is the throat thickness at the jet catcher. TTW is the width of the steel tamper. TTT is the thickness of the top steel tamper. TTL is the length of the steel tamper. EXPL is the weight of the explosive. CEMW is the weight of the cement brick tampers. VOLT is the capacitor bank voltage. LINEL is the line inductance. LOADL is the load inductance.

The load geometries are required for the path length calculations. They can be found using Figure A-2 as a guide. RLOAD is the radius of the load coil. For small loads RLOAD is zero. DLOAD is the depth of the load. WLOAD is the width of the load.

Two filenames are also inputs. They are the best case model results, FILNAM and the worst case model results, FNAME.

Outputs

Outputs for this program consist primarily of currents and fields. TAMW is the total tamper mass. NTOC is the metal mass to explosive ratio. NTOC is the tamper mass to explosive ratio. The

63
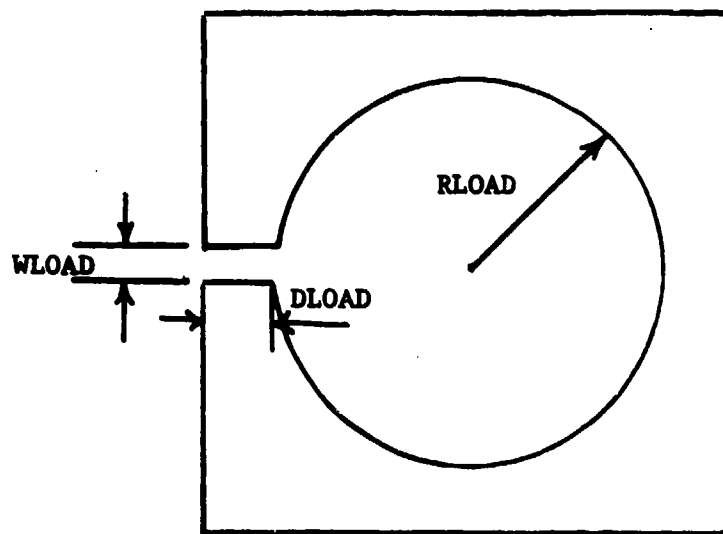
Figure A-2. Load Geometries

detonation velocity is D. The metal velocity is VA. The Gurney angle
is THETD. TIMEL(x) is the time varying Gurney inductance. TIMEI(x)
is the flux conserved current. MAGH(x) and MAGB(x) are the magnetic
field and the magnetic flux density respectively for the flux conserved
model. RES(x) is the time varying resistance. IRES(x) is the current
for the resistance model. MAGRH(x) and MAGRB(x) are the magnetic
field and magnetic flux density respectively for the resistance model.
ISLIP(x) is the current for the sliding contact loss model. HSLIP(x)
and BSLIP(x) are the magnetic field and the magnetic flux density
respectively for the sliding contact loss model. IEFF(x) is the
efficiency model current. HEFF(x) and BEFF(x) are the magnetic field

and magnetic flux density respectively for the efficiency model. IAA(x) is the changing area model current. BAA(x) and HAA(x) are the magnetic flux density and magnetic field respectively for the changing area model.

The program prints tabular output files of these variables. It additionally creates eight output files specifically for plotting the currents described in Chapter VI. A complete copy of the computer program can be found on the following pages.

```
*
*
*
* THIS PROGRAM CALCULATES AND PRINTS THE EXPECTED RESULTS OF A STRIP
* GENERATOR GIVEN THE BANK CAPACITANCE, LINE INDUCTANCE, LOAD INDUCTANCE,
* GENERATOR DIMENSIONS, EXPLOSIVE SIZE, AND TAMPER SIZE.  AT PRESENT,
* THIS PROGRAM ASSUMES THAT THE GENERATOR IS MADE OF COPPER AND THE
* EXPLOSIVE IS DETASHEET.  IF YOU WISH TO CHANGE TO ANOTHER MATERIAL OR
* EXPLOSIVE, PARAMETERS WHICH MUST BE CHANGED ARE INDICATED BY COMMENTS
* SURROUNDED BY A ROW OF *'S.  THIS PROGRAM UTILIZES THE GURNEY EQUA-
* TICNS AND SIMPLE GEOMETRY.  ALTHOUGH THE PROGRAM ALLOWS FOR A TRAPE-
* ZOIDAL GENERATOR, IT ASSUMES THAT THE STEEL TAMPER IS RECTANGULAR IN
* CROSS SECTION.  THIS PROGRAM CALCULATES BOTH A FLUX CONSERVED MODEL
* AND A TIME VARYING RESISTANCE/INDUCTANCE MODEL BASED ON THE MAGNETIC
* SKIN DEPTH.  THIS PROGRAM ALSO CALCULATES THREE EMPIRICAL MODELS, THE
* SLIPPING LOSS EMPIRICAL MODEL, THE FLUX TRAPPING EFFICIENCY MODEL, AND
* THE CHANGING AREA EMPIRICAL MODEL.
*
*
*

      PROGRAM STRIP
      INTEGER LIMIT,LIM1,LIM12,LIM2,THLIM,I,J,K,L,M,N,P,Q,R,S,T,U,V
      INTEGER II,JJ,KK,LL,MM,IJ,IK,CK1,CK2
      REAL TPW,TPT,TPL,TTH,BPL,CWH,CWTL,CWBL,JWTL,JWBL,JCL,TTW,TTT,TTL
      REAL THT,CEMW,EXPL,VOLT,CAP,LINEL,LOADL,VOL1,VOL2,PVOL,METW,TAMMW
      REAL TAMW,MTOC,NTOC,ANUM,ADEN,A,VM1,VM2,VM,VNUM,VDEN,THETA,ARG1,D
      REAL XR,X1,XE,XF1,INTL,THROL,XSTOP,TSTOP,TPTL,TPTW,REST1,CWBM,AA
      REAL ATOT,ARG2,APRIM,THETD,ALPHD,PHID,PHI,ZETA,ZETD,ZETPD,ZETAP,X
      REAL LALPH,ALPHA,Y1,ASUB1,AGEN,XD,GAMAD,GAMA,ASUB2,ASUB3,LGAMA,VA
      REAL XDELT,H3,CENT1,CENT2,CENT,TVL,CNUM,CDEN,IO,TOTL,IT,TPPW,BASE
      REAL SBASE,SHT,TRAPA,IMHT,ZREF,CALH,CALW,XLIM2,XLIM3,B1,B2,H1,H2
      REAL INTL1,INTL2,INTL3,INTL4,ANGLE,A1,LHT,VOL4,L1,L2,XLIM4,SLA1
      REAL SLA2,SLA3,SLA4,SLA5,SLA6,XLIM5,XLIM1,TPPLM,LA3,RLOAD,DLOAD
      REAL WLOAD,DIF,LPHI,LZET,TLOAD,PMAG,ASUB4,ASUB5,MU,REST,LITK,BB
      REAL REST2,SLIPD,POWER,CONS,ROE0,CC,DD,EE,FF,GG,DEC1,DEC2,DEC3
      REAL DEC4,DEC5,DEC6,DEC7,D1,D2,D3,D4,LEX
      REAL AREA(500),MISEC(500),TIMEL(500),TIMEI(500),W(500),LA4(500)
      REAL LA5(500),LA6(500),LA4D(500),LA5D(500),LA6D(500),POS(500)
      REAL LA7(500),LA7D(500),AREA1(500),AREA2(500),AREA3(500),TAU(500)
      REAL ARE1D(500),ARE2D(500),ARE3D(500),TVL1(500),TVL2(500),KO(500)
      REAL AREA4(500),AREA5(500),ARE4D(500),ARE5D(300),TVL4(500)
      REAL TVL3(500),TLEN(500),RLEN(500),LLEN(500),BLEN(500),SIGMA(500)
      REAL PATH(500),MAGB(500),MAGH(500),TVL5(500),RES(500),TEMP(500)
      REAL RAV(500),LAV(500),EARG1(500),EARG2(500),IRES(500),MAGRH(500)
      REAL MAGRB(500),EARG3(500),LA8(500),LA8D(500),EXPO(500),ROE(500)
      REAL SMS(500),EFF(500),AAA(500),ISLIP(500),IEFF(500),IAA(500)
      REAL HSLIP(500),BSLIP(500),HEFF(500),BEFF(500),HAA(500),BAA(500)
      REAL SPHI(500)
      CHARACTER*40 FNAME
      CHARACTER*40 FILNAM
      CHARACTER*40 PLOT1
      CHARACTER*40 PLOT2
      CHARACTER*40 PLOT3
      CHARACTER*40 PLOT4
```

```
      CHARACTER*40 PLOTS
*
* THIS PORTION OF THE PROGRAM HAS THE USER ENTER THE NEEDED PARAMETERS.
*
      PRINT*,'PLEASE ENTER THE WIDTH OF THE PARALLEL PORTION OF THE'
      PRINT*,'TOP PLATE IN CENTIMETERS.>'
      READ*,TPPW
      PRINT*,'PLEASE ENTER THE WIDTH OF THE TOP PLATE AT THE'
      PRINT*,'TRAPEZOIDAL END IN CENTIMETERS.>'
      READ*,TPTW
      PRINT*,'PLEASE ENTER THE THICKNESS OF THE TOP PLATE'
      PRINT*,' IN CENTIMETERS.>'
      READ*,TPT
      PRINT*,'PLEASE ENTER THE LENGTH OF THE TRAPEZOIDAL PORTION OF THE'
      PRINT*,'TOP PLATE IN CENTIMETERS.>'
      READ*,TPTL
      PRINT*,'PLEASE ENTER THE TOTAL LENGTH OF THE TOP PLATE'
      PRINT*,' IN CENTIMETERS.>'
      READ*,TPL
      PRINT*,'PLEASE ENTER THE HEIGHT OF THE TROUGH IN CENTIMETERS.>'
      READ*,TTH
      PRINT*,'PLEASE ENTER THE LENGTH OF THE BOTTOM PLATE'
      PRINT*,' IN CENTIMETERS.>'
      READ*,BPL
      PRINT*,'PLEASE ENTER THE HEIGHT OF THE CUTTING WEDGE'
      PRINT*,' IN CENTIMETERS.>'
      READ*,CWH
      PRINT*,'PLEASE ENTER THE LENGTH OF THE TOP BASE OF THE CUTTING'
      PRINT*,'WEDGE IN CENTIMETERS.>'
      READ*,CWTL
      PRINT*,'PLEASE ENTER THE LENGTH OF THE BOTTOM BASE OF THE CUTTING'
      PRINT*,'WEDGE IN CENTIMETERS.>'
      READ*,CWBL
      PRINT*,'PLEASE ENTER THE LENGTH OF THE TOP BASE OF THE JET WEDGE'
      PRINT*,' IN CENTIMETERS.>'
      READ*,JWTL
      PRINT*,'PLEASE ENTER THE LENGTH OF THE BOTTOM BASE OF THE JET'
      PRINT*,'WEDGE IN CENTIMETERS.>'
      READ*,JWBL
      PRINT*,'PLEASE ENTER THE LENGTH OF THE JET CATCHER'
      PRINT*,' IN CENTIMETERS.>'
      READ*,JCL
      PRINT*,'PLEASE ENTER THE THROAT THICKNESS AT THE JET CATCHER IN'
      PRINT*,'CENTIMETERS.>'
      READ*,THT
      PRINT*,'PLEASE ENTER THE WIDTH OF THE TOP STEEL TAMPER'
      PRINT*,' IN CENTIMETERS.>'
      READ*,TTW
      PRINT*,'PLEASE ENTER THE THICKNESS OF THE TOP STEEL TAMPER IN'
      PRINT*,'CENTIMETERS.>'
      READ*,TTT
      PRINT*,'PLEASE ENTER THE LENGTH OF THE TOP STEEL TAMPER'
      PRINT*,' IN CENTIMETERS.>'
      READ*,TTL
```

```
            PRINT*,'PLEASE ENTER THE WEIGHT OF THE EXPLOSIVE IN POUNDS.>'
            READ*,EXPL
            PRINT*,'PLEASE ENTER THE WEIGHT OF THE TOP CEMENT BRICKS IN'
            PRINT*,'POUNDS.>'
            READ*,CEMW
            PRINT*,'PLEASE ENTER THE BANK VOLTAGE IN VOLTS.>'
            READ*,VOLT
            PRINT*,'PLEASE ENTER THE BANK CAPACITANCE IN MICROFARADS.>'
            READ*,CAP
            CAP=CAP*1E-06
            PRINT*,'PLEASE ENTER THE LINE INDUCTANCE IN NANOHENRIES.>'
            READ*,LINEL
            PRINT*,'PLEASE ENTER THE LOAD INDUCTANCE IN NANOHENRIES.>'
            READ*,LOADL
            PRINT*,'PLEASE ENTER THE RADIUS OF THE LOAD IN CENTIMETERS.>'
            READ*,RLOAD
            PRINT*,'PLEASE ENTER THE DEPTH OF THE LOAD IN CENTIMETERS.>'
            READ*,DLOAD
            PRINT*,'PLEASE ENTER THE WIDTH OF THE LOAD IN CENTIMETERS.>'
            READ*,WLOAD
            LINEL=LINEL*1E-09
            LOADL=LOADL*1E-09
            PRINT*,'PLEASE ENTER THE BEST RESULTS FILENAME.>'
            READ (5,500) FILNAM
500         FORMAT (A40)
            PRINT*,'PLEASE ENTER THE WORST RESULTS FILENAME.>'
            READ (5,500) FNAME
*
* THIS PORTION OF THE PROGRAM CALCULATES THE MASS AND TAMPER RATIOS AND
* USES THE GURNEY EQUATIONS TO DETERMINE A METAL VELOCITY.
*
            VOL1=TPPW*(TPL-TPTL)*TPT
            BASE=TPPW/2.0
            SBASE=TPTW/2.0
            SHT=BASE-SBASE
            IF (SHT.EQ.0.0) THEN
                VOL2=0.0
            ELSE
                TRAPA=ATAN(SHT/TPTL)
                IMHT=BASE/TAN(TRAPA)
                LHT=TPTL-IMHT
                A1=IMHT*BASE
                A2=LHT*SBASE
                VOL2=TPT*(A1-A2)
            END IF
            L1=SQRT((IMHT*IMHT)+(BASE*BASE))-SQRT((LHT*LHT)+(SBASE*SBASE))
            L2=TPL-TPTL
            VOL3=2.0*TTH*(L1+L2)*TPT
            PVOL=VOL1+VOL2+VOL3
            METW=(8.96*PVOL)/1000.0
            CEMW=CEMW/2.20462
            VOL4=TTW*TTT*TTL
            TAMMW=(7.86*VOL4)/1000.0
            TAMW=TAMMW+CEMW
```

68

```
          EXPL=EXPL/2.20462
          MTOC=METW/EXPL
          NTOC=TAMW/EXPL
          ANUM=1.0+(2.0*MTOC)
          ADEN=1.0+(2.0*NTOC)
          A=ANUM/ADEN
          VM1=(1.0+(A*A*A))/(3.0*(1.0+A))
          VM2=NTOC*A*A
          VM3=MTOC
*****************************************************************************
* VNUM WILL HAVE TO BE CHANGED IF THE EXPLOSIVE IS NOT DETASHEET.
*****************************************************************************
          VNUM=2.27
          VDEN=SQRT(VM1+VM2+VM3)
          VM=VNUM/VDEN
*
* THIS PORTION OF THE PROGRAM CALCULATES THETA AND V USING KENNEDY'S
* METHOD AND THE GURNEY EQUATIONS.
*
*****************************************************************************
* D WILL HAVE TO BE CHANGED IF THE EXPLOSIVE IS NOT DETASHEET.
*****************************************************************************
          D=6.0
          ARG1=VM/(2.0*D)
          THETA=2.0*(ASIN(ARG1))
          VA=D*TAN(THETA)
*
* THIS PORTION OF THE PROGRAM CALCULATES THE CHANGING WIDTH OF THE
* GENERATOR.
*
          XE=BPL-CWTL-JCL
          XE=XE*1E01
          XSTOP=XE+((CWH*1E01)/TAN(THETA))
          TSTOP=XSTOP/D
          LIMIT=TSTOP+1
          LIM2=2*LIMIT
          TIME=0.5
          DO 5 I=1,LIMIT,1
             X=D*TIME
             POS(I)=X
             XLIM1=TPTL*1E01
             IF (X.LE.XLIM1) THEN
                BASE=TPPW/2.0
                SBASE=TPTW/2.0
                SHT=BASE-SBASE
                TRAPA=ATAN(SHT/TPTL)
                IMHT=BASE/TAN(TRAPA)
                LHT=(TPTL-IMHT)*1E01
                CALW=(LHT+X)*TAN(TRAPA)
                W(I)=CALW*1E-03*2.0
             ELSE
                W(I)=TPPW*1E-02
             END IF
             TIME=TIME+1.0
```

69

```
5     CONTINUE
*
* THIS PORTION OF THE PROGRAM CALCULATES THE INITIAL INDUCTANCE AND THE
* THROAT INDUCTANCE.
*
      XR=CWBL-CWTL
      TPTLM=TPTL*1E01
      CWBM=CWBL*1E01
      ALPHA=ATAN(XR/CWH)
      XLIM2=(TPL-JCL)*1E01
      XLIM3=(TPL-JWBL)*1E01
      XLIM4=(TPL-JWTL)*1E01
      DO 10 J=1,LIMIT,1
         IF (TPTL.EQ.0.0) THEN
            SLA1=0.5*XR*CWH*1E-04
            X1=BPL-CWBL-JCL
            SLA2=CWH*X1*1E-04
            SLA3=CWH*(JCL-JWBL)*1E-04
            XF1=JWBL-JWTL
            SLA4=0.5*XF1*(CWH-TPT)*1E-04
            SLA5=SLA1+SLA2+SLA3+SLA4
            SLA6=JCL*THT*1E-04
         ELSE
            XR=XR*1E01
            IF (X.LE.XR) THEN
               LA4(K)=0.5*X*(X/TAN(ALPHA))*1E-06
               LA5(K)=0.0
               LA6(K)=0.0
               LA7(K)=0.0
            ELSE IF (X.LE.XLIM2) THEN
               LA4(K)=0.5*XR*(XR/TAN(ALPHA))*1E-06
               LA5(K)=(X-XR)*CWHM*1E-06
               LA6(K)=0.0
               LA7(K)=0.0
            ELSE IF (X.LE.XLIM3) THEN
               LA4(K)=0.5*XR*(XR/TAN(ALPHA))*1E-06
               LA5(K)=(XLIM2-XR)*CWHM*1E-06
               LA6(K)=(X-XLIM2)*((CWH-THT-TPT)*1E01)*1E-06
               LA7(K)=0.0
            ELSE
               ANGLE=ATAN((JWBL-JWTL)/CWH)
               H1=(X-XLIM3)*1E-01
               B1=CWH-THT-TPT
               H2=JWBL-JWTL-H1
               B2=H2/(TAN(ANGLE))
               LA4(K)=0.5*XR*(XR/TAN(ALPHA))*1E-06
               LA5(K)=(XLIM2-XR)*CWHM*1E-06
               LA6(K)=(XLIM3-XLIM2)*((CWH-THT-TPT)*1E01)*1E-05
               LA7(K)=0.5*(B1+B2)*H1*1E-04
            END IF
            XR=XR*1E-01
         END IF
         TIME=TIME+1.0
10    CONTINUE
```

70

```
          DO 15 K=2,LIMIT,1
              L=M-1
              LA4D(1)=LA4(1)
              LA5D(1)=LA5(1)
              LA6D(1)=LA6(1)
              LA7D(1)=LA7(1)
              LA4D(K)=LA4(K)-LA4(L)
              LA5D(K)=LA5(K)-LA5(L)
              LA6D(K)=LA6(K)-LA6(L)
              LA7D(K)=LA7(K)-LA7(L)
15        CONTINUE
          DO 20 M=1,LIMIT,1
              INTL1=((1.2566371*LA4D(M))/W(M))+INTL1
              INTL2=((1.2566371*LA5D(M))/W(M))+INTL2
              INTL3=((1.2566371*LA6D(M))/W(M))+INTL3
              INTL4=((1.2566371*LA7D(M))/W(M))+INTL4
20        CONTINUE
          IF (TPTL.EQ.0.0) THEN
              INTL=(1.2566371*SLA5)/(TPPW*1E-02)
              INTL=INTL*1E-06
          ELSE
              INTL=INTL1+INTL2+INTL3+INTL4
              INTL=INTL*1E-06
          END IF
          THLIM=((TPL-JCL)*1E01)/D
          TIME=0.0
          DO 25 N=1,LIMIT,1
              XLIMS=THLIM*D
              X=D*TIME
              IF (X.LE.XLIMS) THEN
                  LA8(N)=0.0
              ELSE
                  LA8(N)=(((BPL-JWBL)*1E01)-X)*(THT*1E01)*1E-06
              END IF
              TIME=TIME+1.0
25        CONTINUE
          DO 30 P=2,LIMIT,1
              Q=P-1
              LA8D(1)=LA8(1)
              LA8D(P)=LA8(P)-LA8(Q)
30        CONTINUE
          IF (TPTL.EQ.0.0) THEN
              THROL=(1.2566371*SLA6)/(TPPW*1E-02)
          ELSE
              DO 35 R=1,LIMIT,1
                  THROL=(1.2566371*LA8D(R))/W(R)+THROL
35        CONTINUE
          END IF
          THROL=THROL*1E-06
*
* THIS PORTION OF THE PROGRAM CALCULATES HOW THE INDUCTANCE CHANGES
* WITH TIME.  IT ASSUMES A CONSTANT DETONATION VELOCITY.  IT FURTHER
* ASSUMES THAT THE METAL LINER IS TOTALLY ELASTIC AND THAT THE LOAD AND
* THROAT INDUCTANCES DO NOT VARY WITH TIME.
```

71

```fortran
      XE=BPL-CWTL-JCL
      XE=XE*1E01
      XSTOP=XE+(((CWH-THT-TPT)*1E01)/TAN(THETA))
      TSTOP=XSTOP/D
      ARG2=CWH/(CWBL-CWTL)
      ALPHA=ATAN(ARG2)
      THETD=THETA*(180.0/3.1415927)
      ALPHD=ALPHA*(180.0/3.1415927)
      PHID=180.0-THETD-ALPHD
      PHI=PHID*(3.1415928/180.0)
      ZETA=ATAN(XF1/CWH)
      ZETD=ZETA*(180.0/3.1415927)
      ZETPD=90.0+ZETD
      ZETAP=ZETPD*(3.1415927/180.0)
      ALPHA=ALPHD*(3.1415927/180.0)
      XR=CWBL-CWTL
      XR=XR*1E01
      X1=BPL-CWBL-JCL
      XF1=JWBL-JWTL
      XO=CWH/TAN(THETA)
      XO=XO*1E01
      LIMIT=TSTOP+1
      TIME=0.0
      DO 40 S=1,LIMIT,1
         X=D*TIME
         XLIM=XR+XO
         XF=(BPL-CWTL-JWTL)*1E01
         IF (TPTL.EQ.0.0) THEN
               IF (X.LE.XLIM) THEN
               LALPH=SIN(THETA)*(X/(SIN(PHI)))
               Y1=LALPH*SIN(ALPHA)
               ASUB1=0.5*X*Y1
               AGEN=(SLA5*1E06)-ASUB1
               AREA(S)=AGEN*1E-06
               MISEC(S)=TIME
            ELSE IF (X.LE.XF) THEN
               ASUB1=0.5*XLIM*CWH*1E01
               ASUB2=(X-XLIM)*CWH*1E01
               AGEN=(SLA5*1E06)-ASUB1-ASUB2
               AREA(S)=AGEN*1E-06
               MISEC(S)=TIME
            ELSE
               ASUB1=0.5*XLIM*CWH*1E01
               ASUB2=(X-XLIM)*CWH*1E01
               GAMAD=180.0-ZETPD-THETD
               GAMA=GAMAD*(3.1415927/180.0)
               XDELT=X-XF
               LGAMA=SIN(THETA)*(XDELT/SIN(GAMA))
               H3=LGAMA*SIN(GAMA)
               CENT1=SQRT((LGAMA*LGAMA)-(H3*H3))
               CENT2=SQRT((XDELT*XDELT)-(H3*H3))
               CENT=CENT1+CENT2
               ASUB3=0.5*CENT*H3
```

```fortran
                    ASUB4=((THT*TPT)*(JCL-JWBL)*1E02)
                    ASUB5=.5*(TPT*TPT*1E02)/TAN(THETA)
                    AGEN=(SLA5*1E05)-ASUB1-ASUB2+ASUB3-ASUB4+ASUB5
                    AREA(S)=AGEN*1E-06
                    MISEC(S)=TIME
                 END IF
                 TIME=TIME+1.0
              ELSE
                 IF (X.LE.XLIM) THEN
                    LALPH=SIN(THETA)*(X/(SIN(PHI)))
                    Y1=LALPH*SIN(ALPHA)
                    ASUB1=0.5*X*Y1
                    AREA1(S)=ASUB1*1E-06
                    AREA2(S)=0.0
                    AREA3(S)=0.0
                    AREA4(S)=0.0
                    AREA5(S)=0.0
                    MISEC(S)=TIME
                 ELSE IF (X.LE.XF) THEN
                    AREA1(S)=0.5*XLIM*CWH*1E01*1E-06
                    AREA2(S)=(X-XLIM)*CWH*1E01*1E-06
                    AREA3(S)=0.0
                    AREA4(S)=0.0
                    AREA5(S)=0.0
                    MISEC(S)=TIME
                 ELSE
                    AREA1(S)=0.5*XLIM*CWH*1E01*1E-06
                    AREA2(S)=(X-XLIM)*CWH*1E01*1E-06
                    GAMAD=180.0-ZETPD-THETD
                    GAMA=GAMAD*(3.1415927/180.0)
                    XDELT=X-XF
                    LGAMA=SIN(THETA)*(XDELT/SIN(GAMA))
                    H3=LGAMA*SIN(GAMA)
                    CENT1=SQRT((LGAMA*LGAMA)-(H3*H3))
                    CENT2=SQRT((XDELT*XDELT)-(H3*H3))
                    CENT=CENT1+CENT2
                    AREA3(S)=0.5*CENT*H3*1E-06
                    AREA4(S)=((THT*TPT)*(JCL-JWBL))*1E-04
                    AREA5(S)=(0.5*(TPT*TPT)/TAN(THETA))*1E-04
                    MISEC(S)=TIME
                 END IF
                 TIME=TIME+1.0
              END IF
40         CONTINUE
           IF (TPTL.EQ.0.0) THEN
              DO 45 T=1,LIMIT,1
              TVL=((1.2566371*AREA(T))/(TPPW*1E-02))*1E-06
              TIMEL(T)=TVL
45         CONTINUE
           ELSE
              DO 50 U=2,LIMIT,1
              V=U-1
              ARE1D(1)=AREA1(1)
              ARE2D(1)=AREA2(1)
```

73

```
                          ARE3D(1)=AREA3(1)
                          ARE4D(1)=AREA4(1)
                          ARE5D(1)=AREA5(1)
                          ARE1D(U)=AREA1(U)-AREA1(V)
                          ARE2D(U)=AREA2(U)-AREA2(V)
                          ARE3D(U)=AREA3(U)-AREA3(V)
                          ARE4D(U)=AREA4(U)-AREA4(V)
                          ARE5D(U)=AREA5(U)-AREA5(V)
50          CONTINUE
            DO 55 I=2,LIMIT,1
                J=I-1
                TVL1(1)=((1.2566371*ARE1D(1))/W(1))*1E-06
                TVL2(1)=((1.2566371*ARE2D(1))/W(1))*1E-06
                TVL3(1)=((1.2566371*ARE3D(1))/W(1))*1E-06
                TVL4(1)=((1.2566371*ARE4D(1))/W(1))*1E-06
                TVL5(1)=((1.2566371*ARE5D(1))/W(1))*1E-06
                TVL1(I)=(((1.2566371*ARE1D(I))/W(I))*1E-06)+TVL1(J)
                TVL2(I)=(((1.2566371*ARE2D(I))/W(I))*1E-06)+TVL2(J)
                TVL3(I)=(((1.2566371*ARE3D(I))/W(I))*1E-06)+TVL3(J)
                TVL4(I)=(((1.2566371*ARE4D(I))/W(I))*1E-06)+TVL4(J)
                TVL5(I)=(((1.2566371*ARE5D(I))/W(I))*1E-06)+TVL5(J)
55          CONTINUE
            DO 60 K=1,LIMIT,1
                TVL=INTL-TVL1(K)-TVL2(K)+TVL3(K)+TVL4(K)-TVL5(K)
                TIMEL(K)=TVL
60          CONTINUE
        END IF
*
* THIS PORTION OF THE PROGRAM CALCULATES AND PRINTS THE CHANGING CURRENT.
*
        DO 65 L=1,LIMIT,1
            CNUM=INTL+THROL+LOADL
            CDEN=THROL+LOADL+TIMEL(L)
            TOTL=CNUM+LINEL
            IO=VOLT*(SQRT(CAP/TOTL))
            IT=(CNUM/CDEN)*IO*1E-03
            TIMEI(L)=IT
            TIMEL(L)=TIMEL(L)*1E09
65      CONTINUE
*
* THIS PORTION OF THE PROGRAM CALCULATES THE CHANGING PATH LENGTH OF
* THE SYSTEM.
*
        IF (RLOAD.EQ.0.0) THEN
            TLOAD=(2.0*3.1415927*RLOAD)+((2.0*DLOAD)+WLOAD)
        ELSE
            TLOAD=(2.0*3.1415927*RLOAD)-WLOAD+(2.0*DLOAD)
        END IF
        TIME=0.0
        DO 70 L=1,LIMIT,1
            X=D*TIME
            IF (X.LE.XLIM) THEN
                TLEN(L)=TPL-JWTL-CWTL-(X*1E-01)
                LALPH=SIN(THETA)*(X/(SIN(PHI)))*1E-01
```

74

```
                          DIF=CWBL-CWTL
                          LPHI=SIN(ALPHA)*(X/(SIN(PHI)))*1E-01
                          LLEN(L)=(SQRT((CWH*CWH)+(DIF*DIF)))-LALPH+LPHI
                          BLEN(L)=TPL-CWBL+TLOAD
                          RLEN(L)=SQRT(((JWBL-JWTL)*(JWBL-JWTL))+(CWH*CWH))+JCL
                     ELSE IF (X.LE.XF) THEN
                          TLEN(L)=TPL-JWTL-CWTL-(X*1E-01)
                          LLEN(L)=CWH/SIN(THETA)
                          BLEN(L)=TPL-CWTL+(CWH/TAN(THETA))+TLOAD-(X*1E-01)
                          RLEN(L)=SQRT(((JWBL-JWTL)*(JWBL-JWTL))+(CWH*CWH))+JCL
                     ELSE
                          TLEN(L)=0.0
                          XDELT=(X-XF)*1E-01
                          GAMAD=180.0-ZETPD-THETD
                          GAMA=GAMAD*(3.1415927/180.0)
                          LZET=SIN(ZETAP)*(XDELT/(SIN(GAMA)))
                          LLEN(L)=(CWH/SIN(THETA))-LZET
                          BLEN(L)=TPL-CWTL+(CWH/TAN(THETA))+TLOAD-(X*1E-01)
                          LGAMA=SIN(THETA)*(XDELT/SIN(GAMA))
                          RLEN(L)=(CWH/COS(ZETA))-LGAMA+JCL
                     END IF
                     TIME=TIME+1.0
  70         CONTINUE
             DO 75 M=1,LIMIT,1
                  PATH(M)=(TLEN(M)+LLEN(M)+RLEN(M)+BLEN(M))*1E-02
  75         CONTINUE
 *
 * THIS PORTION OF THE PROGRAM CALCULATES THE CHANGING MAGNETIC FIELDS.
 *
             IF (TPTL.EQ.0.0) THEN
                  DO 80 N=1,LIMIT,1
                       MAGH(N)=(TIMEI(N)*1E03)/(TPPW*1E-02)
                       MAGB(N)=MAGH(N)*(4.0*3.1415927*1E-09)
  80              CONTINUE
             ELSE
                  DO 85 P=1,LIMIT,1
                       MAGH(P)=(TIMEI(P)*1E03)/W(P)
                       MAGB(P)=MAGH(P)*(4.0*3.1415927*1E-09)
  85              CONTINUE
             END IF
 *
 * THIS PORTION OF THE PROGRAM USES THE STRENGTH OF THE IDEAL MAGNETIC
 * FIELD TO CALCULATE A CHANGING RESISTANCE BASED ON THE MAGNETIC SKIN
 * DEPTH.  IT FURTHER CALCULATES A RESISTANCE DUE TO THE RESISTANCE OF THE
 * COPPER PLATES.  IT THEN CALCULATES THE CHANGING CURRENT AND MAGNETIC
 * FIELDS GENERATED FROM THIS TIME VARYING RESISTANCE.
 *
 *************************************************************************
 * MU MAY HAVE TO BE CHANGED IF THE METAL IS NOT COPPER.  ROE0 WILL HAVE
 * TO BE CHANGED IF THE METAL IS NOT COPPER.  LITK MAY HAVE TO BE CHANGED
 * IF THE METAL IS NOT COPPER.  CONS WILL HAVE TO BE CHANGED IF THE METAL
 * IS NOT COPPER.
 *************************************************************************
             MU=4.0*3.1415927*1E-07
```

```fortran
          LITK=1E-03
          ROE0=1.72*1E-08
          CONS=1170.0
          DO 90 Q=1,LIMIT,1
              TEMP(Q)=CONS*(MAGB(Q)*MAGB(Q))
              ROE(Q)=ROE0*(1.0+(LITK*TEMP(Q)))
              SIGMA(Q)=1.0/ROE(Q)
              KO(Q)=1.0/(SIGMA(Q)*MU)
90        CONTINUE
          THICK=TPT*1E-02
          DO 95 R=2,LIMIT,1
              S=R-1
              TAU(R)=MAGH(R)/((MAGH(R)-MAGH(S)))/((MISEC(R)-MISEC(S))*1E-06)
              SPHI(R)=2.0*SQRT((KO(R)*R*1E-06))
95        CONTINUE
          DO 100 T=2,LIMIT,1
              IF (TPTL.EQ.0.0) THEN
                  REST1=TAU(T)/(SIGMA(T)*MU)
                  REST2=SQRT(REST1)
                  REST=SIGMA(T)*REST2
                  IF (SPHI(T).LE.THICK) THEN
                   RES(T)=(1.0/REST)+((ROE(T)*PATH(T))/((TPPW*SPHI(T)*1E-02)))
                  ELSE
                      RES(T)=(1.0/REST)+((ROE(T)*PATH(T))/(TPPW*THICK*1E-02))
                  END IF
              ELSE
                  REST1=TAU(T)/(SIGMA(T)*MU)
                  REST2=SQRT(REST1)
                  REST=SIGMA(T)*REST2
                  IF(SPHI(T).LE.THICK) THEN
                      RES(T)=(1.0/REST)+((ROE(T)*PATH(T))/(W(T)*SPHI(T)))
                  ELSE
                      RES(T)=(1.0/REST)+((ROE(T)*PATH(T))/(W(T)*THICK))
                  END IF
              END IF
100       CONTINUE
          RES(1)=RES(2)
          DO 105 U=2,LIMIT,1
              V=U-1
              RAV(U)=(RES(U)+RES(V))/2.0
              LAV(U)=((TIMEL(U)+TIMEL(V))/2.0)*1E-09+THROL+LOADL
              EARG1(U)=(RAV(U)/LAV(U))*-1.0*1E-06
              EARG2(U)=IO*((TIMEL(1)*1E-09)+THROL+LOADL)/((TIMEL(U)*1E-09)+
      +THROL+LOADL)
105       CONTINUE
          EARG1(1)=(RES(1)/((TIMEL(1)*1E-09)+THROL+LOADL))*-1.0*1E-06
          EARG2(1)=IO
          DO 110 I=2,LIMIT,1
              J=I-1
              EARG3(1)=0.0
              EARG3(I)=EARG1(I)+EARG3(J)
110       CONTINUE
          DO 115 K=1,LIMIT,1
              EXPO(K)=EXP(EARG3(K))
```

```
115    CONTINUE
       DO 120 L=1,LIMIT,1
           IRES(L)=EARG2(L)*EXPO(L)*1E-03
120    CONTINUE
       IF (TPTL.EQ.0.0) THEN
           DO 125 N=1,LIMIT,1
               MAGRH(N)=(IRES(N)/(TPPW*1E-02))*1E03
               MAGRB(N)=MAGRH(N)*(4.0*3.1415927*1E-09)
125        CONTINUE
       ELSE
           DO 130 P=1,LIMIT,1
               MAGRH(P)=(IRES(P)/W(P))*1E03
               MAGRB(P)=MAGRH(P)*(4.0*3.1415927*1E-09)
130        CONTINUE
       END IF
*
* THIS PORTION OF THE PROGRAM USES THE EMPIRICALLY DEVELOPED MODELS
* TO DESCRIBE THE CURRENT AND MAGNETIC FIELDS WHICH ACCOUNT FOR THE
* THE FLUX LOSSES DUE TO A SLIDING CONTACT, THE LOSSES DUE TO A CHANGING
* AREA, AND THE LOSSES DUE TO A FLUX TRAPPING EFFICIENCY.
*
       OPEN (UNIT=1,NAME=PLOT4,TYPE='NEW')
       WRITE (1,700)
700    FORMAT (' PLOTS OF RESISTANCE MODEL CURRENTS ')
       WRITE (1,*) LIMIT  .
       DO 800 I=1,LIMIT,1
           J=I-1
           WRITE (1,*) J
800    CONTINUE
       DO 805 K=1,LIMIT,1
           A=IRES(K)*1E-03
           WRITE (1,*) A
805    CONTINUE
       CLOSE (UNIT=1)
       OPEN (UNIT=1,NAME=PLOT5,TYPE='NEW')
       WRITE (1,705)
705    FORMAT (' PLOTS OF IDEAL MODEL CURRENTS ')
       WRITE (1,*) LIMIT
       DO 810 L=1,LIMIT,1
           M=L-1
           WRITE (1,*) M
810    CONTINUE
       DO 815 N=1,LIMIT,1
           A=TIMEI(N)*1E-03
           WRITE (1,*) A
815    CONTINUE
*
* THIS PORTION OF THE PROGRAM SETS THE VALUES FOR THE BEST CASES FOR
* THE EMPIRICAL MODELS.  THIS PORTION OF THE PROGRAM INITIALIZES THE
* SMALL S VALUES FOR THE BEST CASE FOR THE SLIPPING CONTACT LOSS MODEL.
*
       II=LIMIT-18
       JJ=LIMIT-81
       AA=0.3102
```

```
          BB=0.2015
          DEC1=BB/(II-JJ)
          DEC2=(AA-BB)/(LIMIT-II)
*
* THIS PORTION OF THE PROGRAM INITIALIZES THE VALUES FOR THE BEST CASE
* EFFICIENCY MODEL.
*
          CK1=1
          KK=LIMIT-10
          LL=LIMIT-101
          CC=63.839
          DD=79.056
          DEC3=(DD-CC)/(LIMIT-KK)
          DEC4=(100.0-DD)/(KK-LL)
*
* THIS PORTION OF THE PROGRAM INITIALIZES THE VALUES FOR THE BEST CASE
* CHANGING AREA EFFICIENCY MODEL.
*
          CK2=1
          MM=LIMIT-5
          IJ=LIMIT-44
          IK=LIMIT-81
          EE=0.0009924
          FF=0.0006931
          GG=0.0005749
          DEC5=(EE-FF)/(LIMIT-MM)
          DEC6=(FF-GG)/(MM-IJ)
          DEC7=GG/(IJ-IK)
*
* THE FIRST ITERATION PRODUCES THE BEST CASE PLOTS FOR THE EMPIRICAL
* MODELS.  THE SECOND ITERATION PRODUCES THE WORST CASE PLOTS FOR THE
* EMPIRICAL MODELS.
*
          OPEN (UNIT=1,NAME=FILNAM,TYPE='NEW')
          WRITE (1,710)
710       FORMAT (' THE FOLLOWING RESULTS AND PLOTS ARE FOR THE BEST CASE ')
          IO=IO*1E-03
          DO 900 I=1,2,1
*
* THIS PORTION OF THE PROGRAM CALCULATES THE SMALL S VALUES.
*
              DO 905 J=1,JJ,1
                  SMS(J)=0.0
905           CONTINUE
              JJ=JJ+1
              D1=DEC1
              DO 910 K=JJ,II,1
                  SMS(K)=D1
                  D1=D1+DEC1
910           CONTINUE
              D2=SMS(II)+DEC2
              II=II+1
              DO 915 L=II,LIMIT,1
                  SMS(L)=D2
```

78

```
                    D2=D2+DEC2
915         CONTINUE
*
* THIS PORTION OF THE PROGRAM CALCULATES THE EFFICIENCY VALUES.
*
            DO 920 M=1,LL,1
                EFF(M)=100.0
920         CONTINUE
            D3=DEC4
            LL=LL+1
            DO 925 N=LL,KK,1
                EFF(N)=100.0-D3
                D3=D3+DEC4
925         CONTINUE
            IF (CK1.EQ.1) THEN
                D4=100.0-EFF(KK)-DEC3
                KK=KK+1
                DO 930 P=KK,LIMIT,1
                    EFF(P)=100.0-D4
                    D4=D4+DEC3
930             CONTINUE
            ELSE
            END IF
            DO 935 Q=1,LIMIT,1
                EFF(Q)=EFF(Q)/100.0
935         CONTINUE
*
* THIS PORTION OF THE PROGRAM CALCULATES THE CHANGING AREA FOR THE
* CHANGING AREA EMPIRICAL MODEL.
*
            DO 940 R=1,IK,1
                AAA(R)=0.0
940         CONTINUE
            IK=IK+1
            D5=DEC7
            DO 945 S=IK,IJ,1
                AAA(S)=D5
                D5=D5+DEC7
945         CONTINUE
            IF (CK2.EQ.1) THEN
                D6=AAA(IJ)+DEC6
                IJ=IJ+1
                DO 950 T=IJ,MM,1
                    AAA(T)=D6
                    D6=D6+DEC6
950             CONTINUE
                D7=AAA(MM)+DEC5
                MM=MM+1
                DO 955 U=MM,LIMIT,1
                    AAA(U)=D7
                    D7=D7+DEC5
955             CONTINUE
            ELSE
            END IF
```

```
*
* THIS PORTION OF THE PROGRAM CALCULATES THE CURRENTS DUE TO SLIPPING
* CONTACT LOSSES.
*
          DO 960 V=1,LIMIT,1
              IF(TPTL.EQ.0.0) THEN
                  POWER=1.0-((SMS(V)*2.0)/CWH)
                  ISLIP(V)=IO*((IRES(V)/IO))**POWER
                  HSLIP(V)=(ISLIP(V)/(TPPW*1E-02))*1E03
                  BSLIP(V)=HSLIP(V)*MU
              ELSE
                  POWER=1.0-((SMS(V)*2.0)/(W(V)*1E02))
                  ISLIP(V)=IO*((IRES(V)/IO))**POWER
                  HSLIP(V)=(ISLIP(V)/W(V))*1E03
                  BSLIP(V)=HSLIP(V)*MU
              END IF
960       CONTINUE
*
* THIS PORTION OF THE PROGRAM CALCULATES THE CURRENTS DUE TO FLUX TRAPPING
* EFFICIENCY.
*
          DO 965 J=1,LIMIT,1
              IF (TPTL.EQ.0.0) THEN
                  IEFF(J)=EFF(J)*IRES(J)
                  HEFF(J)=(IEFF(J)/(TPPW*1E-02))*1E03
                  BEFF(J)=HEFF(J)*MU
              ELSE
                  IEFF(J)=EFF(J)*IRES(J)
                  HEFF(J)=(IEFF(J)/W(J))*1E03
                  BEFF(J)=HEFF(J)*MU
              END IF
965       CONTINUE
*
* THIS PORTION OF THE PROGRAM CALCULATES THE CURRENTS DUE TO THE CHANGING
* AREA EMPIRICAL MODEL.
*
          DO 970 K=1,LIMIT,1
              IF (TPTL.EQ.0.0) THEN
                  LEX=((1.2566371*AAA(K))/(TPPW*1E-02))*1E-06
                  A=EXPO(K)
                  B=CNUM
                  C=((TIMEL(K)+LOADL)*1E-09)+THROL+LEX
                  IAA(K)=IO*(B/C)*A
                  HAA(K)=(IAA(K)/(TPPW*1E-02))*1E03
                  BAA(K)=HAA(K)*MU
              ELSE
                  LEX=((1.2566371*AAA(K))/W(K))*1E-06
                  A=EXPO(K)
                  B=CNUM
                  C=((TIMEL(K)+LOADL)*1E-09)+THROL+LEX
                  IAA(K)=IO*(B/C)*A
                  HAA(K)=(IAA(K)/W(K))*1E03
                  BAA(K)=HAA(K)*MU
              END IF
```

```
970        CONTINUE
           WRITE (1,715)
715        FORMAT (' TIME      IRES       ISLIP       IEFF       IAA')
              DO 975 L=1,LIMIT,1
                 M=L-1
                 WRITE (1,720) M,IRES(L),ISLIP(L),IEFF(L),IAA(L)
720              FORMAT (I6,G15.4,G15.4,G15.4,G15.4)
975        CONTINUE
*
* THIS PORTION OF THE PROGRAM SETS UP THE PLOTTING FILES FOR THE SLIPPING
* CURRENT.
*
           OPEN (UNIT=1,NAME=PLOT1,TYPE='NEW')
           WRITE (1,500) PLOT1
           WRITE (1,*) LIMIT
           DO 980 N=1,LIMIT,1
              P=N-1
              WRITE (1,*) P
980        CONTINUE
           DO 985 Q=1,LIMIT,1
              A=ISLIP(Q)*1E-03
              WRITE (1,*) A
985        CONTINUE
           CLOSE (UNIT=1)
*
* THIS PORTION OF THE PROGRAM SETS UP THE PLOTTING FILES FOR THE EFFICIENCY
* CURRENT.
*
           OPEN (UNIT=1,NAME=PLOT2,TYPE='NEW')
           WRITE (1,500) PLOT2
           WRITE (1,*) LIMIT
           DO 990 R=1,LIMIT,1
              S=R-1
              WRITE (1,*) S
990        CONTINUE
           DO 995 T=1,LIMIT,1
              A=IEFF(T)*1E-03
              WRITE (1,*) A
995        CONTINUE
           CLOSE (UNIT=1)
*
* THIS PORTION OF THE PROGRAM SETS UP THE PLOTTING FILES FOR THE CHANGING
* AREA CURRENT.
*
           OPEN (UNIT=1,NAME=PLOT3,TYPE='NEW')
           WRITE (1,500) PLOT3
           WRITE (1,*) LIMIT
           DO 1000 U=1,LIMIT,1
              V=U-1
              WRITE (1,*) V
1000       CONTINUE
           DO 1005 J=1,LIMIT,1
              A=IAA(J)*1E-03
              WRITE (1,*) A
```

81

```
1005      CONTINUE
          CLOSE (UNIT=1)
*
* THIS PORTION OF THE PROGRAM INITIALIZES THE VALUES FOR THE WORST CASE
* FOR THE EMPIRICAL MODELS.  THIS PORTION OF THE PROGRAM INITIALIZES THE
* S VALUES FOR THE SLIPPING LOSS MODEL.
*
          II=LIMIT-45
          JJ=LIMIT-84
          AA=0.4800
          BB=0.1348
          DEC1=BB/(II-JJ)
          DEC2=(AA-BB)/(LIMIT-II)
*
* THIS PORTION OF THE PROGRAM INITIALIZES THE VALUES FOR THE WORST CASE
* FOR THE EFFICIENCY MODEL.
*
          CK1=0
          KK=LIMIT
          LL=LIMIT-59
          CC=52.8528
          DEC3=0.0
          DEC4=(100.0-CC)/(LIMIT-LL)
          DD=0.0
*
* THIS PORTION OF THE PROGRAM INITIALIZES THE VALUES FOR THE WORST CASE
* FOR THE CHANGING AREA EMPIRICAL MODEL.
*
          CK2=0
          IJ=LIMIT
          IK=LIMIT-56
          EE=0.0010029
          DEC5=0.0
          DEC6=0.0
          DEC7=EE/(LIMIT-IK)
          FF=0.0
          GG=0.0
          MM=0
          OPEN (UNIT=1,NAME=FNAME,TYPE='NEW')
          WRITE (1,725)
725       FORMAT ('  THE FOLLOWING ARE THE RESULTS FOR THE WORST CASE ')
900   CONTINUE
*
* THIS PORTION OF THE PROGRAM PRINTS THE DATA DEVELOPED FOR EACH
* OF THE MODELS.
*
200   FORMAT (' THE LINE INDUCTANCE IS: ',F12.4,' NANOHENRIES')
      WRITE (1,205) INTL
205   FORMAT (' THE GENERATOR INDUCTANCE IS: ',F12.4,' NANOHENRIES')
      WRITE (1,210) LOADL
210   FORMAT (' THE LOAD INDUCTANCE IS: ',F12.4,' NANOHENRIES')
      WRITE (1,215) CAP
215   FORMAT(' THE BANK CAPACITANCE IS: ',F12.4,' MICROFARADS')
      WRITE (1,220) VOLT
```

82

```
220     FORMAT(' THE BANK VOLTAGE IS: ',F12.4,' KILOVOLTS')
        WRITE (1,225) EXPL
225     FORMAT(' THERE ARE: ',F12.4,' KILOGRAMS OF EXPLOSIVES')
        WRITE (1,230) TAMW
230     FORMAT(' THERE ARE:',F12.4,' KILOGRAMS OF TAMPER')
        WRITE (1,235) MTOC
235     FORMAT(' THE MASS TO EXPLOSIVE RATIO IS: ',F12.4)
        WRITE (1,240) NTOC
240     FORMAT(' THE TAMPER RATIO IS: ',F12.4)
        WRITE (1,245) D
245     FORMAT(' THE DETONATION VELOCITY IS: ',F12.4,' MM/MICROSECONDS')
        WRITE (1,250) VA
250     FORMAT(' THE METAL VELOCITY IS: ',F12.4,' MM/MICROSECONDS')
        WRITE (1,255) THETD
255     FORMAT(' THE GURNEY ANGLE IS: ',F12.4,' DEGREES')
        WRITE (1,260) LIMIT
260     FORMAT(' THE LIMIT IS: ',I10)
        WRITE (1,265)
265     FORMAT(' THE RESULTS FOR THE FLUX CONSERVED MODEL ARE:')
        WRITE (1,270)
270     FORMAT(' TIME(MICROSECONDS)    INDUCTANCE(NANOHENRIES)')
        DO 150 T=1,LIMIT,1
        WRITE (1,275) MISEC(T),TIMEL(T)
275     FORMAT(' ',4X,F12.4,10X,F12.4)
150     CONTINUE
        WRITE (1,280)
280     FORMAT(' TIME(MICROSECONDS)    CURRENT(KAMPS)')
        DO 155 U=1,LIMIT,1
        WRITE (1,285) MISEC(U),TIMEI(U)
285     FORMAT(' ',4X,F12.4,6X,F12.4)
155     CONTINUE
        WRITE (1,290)
290     FORMAT(' TIME(MICROSECONDS)',10X,'HFIELD(AMPS/METER)',3X,'BFIELD(
       +MEGAGAUSS)')
        DO 160 V=1,LIMIT,1
        WRITE (1,295) MISEC(V),MAGH(V),MAGB(V)
295     FORMAT(' ',4X,F12.4,4X,G20.4,2X,G20.4)
160     CONTINUE
        WRITE (1,300)
300     FORMAT (' A TIME VARYING RESISTANCE IS:')
        WRITE (1,305)
305     FORMAT (' TIME(MICROSECONDS)        RESISTANCE(OHMS)')
        DO 165 I=1,LIMIT,1
        WRITE (1,310) MISEC(I),RES(I)
310     FORMAT(' ',F12.4,6X,G20.4)
165     CONTINUE
        WRITE (1,315)
315     FORMAT (' THE RESULTS FOR THE TIME VARYING RESISTANCE MODEL ARE:')
        WRITE (1,320)
320     FORMAT (' TIME(MICROSECONDS)',3X,'CURRENT(KAMPS)')
        DO 170 J=1,LIMIT,1
        WRITE (1,325) MISEC(J),IRES(J)
325     FORMAT (' ',4X,F12.4,6X,F12.4)
170     CONTINUE
```

```
          WRITE (1,330)
330       FORMAT (' TIME(MICROSECONDS)',10X,'HFIELD(AMPS/METER)',3X,'BFIELD(
         +MEGAGAUSS)')
          DO 175 K=1,LIMIT,1
              WRITE (1,335) MISEC(K),MAGRH(K),MAGRB(K)
335           FORMAT (' ',4X,F12.4,4X,G20.4,2X,G20.4)
175       CONTINUE
          WRITE (1,340)
340       FORMAT (' THE RESULTS FOR THE SLIPPING LOSS MODEL ARE:')
          WRITE (1,345)
345       FORMAT (' TIME(MICROSECONDS)',3X,'CURRENT(KAMPS)')
          DO 180 L=1,LIMIT,1
              WRITE (1,350) MISEC(L),ISLIP(L)
350           FORMAT (' ',4X,F12.4,6X,F12.4)
180       CONTINUE
          WRITE (1,355)
355       FORMAT (' TIME(MICROSECONDS)',10X,'HFIELD(AMPS/METER)',3X,'BFIELD(
         +MEGAGAUSS)')
          DO 185 M=1,LIMIT,1
              WRITE (1,360) MISEC(M),HSLIP(M),BSLIP(M)
360           FORMAT (' ',4X,F12.4,4X,G20.4,2X,G20.4)
185       CONTINUE
          WRITE (1,365)
365       FORMAT (' THE RESULTS FOR THE EFFICIENCY MODEL ARE:')
          WRITE (1,370)
370       FORMAT (' TIME(MICROSECONDS)',3X,'CURRENT(KAMPS)')
          DO 190 N=1,LIMIT,1
              WRITE (1,375) MISEC(N),IEFF(N)
375           FORMAT (' ',4X,F12.4,6X,F12.4)
190       CONTINUE
          WRITE (1,380)
380       FORMAT (' TIME(MICROSECONDS)',10X,'HFIELD(AMPS/METER)',3X,'BFIELD(
         +MEGAGAUSS)')
          DO 195 P=1,LIMIT,1
              WRITE (1,385) MISEC(P),HEFF(P),BEFF(P)
385           FORMAT (' ',4X,F12.4,4X,G20.4,2X,G20.4)
195       CONTINUE
          WRITE (1,390)
390       FORMAT(' THE RESULTS FOR THE CHANGING AREA LOSS MODEL ARE:')
          WRITE (1,395)
395       FORMAT (' TIME(MICROSECONDS)',3X,'CURRENT(KAMPS)')
          DO 600 Q=1,LIMIT,1
              WRITE (1,400) MISEC(Q),IAA(Q)
400           FORMAT (' ',4X,F12.4,6X,F12.4)
600       CONTINUE
          WRITE (1,405)
405       FORMAT (' TIME(MICROSECONDS)',10X,'HFIELD(AMPS/METER)',3X,'BFIELD(
         +MEGAGAUSS)')
          DO 605 R=1,LIMIT,1
              WRITE (1,410) MISEC(R),HAA(R),BAA(R)
410           FORMAT (' ',4X,F12.4,4X,G20.4,2X,G20.4)
605       CONTINUE
          END
```

Appendix B

Appendix B contains the curves of the measured and calculated data used for analysis in Chapter VI. The curves for Test 1 were presented in Chapter VI. This appendix contains the same curves for the remaining tests. They include the experimental currents, the bubble heights, efficiencies, and additional areas. Also included are the output currents of each of these models.
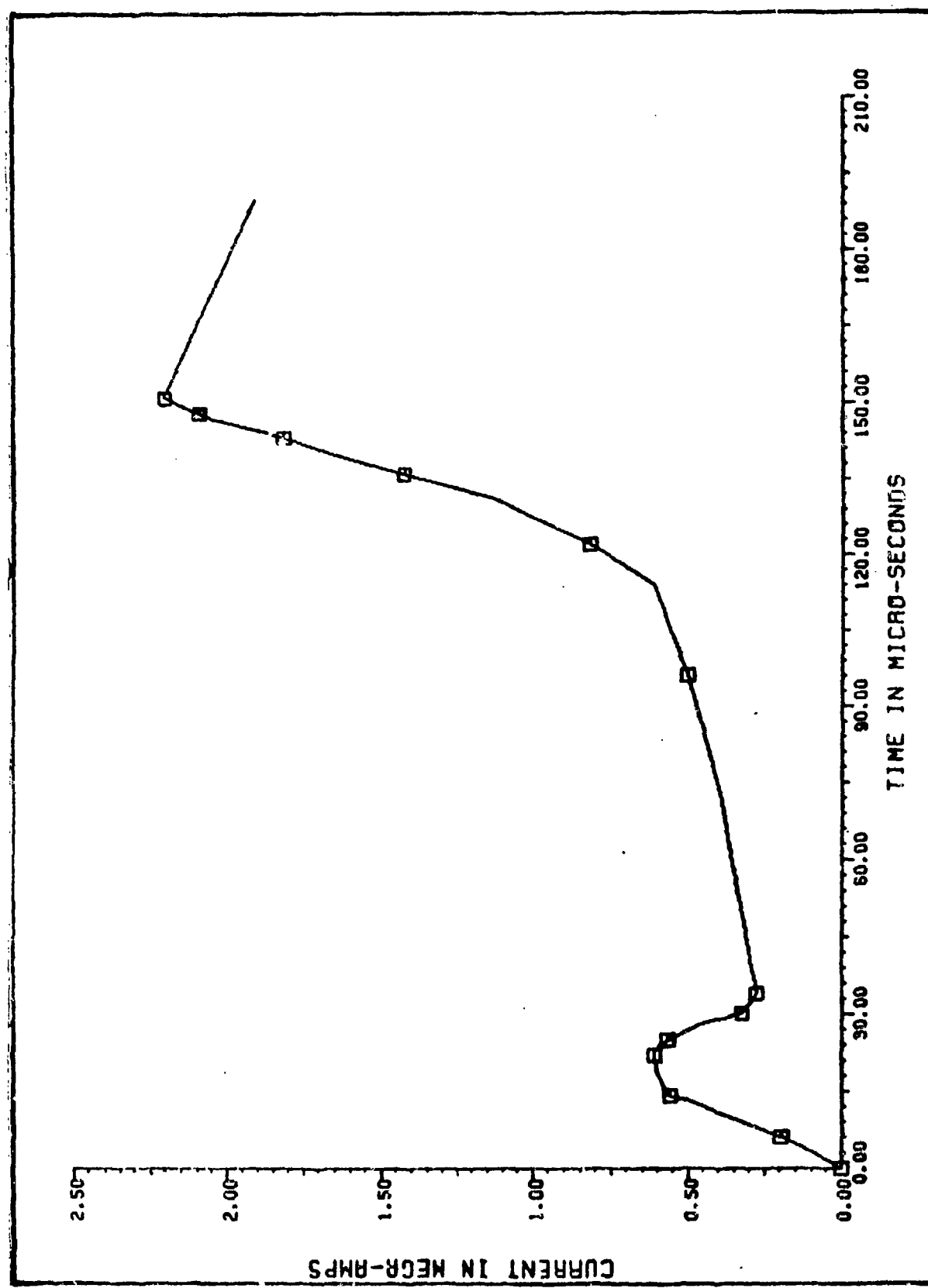
Figure B-1. Experimental Current Test 2
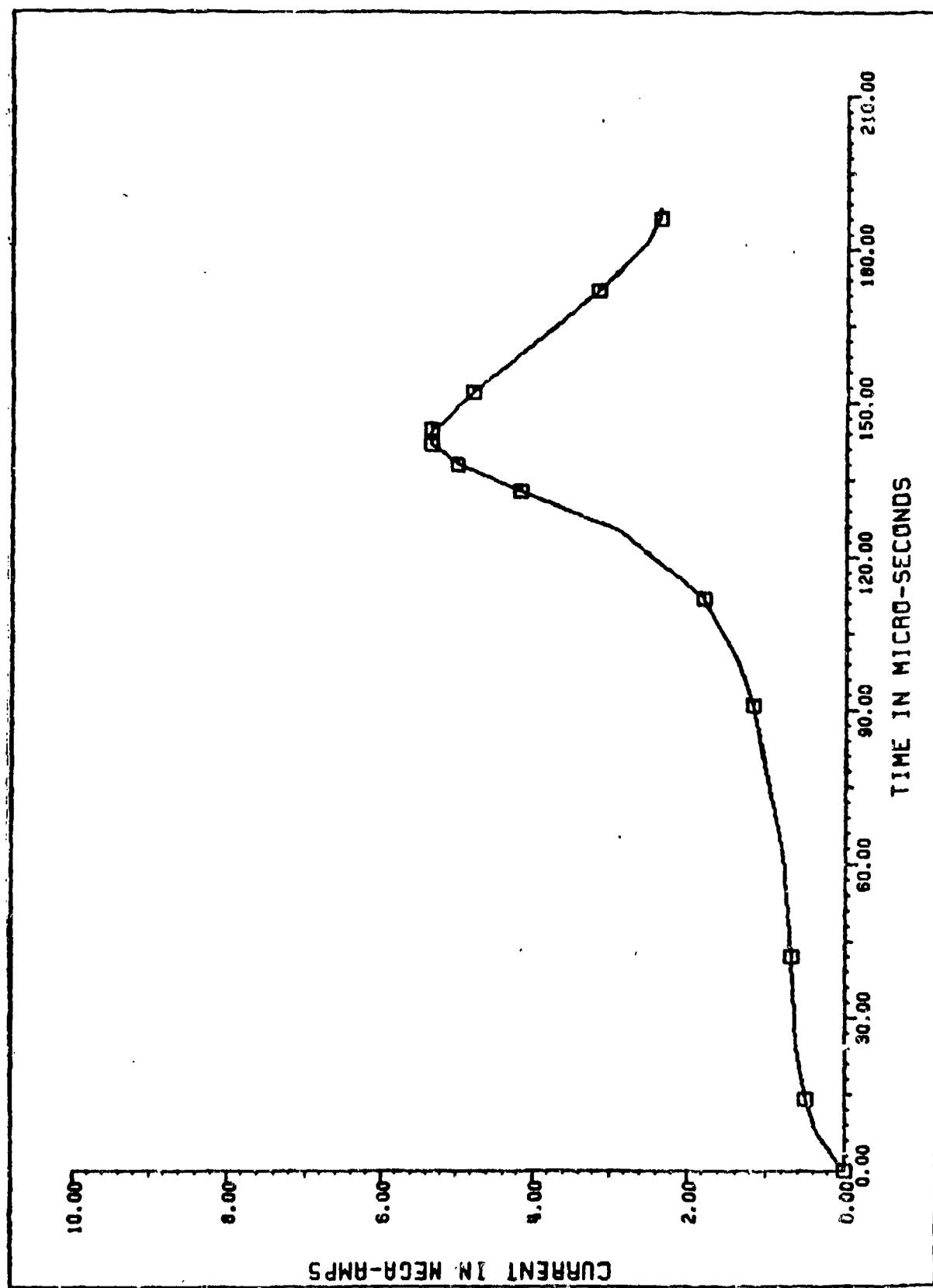
Figure B-2. Experimental Current Test 3
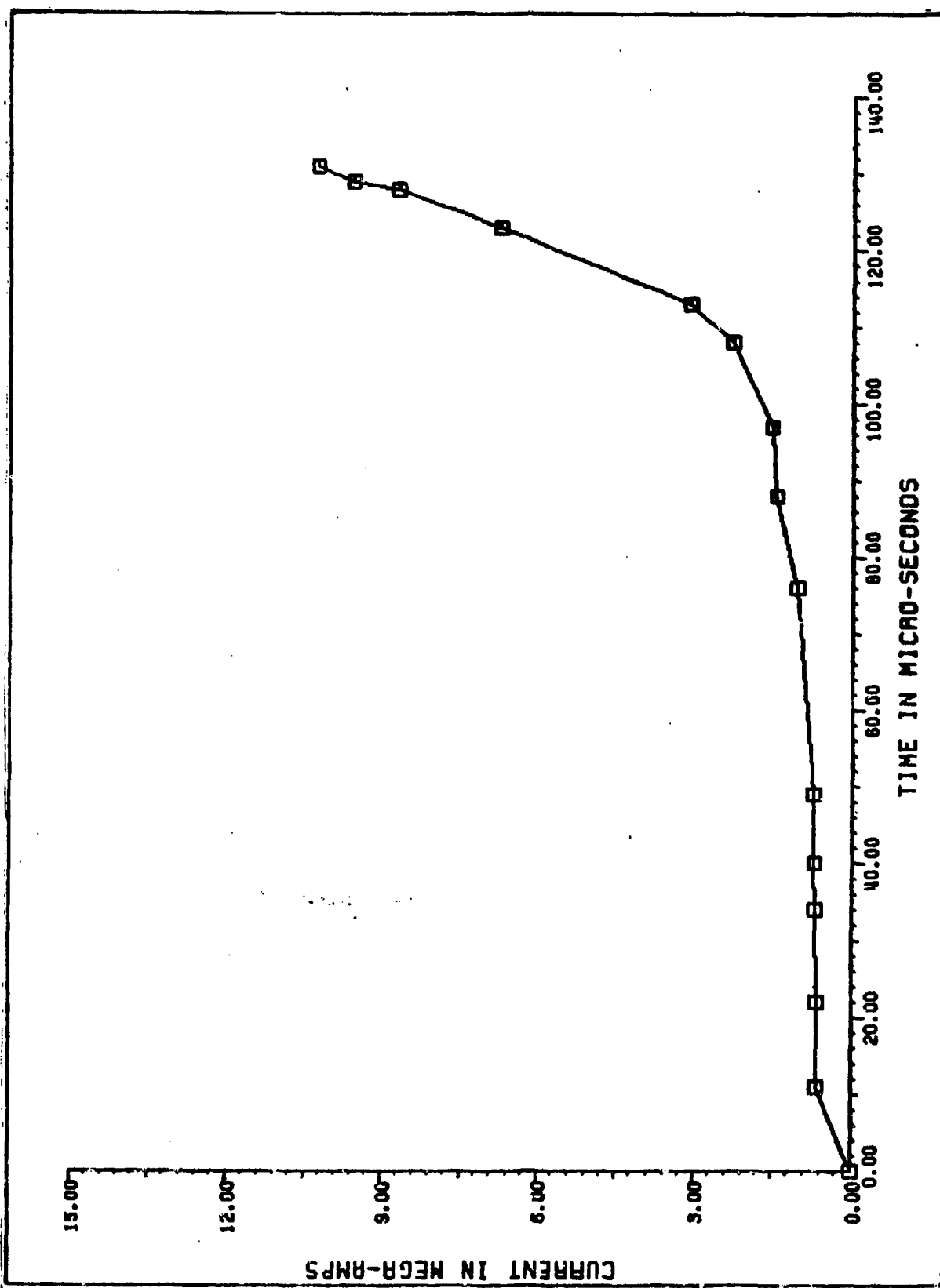
Figure B-3. Experimental Current Test 4
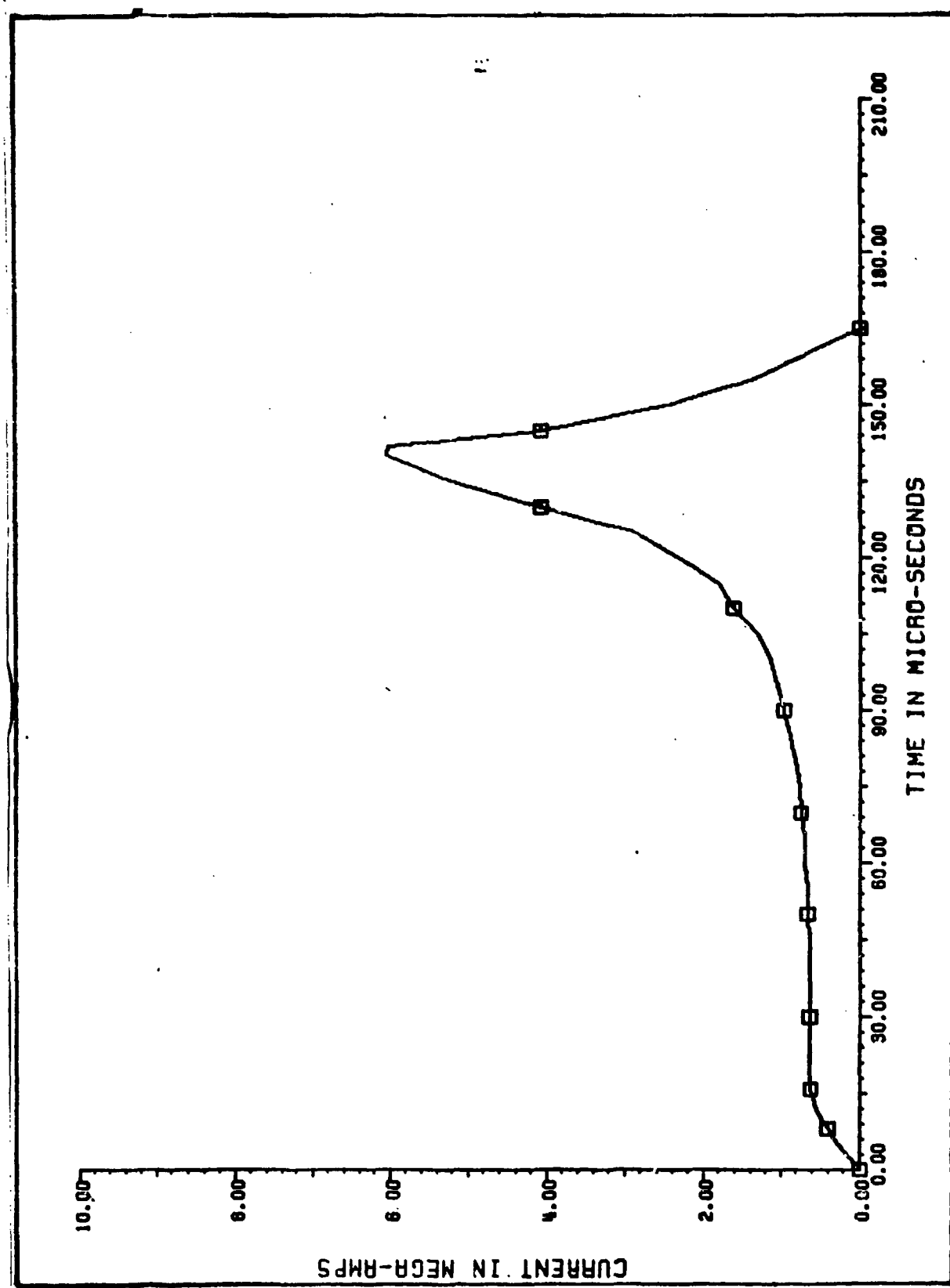
Figure B-4. Experimental Current Test 5
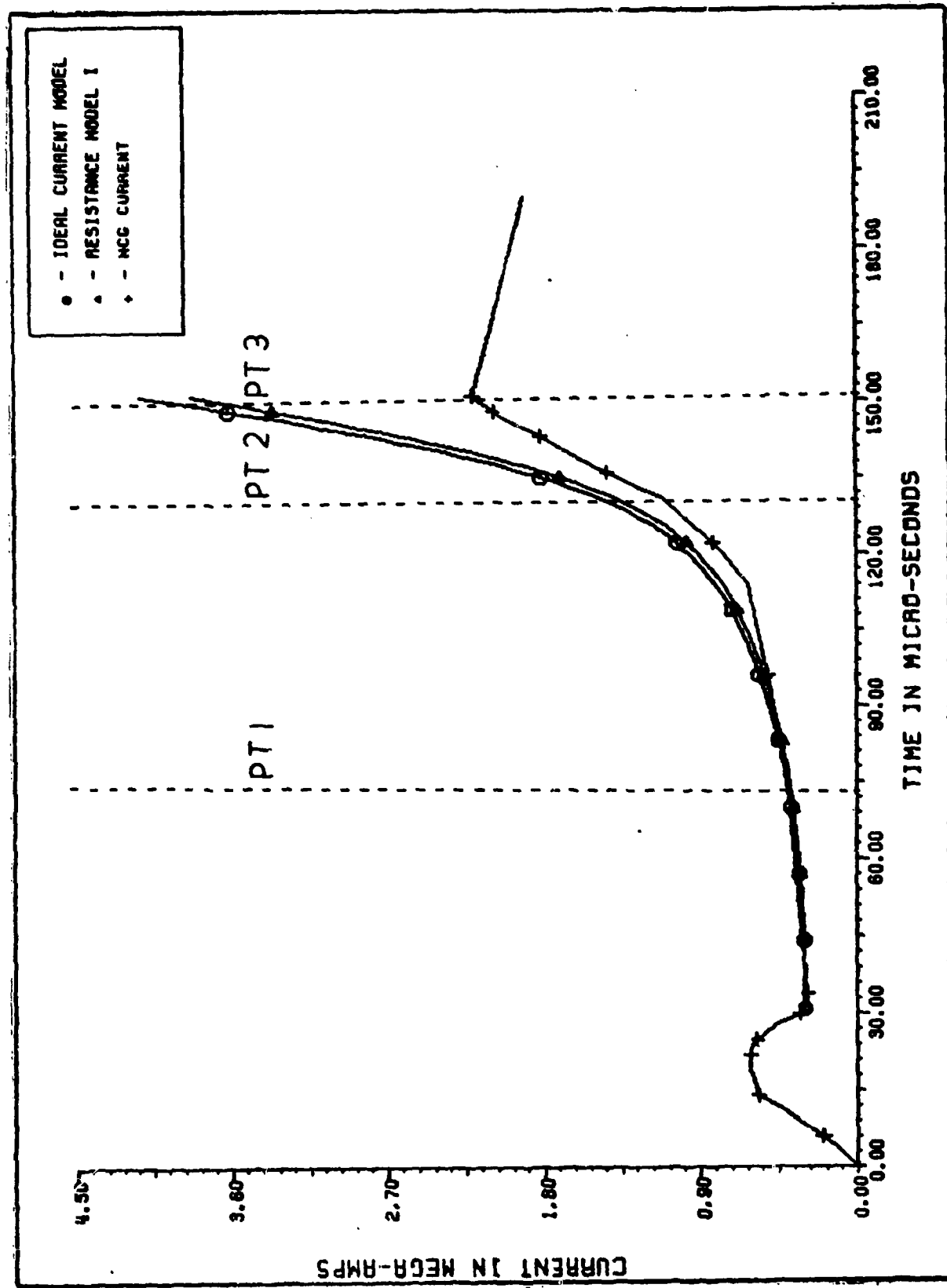
Figure B-5. Equivalent Circuit Currents Test 2
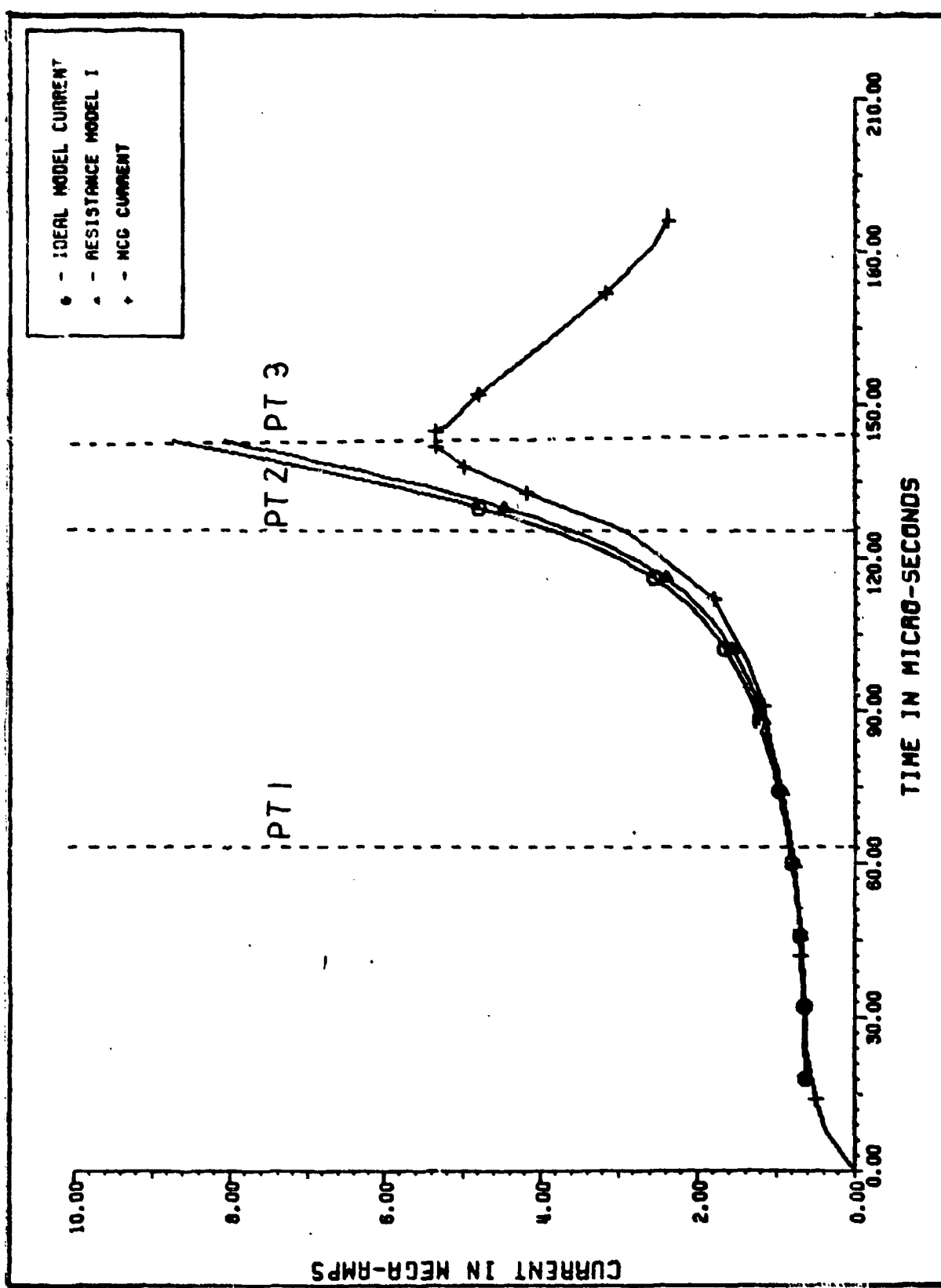
Figure B-6. Equivalent Circuit Currents Test 3
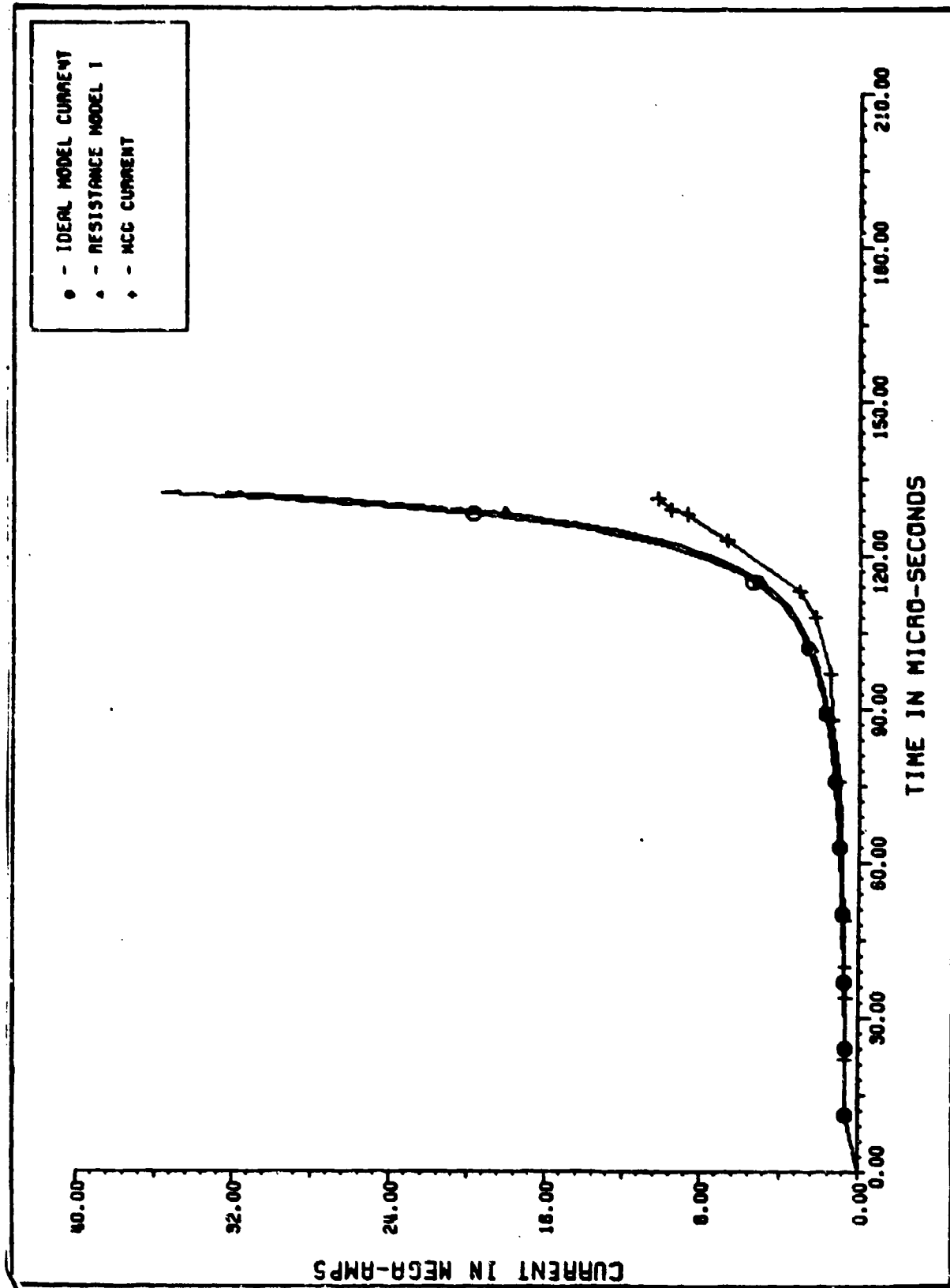
Figure B-7. Equivalent Circuit Currents Test 4
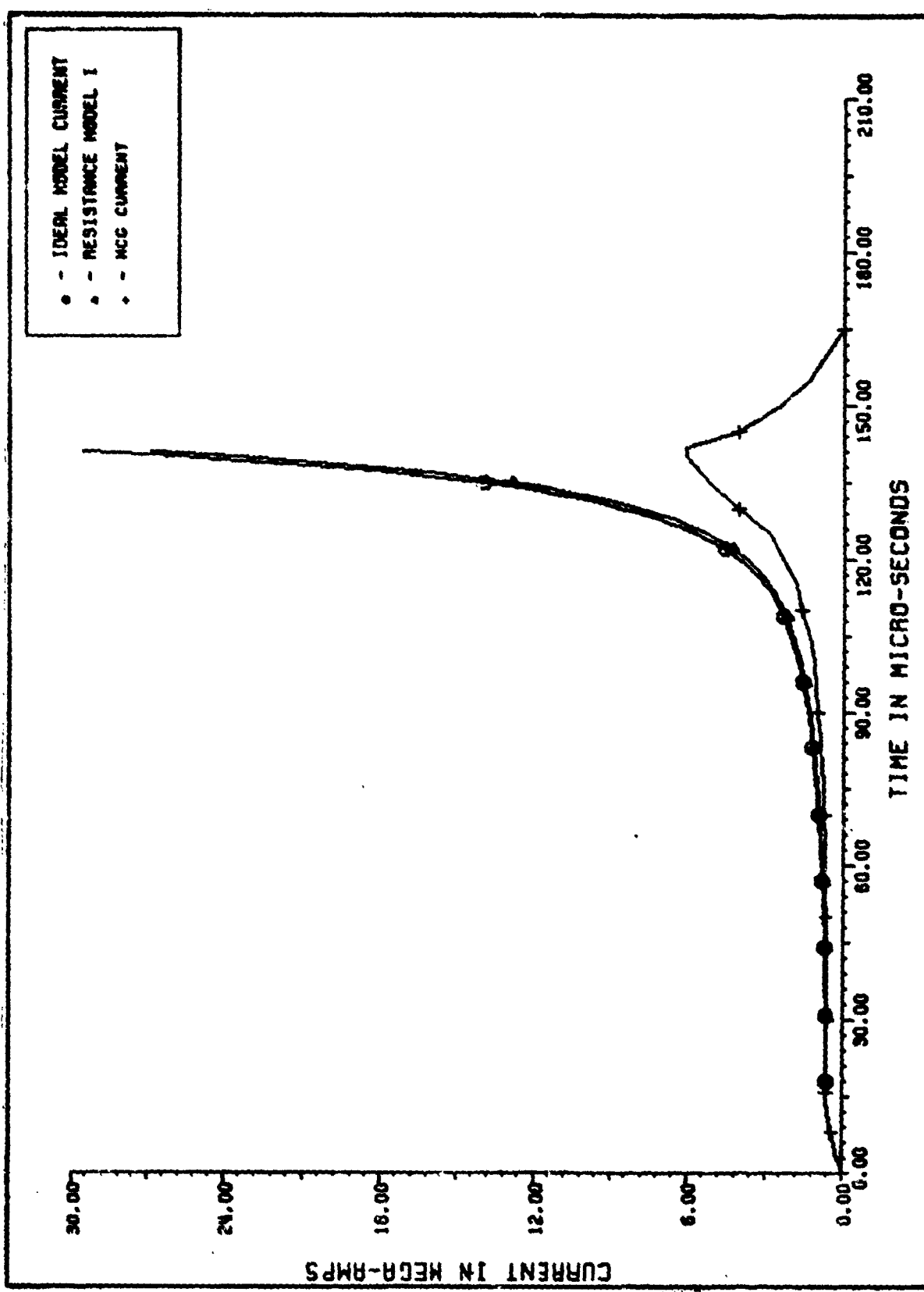
Figure B-8. Equivalent Circuit Currents Test 5

The figure shows a plot with the following axis labels:

Y-axis: CURRENT IN MEGA-AMPS, with values 0.00, 6.00, 12.00, 18.00, 24.00, 30.00

X-axis: TIME IN MICRO-SECONDS, with values 0.00, 30.00, 60.00, 90.00, 120.00, 150.00, 180.00, 210.00

Legend:
● — IDEAL MODEL CURRENT
▲ — RESISTANCE MODEL I
+ — MCG CURRENT
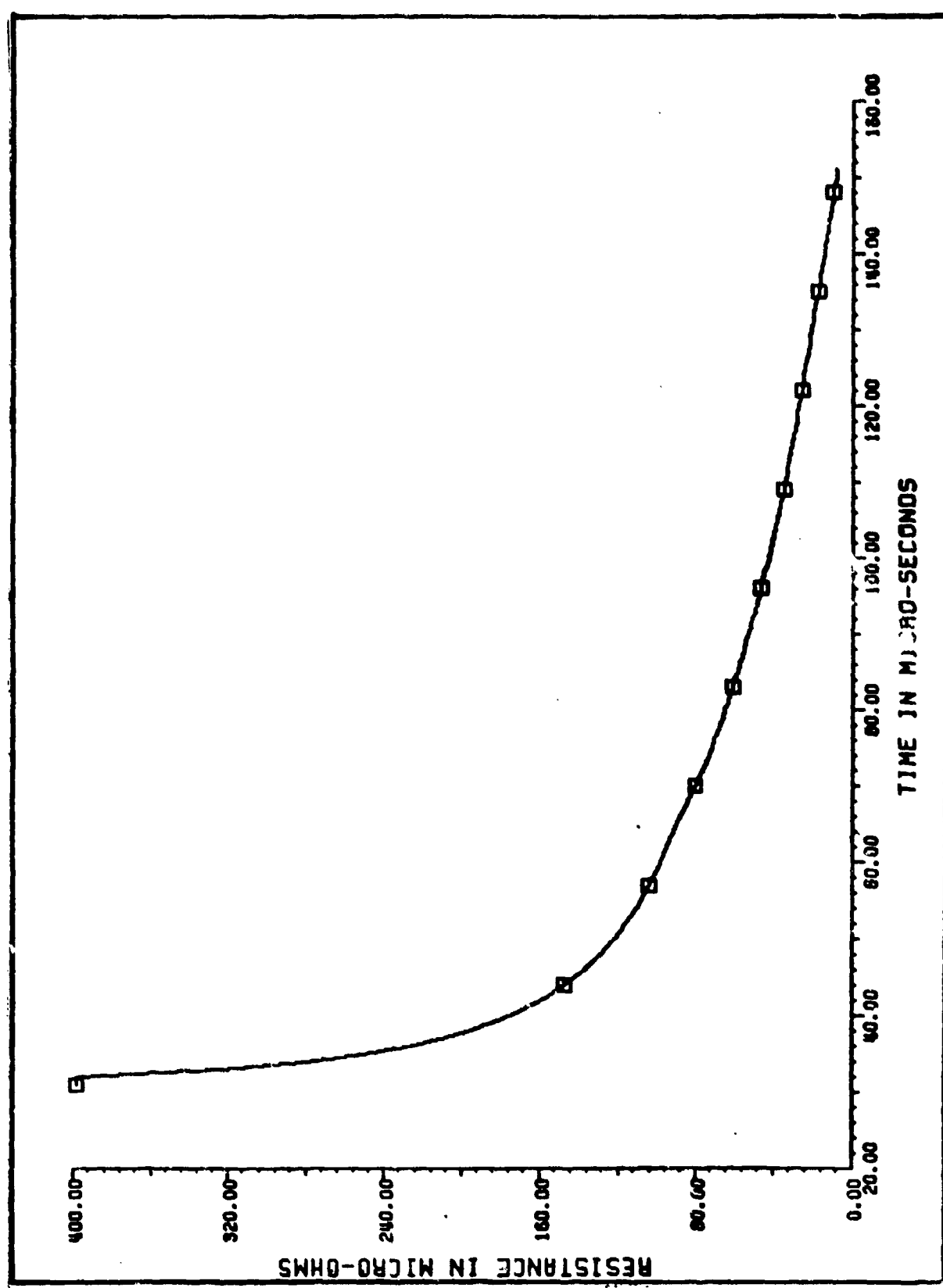
Figure B-9. Time Varying Resistance Test 2

94
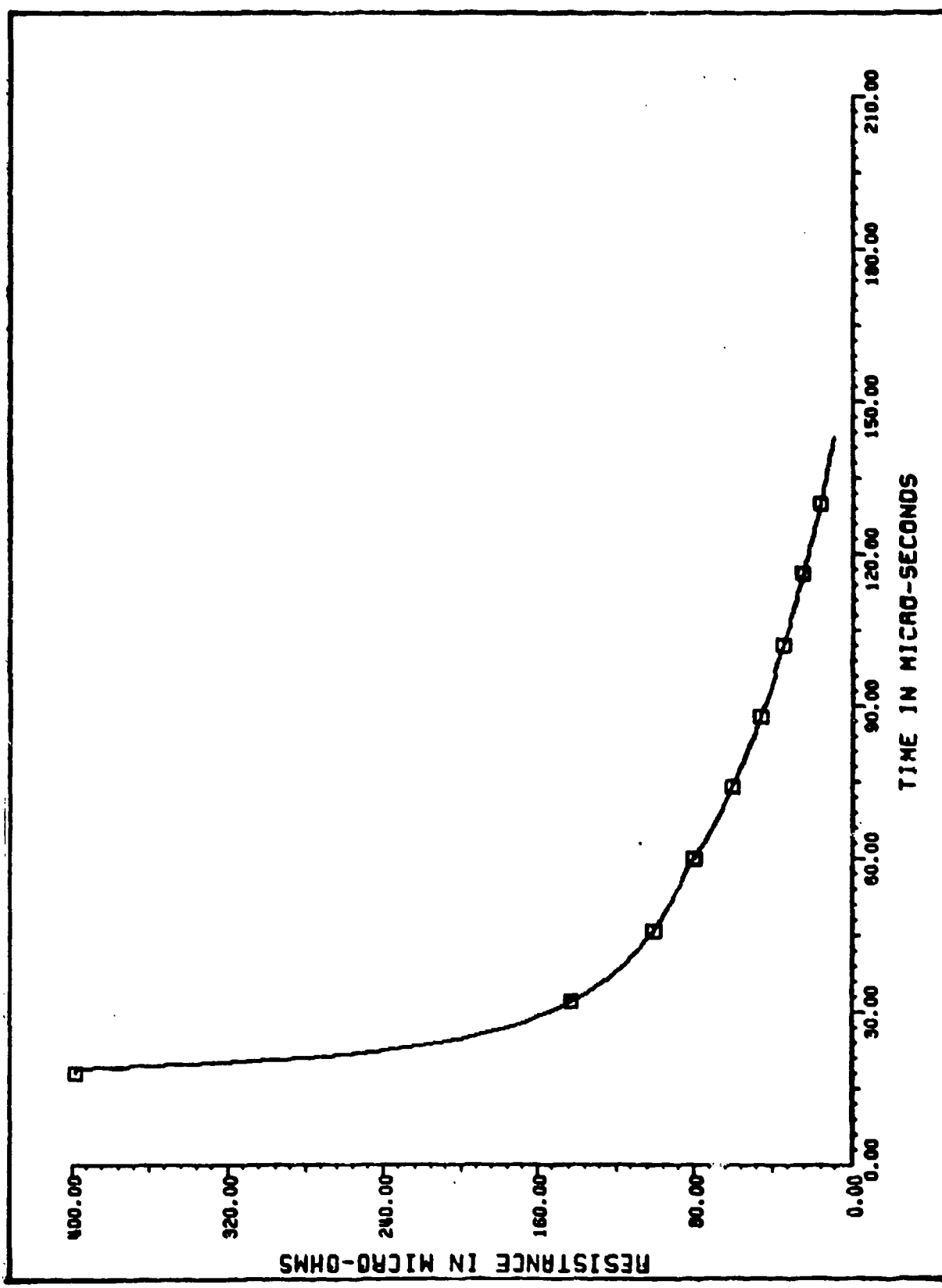
Figure B-10. Time Varying Resistance Test 3

95
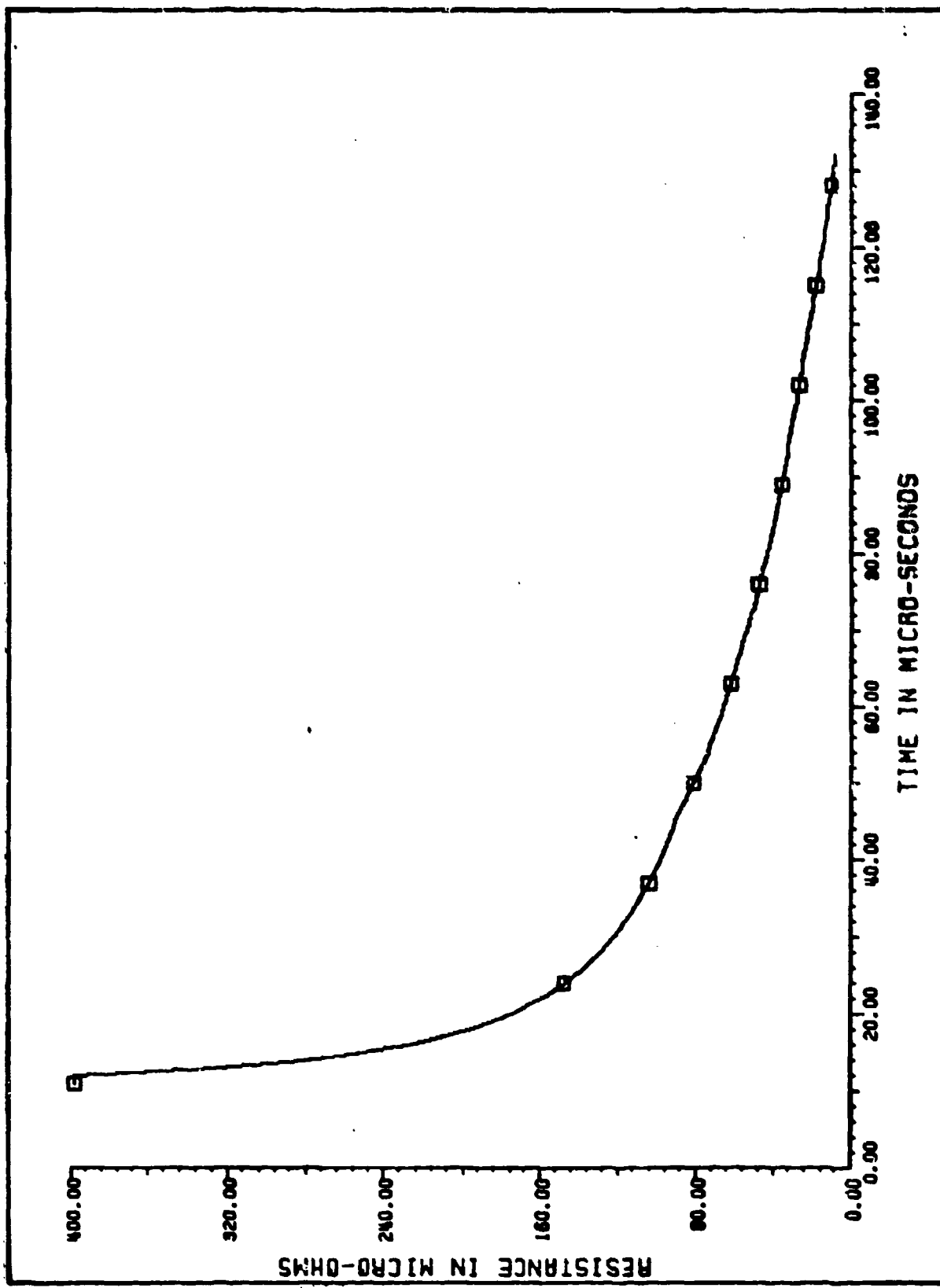
Figure B-11. Time Varying Resistance Test 4
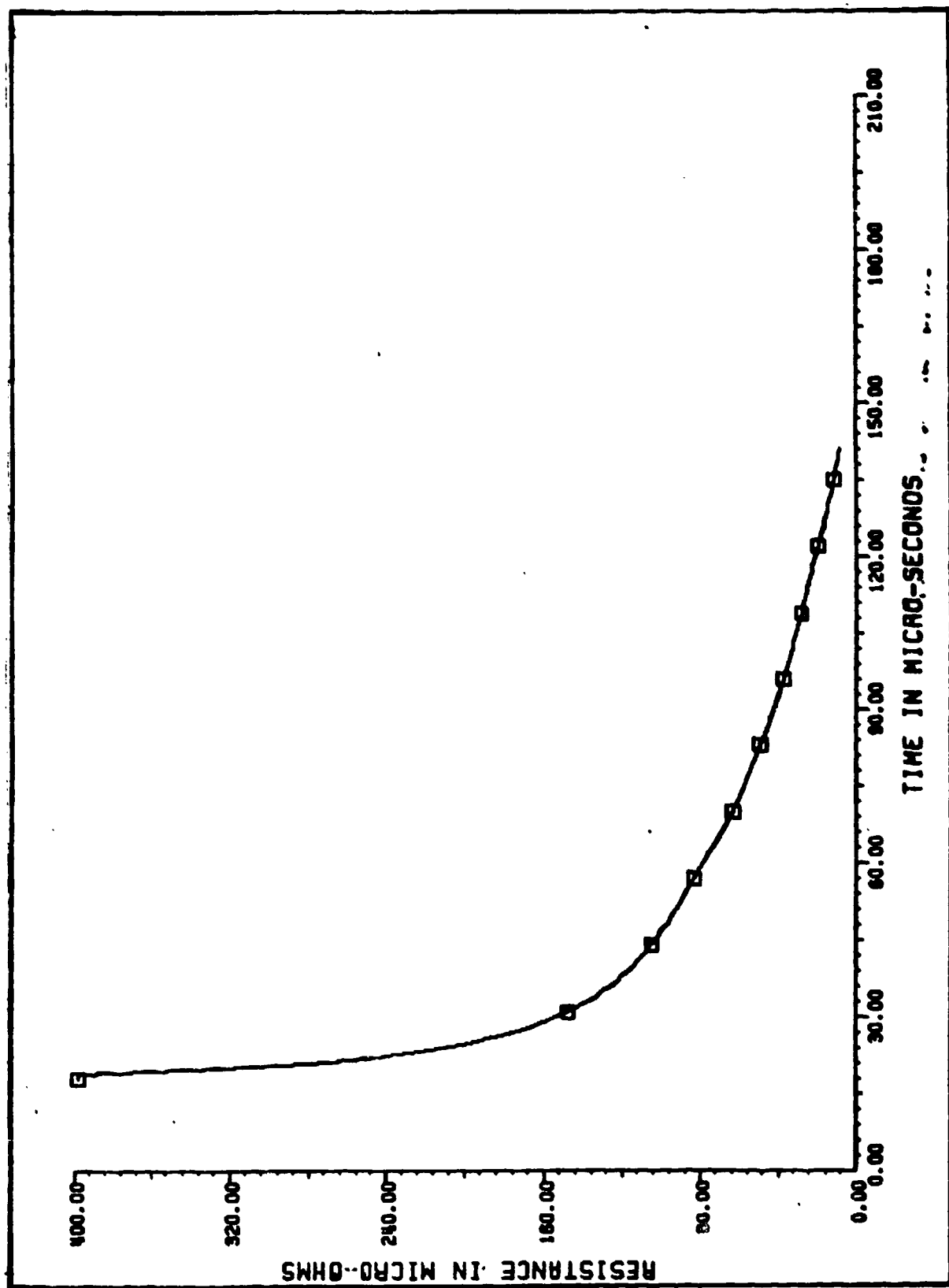
Figure B-12. Time Varying Resistance Test 5
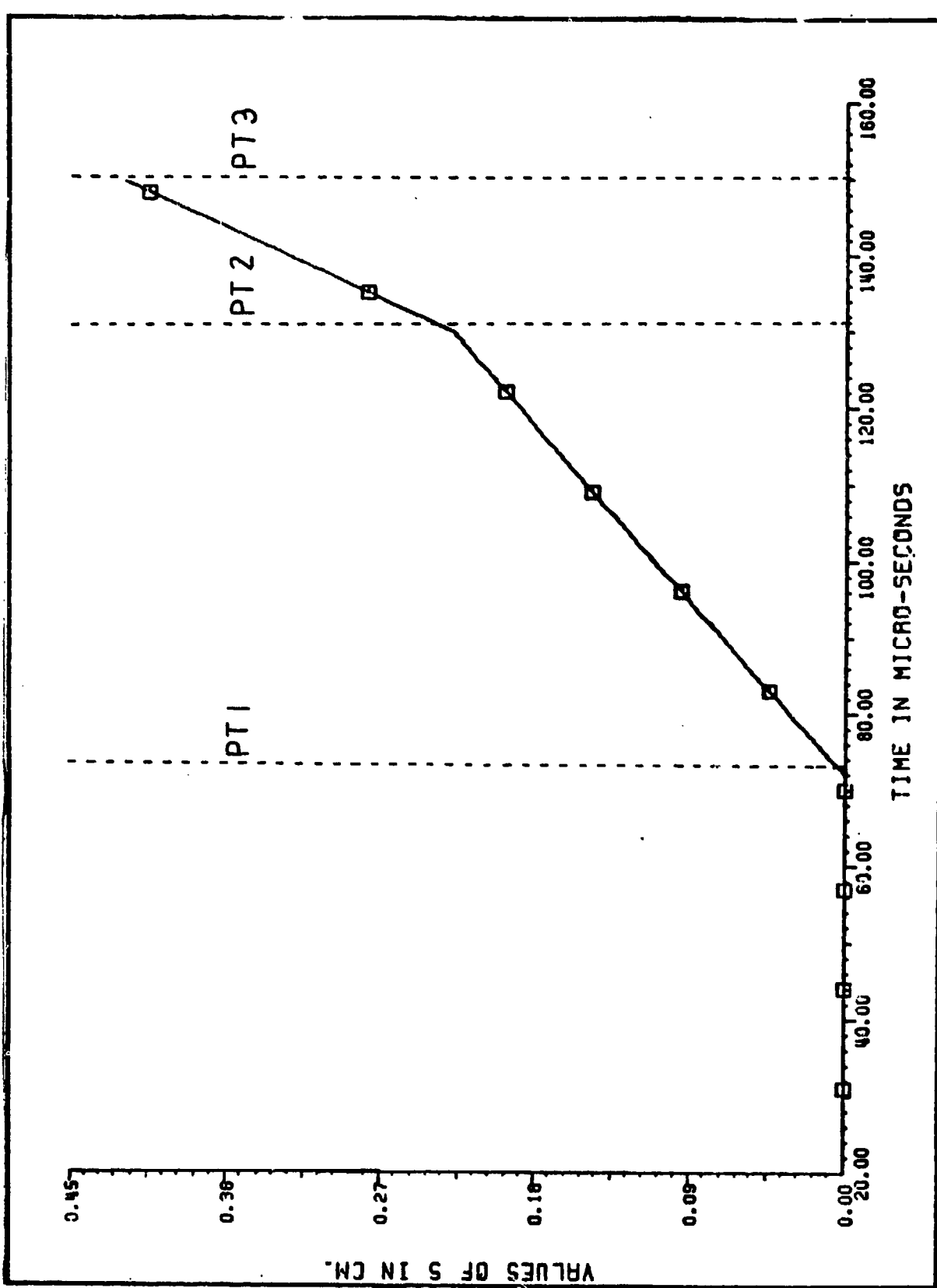
Figure B-13. S Curve Test 2

98
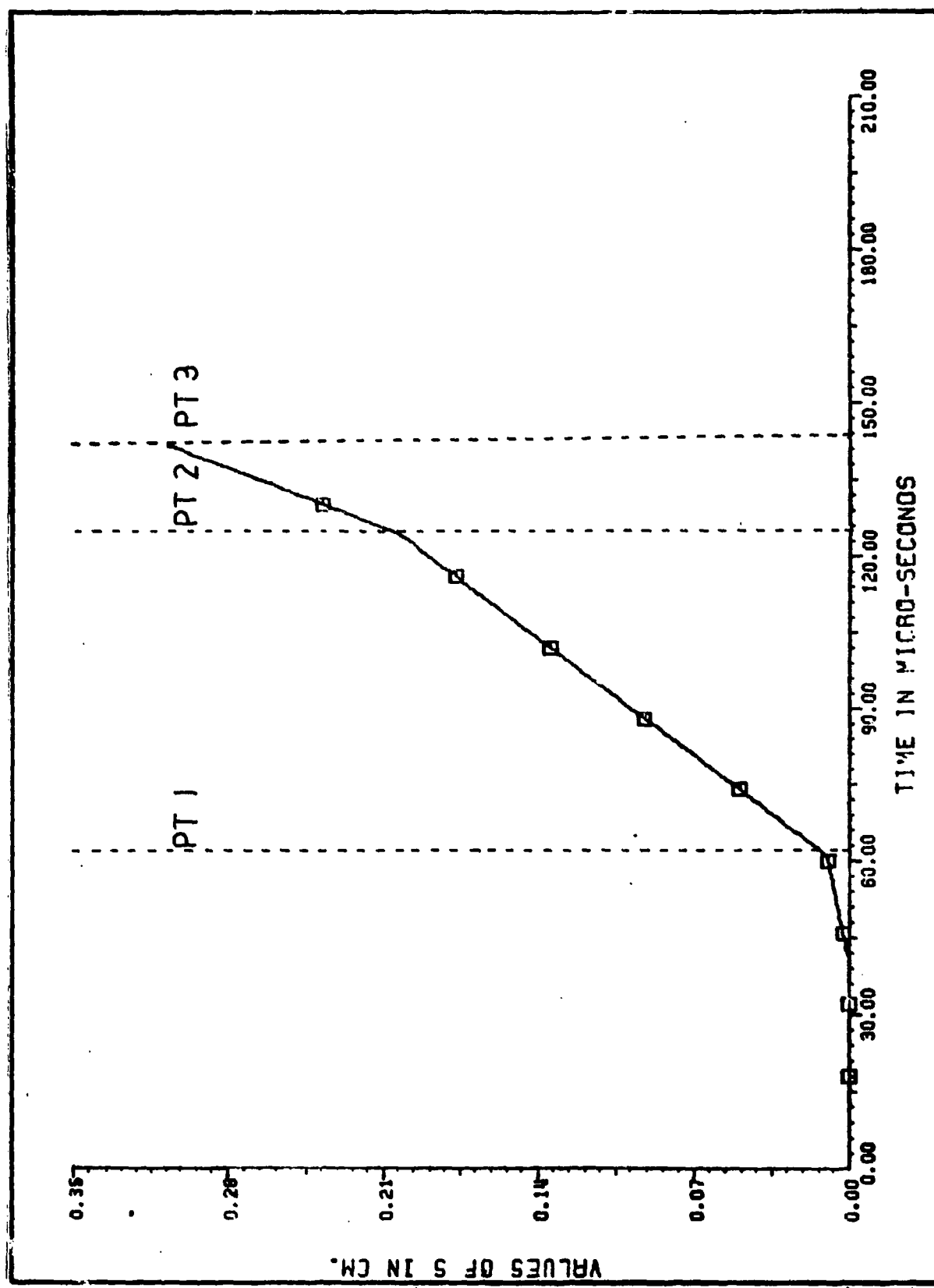
Figure B-14. S Curve Test 3
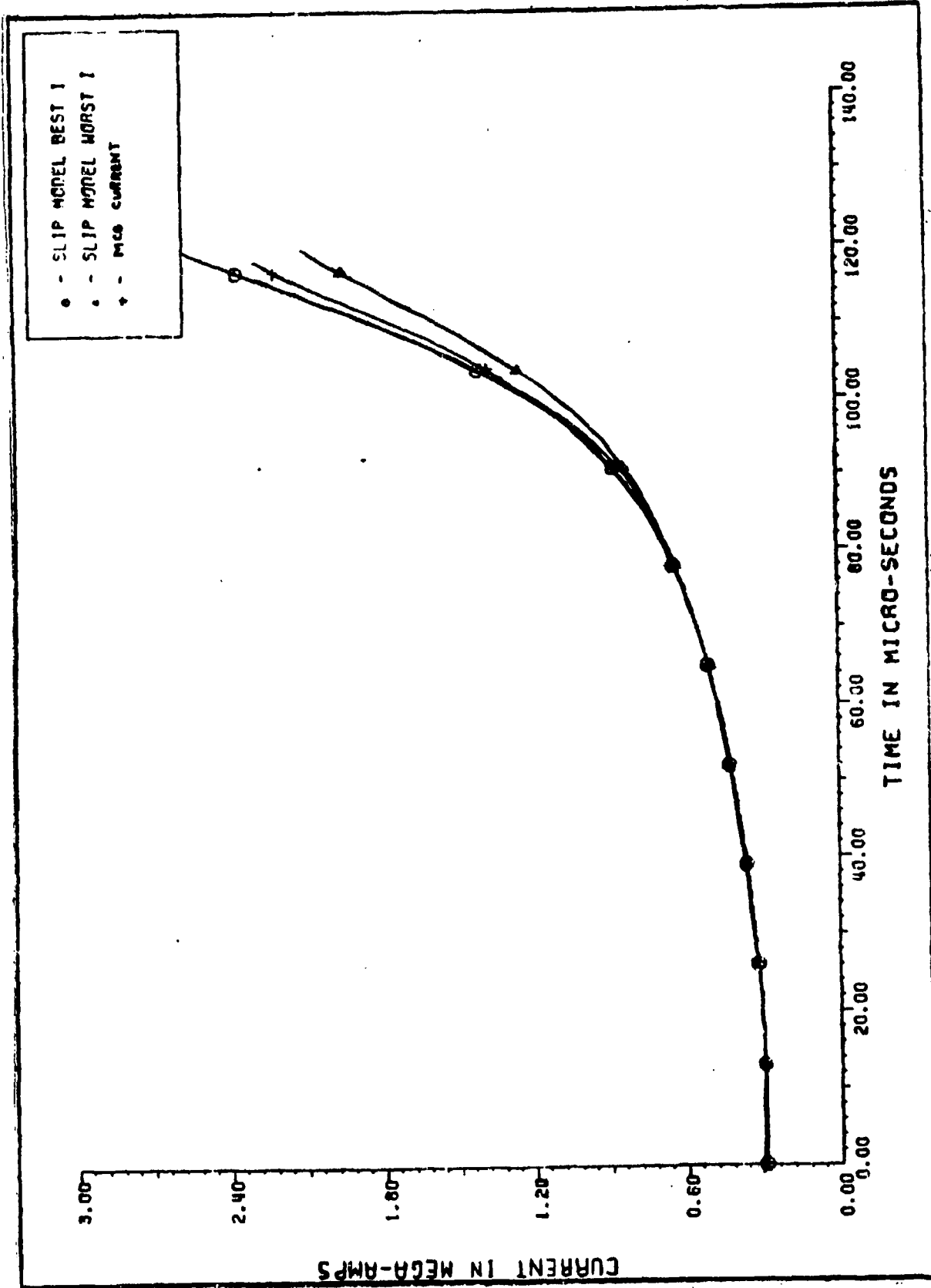
Figure B-15. Slipping Currents Test 2
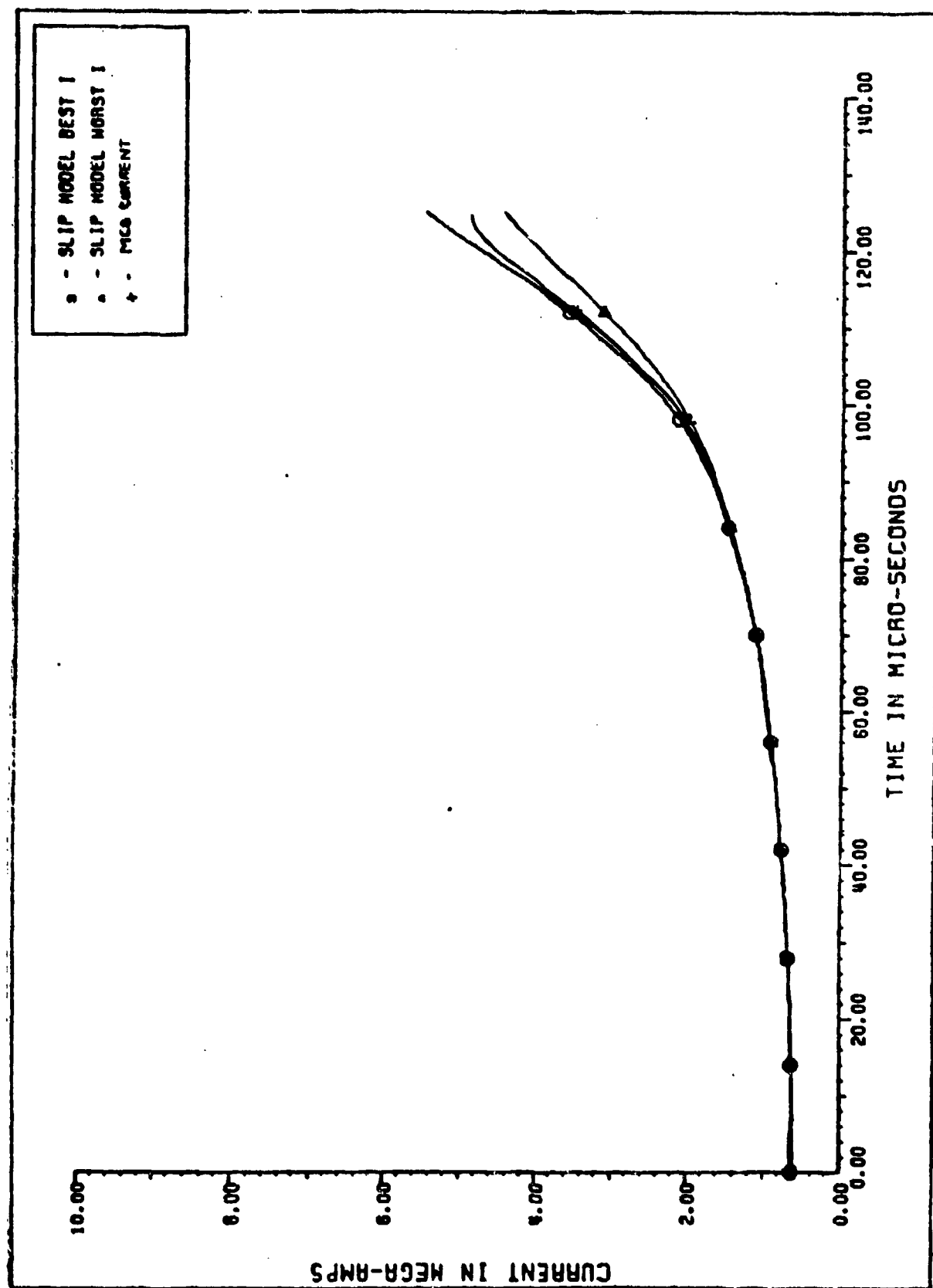
Figure B-16. Slipping Currents Test 3

101
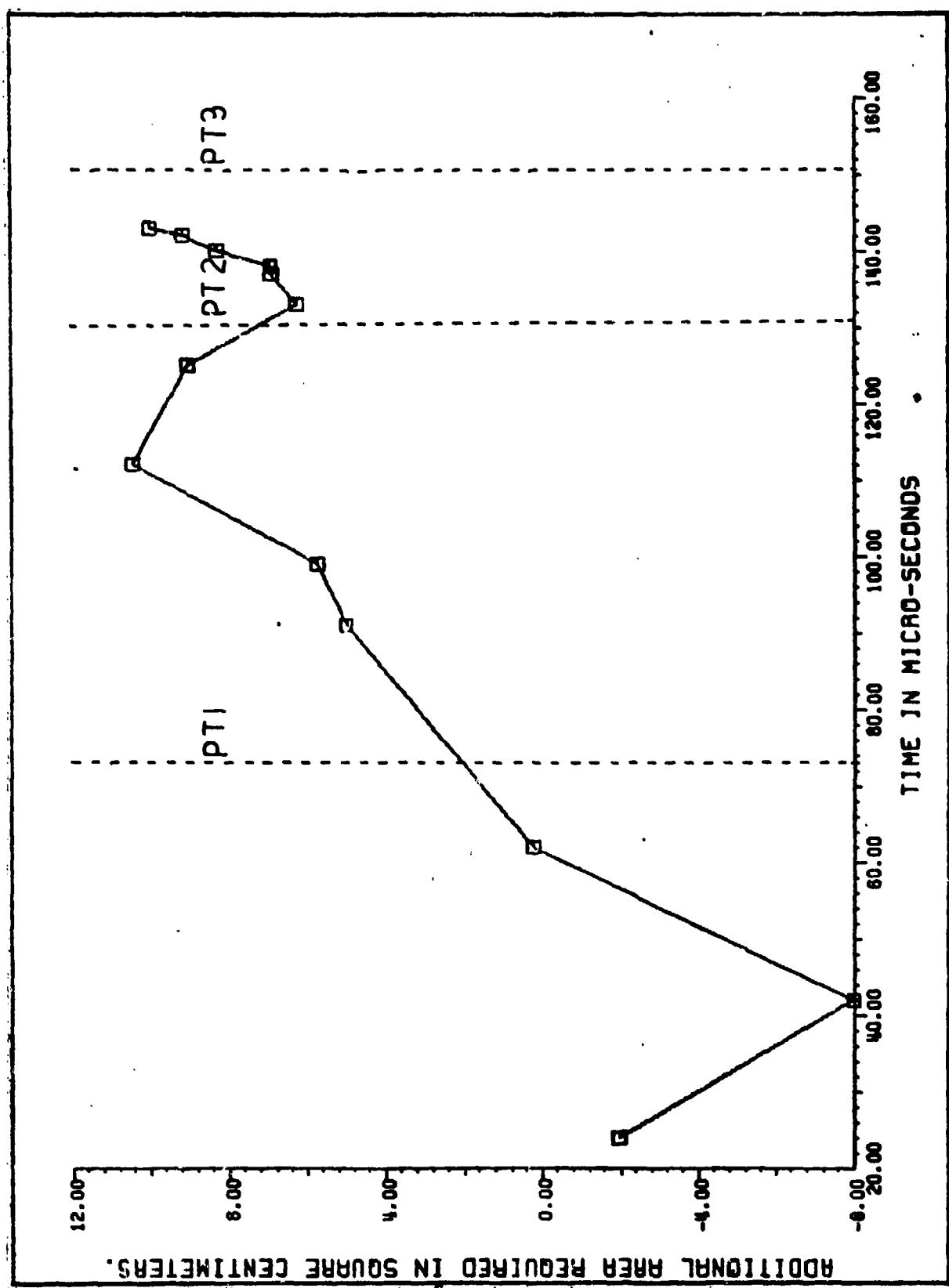
Figure B-17. Additional Area Test 2

The chart shows ADDITIONAL AREA REQUIRED IN SQUARE CENTIMETERS (vertical axis, ranging from -6.00 to 12.00) plotted against TIME IN MICRO-SECONDS (horizontal axis, ranging from 20.00 to 160.00). Vertical dashed reference lines are labeled PT1, PT2, and PT3.
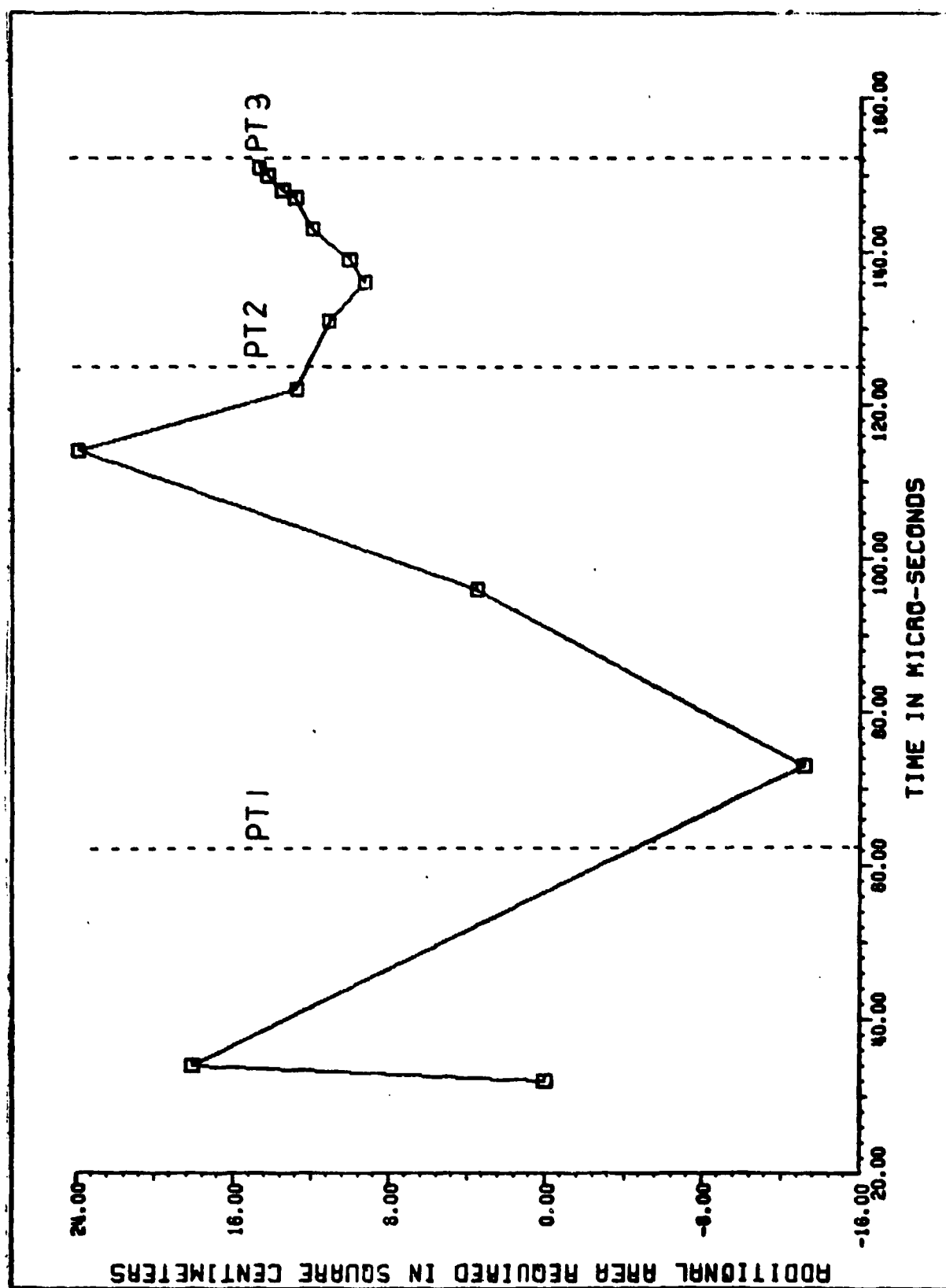
Figure B-18. Additional Area Test 3
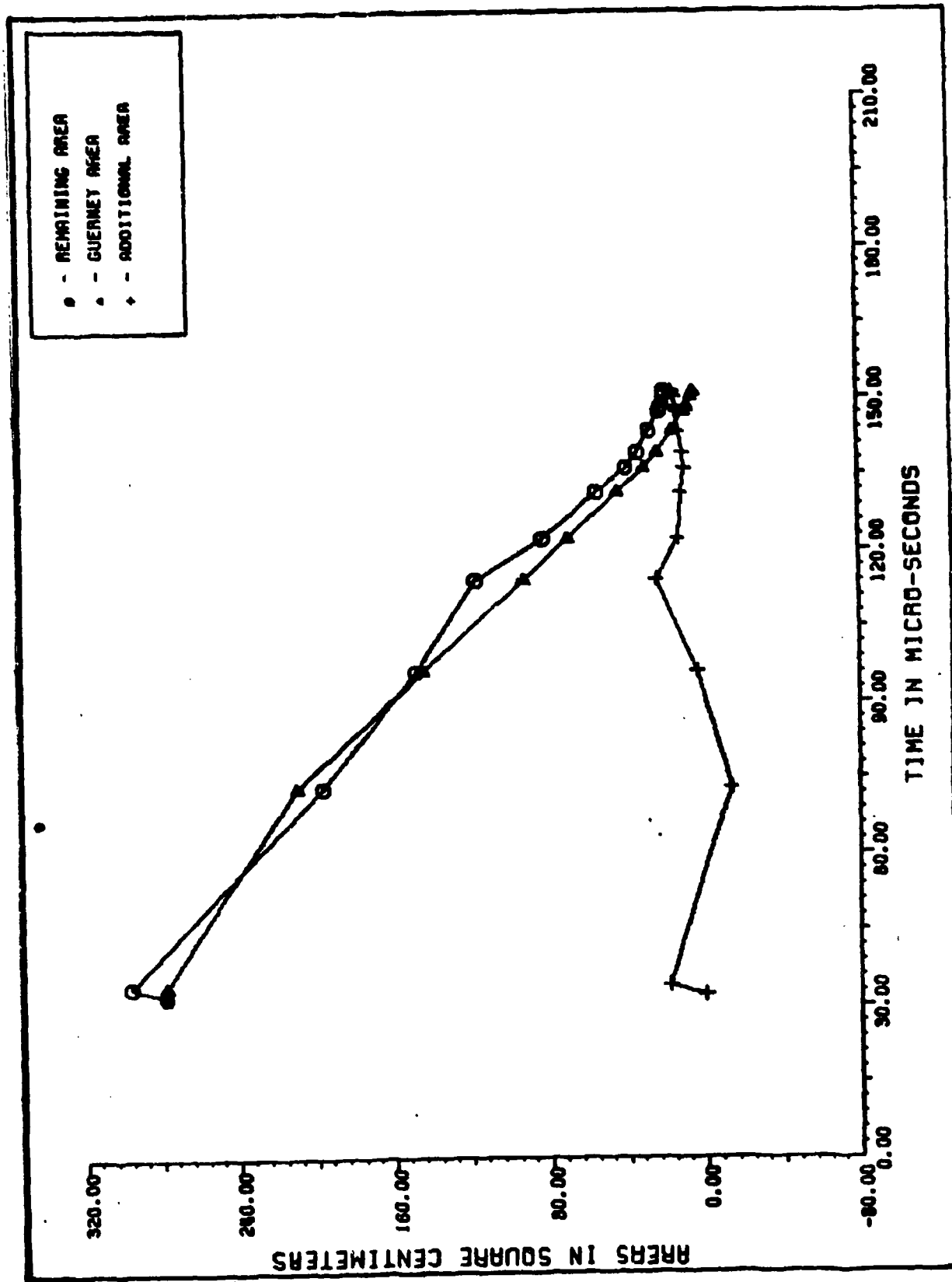
Figure B-19. Changing Areas Test 2
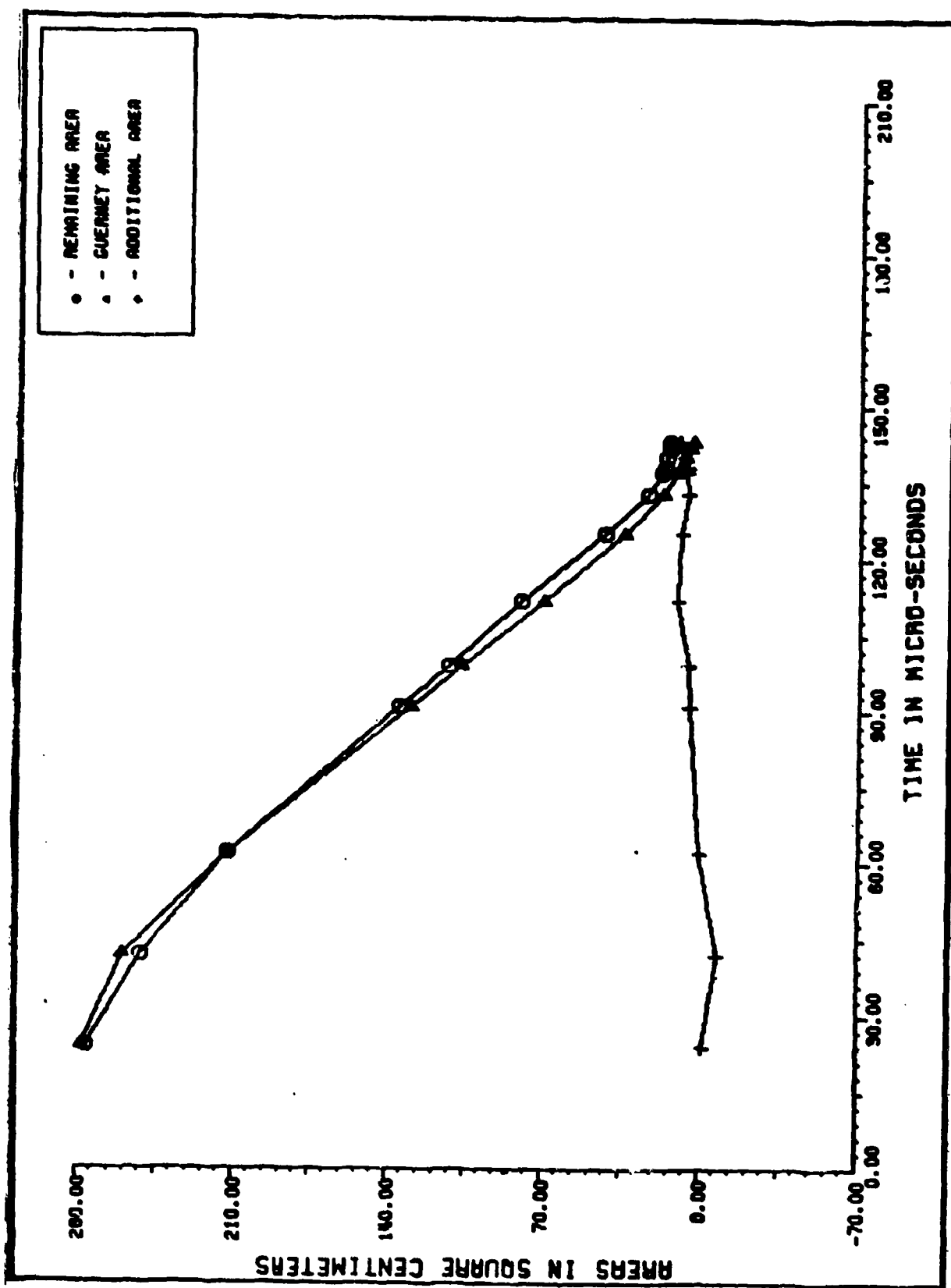
Figure B-20. Changing Areas Test 3

105
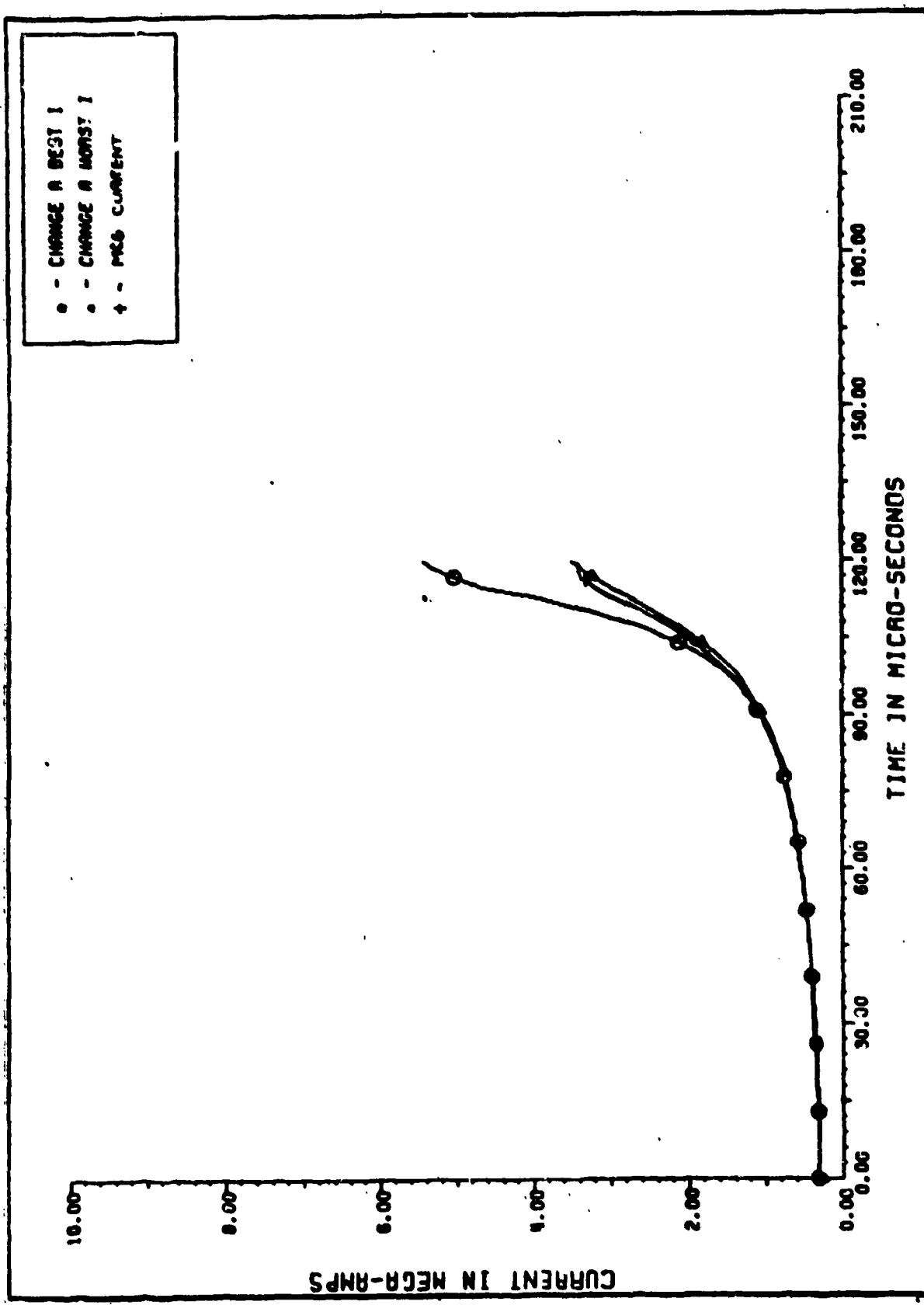
Figure B-21. Changing Area Currents Test 2

CURRENT IN MEGA-AMPS

TIME IN MICRO-SECONDS

- - CHANGE AREA BEST 1
- - CHANGE AREA WORST 1
+ - MCG CURRENT
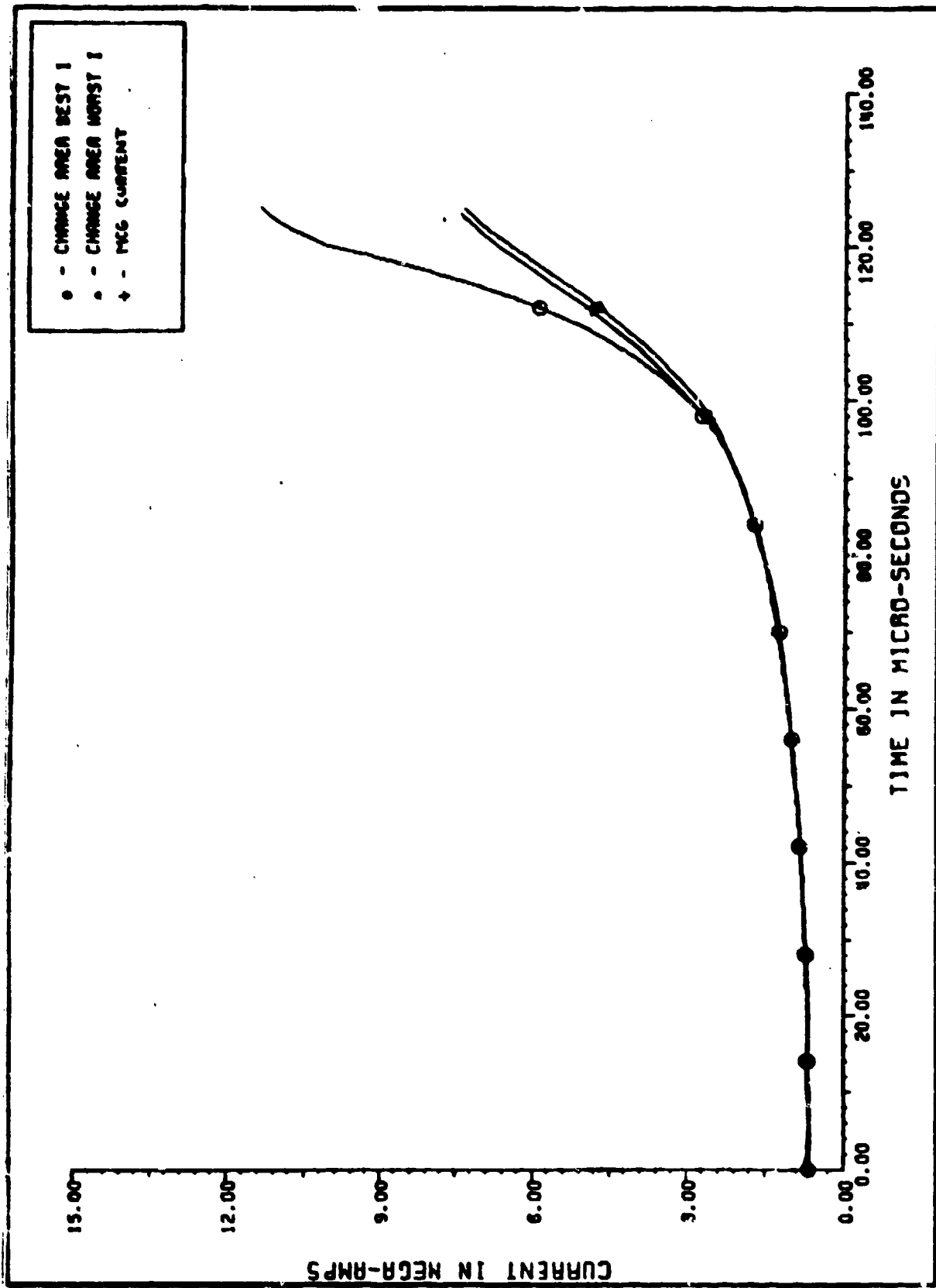
Figure B-22. Changing Area Currents Test 3

107
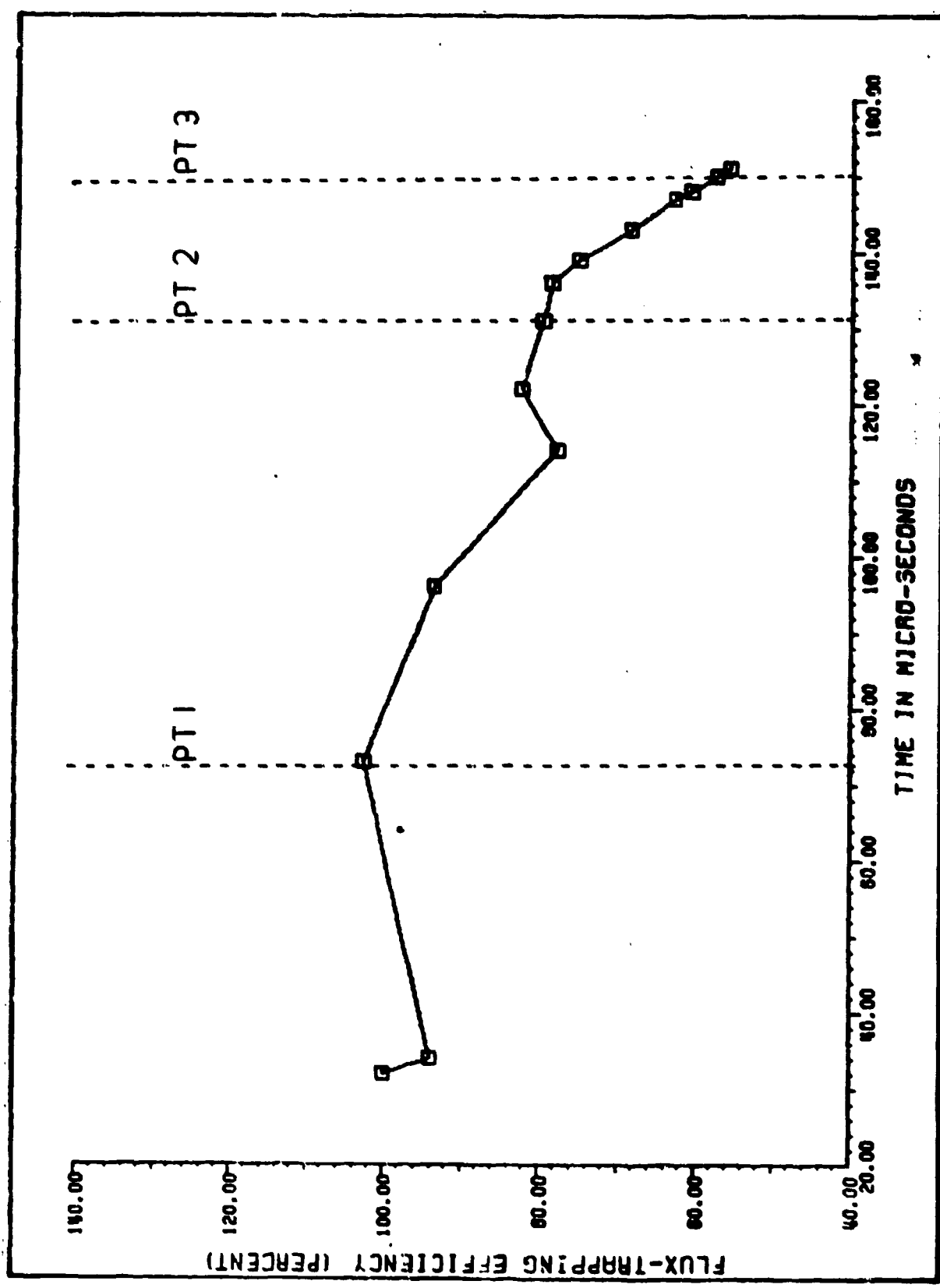
Figure B-23. Efficiency Test 2
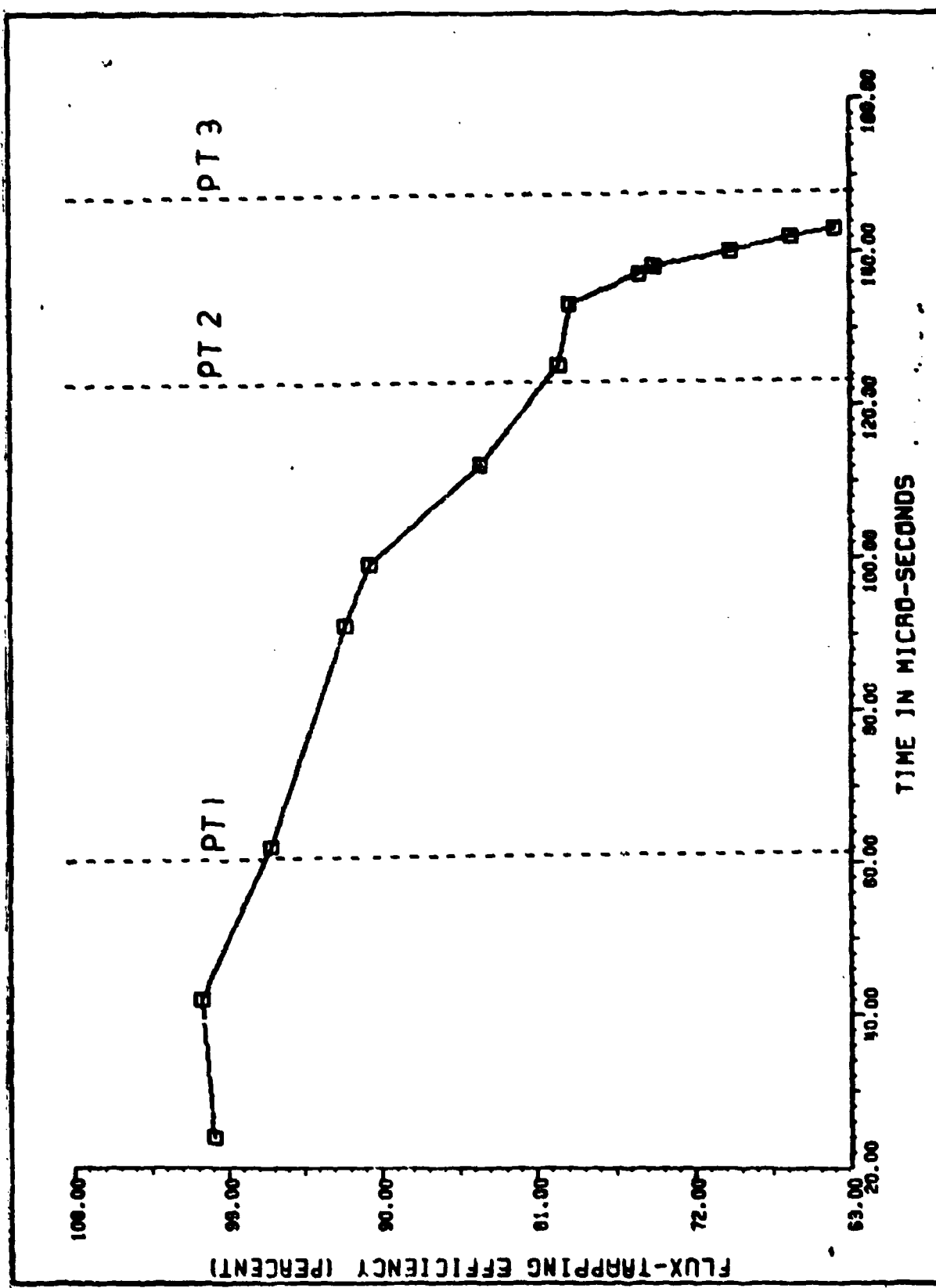
Figure B-24. Efficiency Test 3

109
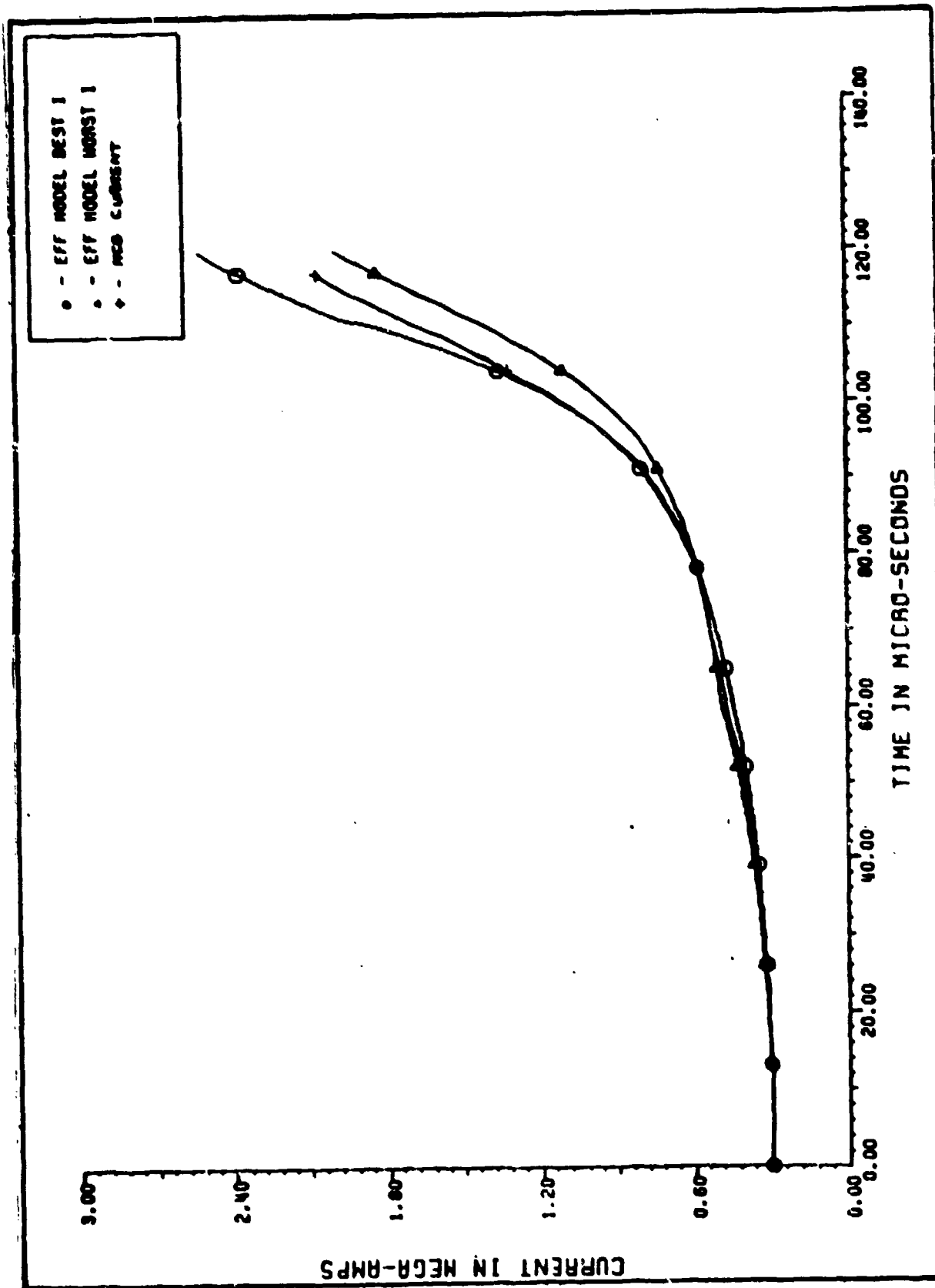
Figure B-25. Efficiency Currents Test 2

Figure B-26. Efficiency Currents Test 3

111
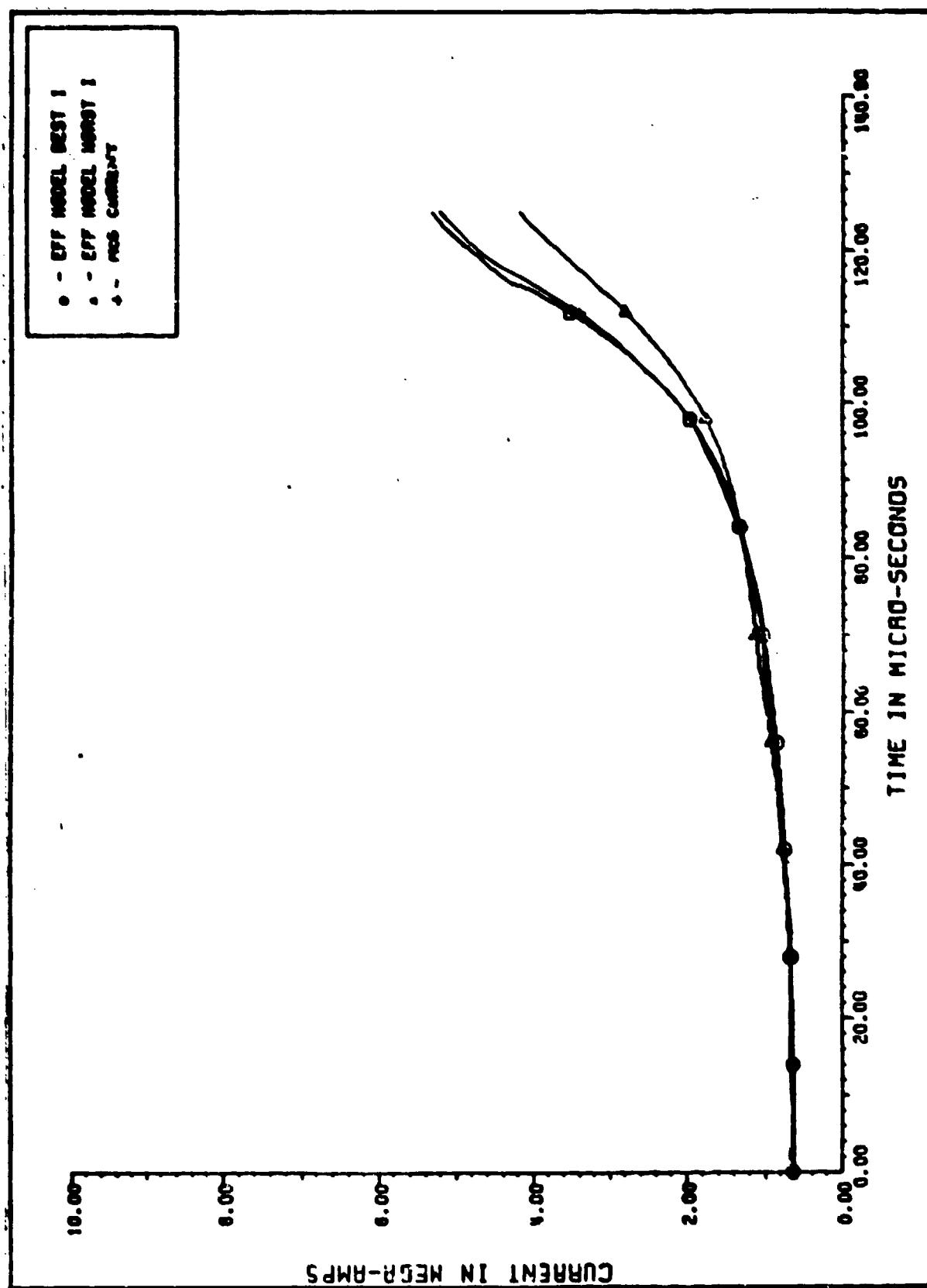
Bibliography

1. Knoepfel, Heinz. _Pulsed High Magnetic Fields_. New York, NY: American Elsevier Publishing Company, 1970.

2. Herlach, Fritz. "Flux Loss and Energy Balance in Magnetic Flux Compression Experiments," _Journal of Applied Physics_, 39, (11):5191-5204 (October 1968).

3. Reinovsky, Robert E., Research Physicist, Simulators and Advanced Weapons Concepts Branch, Kirtland AFB, New Mexico (personal correspondence), September 1983.

4. Plonsey, Robert and Robert E. Collin. _Principles and Applications of Electromagnetic Fields_. New York: McGraw-Hill Book Company, 1961.

5. Lehner, G., J. G. Linhart, and J. P. Somcn. "Limitations on Magnetic Fields Obtained by Flux Compression I," _Nuclear Fusion_, 4, 362-379 (1964).

6. Kennedy, J. E. _Gurney Energy of Explosives: Estimation of the Velocity and Impulse Imparted to Driver Metal_. Sandia Laboratories Report No SC-RR-70-790, December 1970.

7. Gerasimov, L. S. and V. I. Ikryannikov. "Magnetic Accumulation in a Plane Liner of Finite Thickness," _Soviet Physics Technical Physics_, 23, (2):147-149 (February 1978).

8. Tucker, T. J. and B. N. Turnman. "Modeling and Scaling Experiments of Explosive Driven Pulse Power Systems," _Proceedings of the Third IEEE International Pulse Power Conference:_ 334-336 (June 1981).

9. Lewin, J. D. and P. F. Smith. "Production of Very High Magnetic Fields by Flux Compression," _Review of Scientific Instruments_, 35, 541-548 (May 1964).

10. Herlach, F. "Megagauss Magnetic Fields," _Reports on Progress in Physics_, 31, 341-417 (1968).

11. Damerow, R. H., J. C. Crawford, D. B. Thomson, R. S. Caird, K. J. Ewing, W. B. Garn, and C. M. Fowler. "Use of Explosive Generators to Power the θ Pinch," _Symposium on Engineering Problems of Fusion Research:_ DI8-1-DI8-6 (1968).

12. Fowler, C. M., R. S. Caird, and W. B. Garn. _An Introduction to Explosive Magnetic Flux Compression Generators_. Los Alamos, New Mexico: Los Alamos Scientific Laboratory of University of California, March 1975 (Report LA-5890-MS).

13. Schwab, Adolf J. _High-Voltage Measurement Techniques_. Cambridge, MA: M. I. T. Press, 1970.

VITA

Mary Jeffrey

Mary Patricia Jeffrey was born 14 November 1954 in Milwaukee, Wisconsin. She graduated from high school in Kaukauna, Wisconsin in 1973. She entered the Air Force in 1973 and served as a communications specialist. In 1976 she entered the Air Force Academy and received the degree of Bachelor of Science in Electrical Engineering and an Air Force commission in 1980. She entered the School of Engineering, Air Force Institute of Technology in June 1982.

> Permanent address: Mounted Route 8
> Box 145
> Cumberland Head
> Plattsburgh, New York 12901

James Hebert

James Leland Hebert was born on 29 June 1950 in Port Arthur, Texas. He graduated from Castle Heights Military Academy in 1968. He entered the Air Force in 1969 and served as a voice processing technician obtaining the rank of MSgt. Through AECP, he received a Bachelor of Science in Electrical Engineering from Texas Tech University in May 1982. Upon graduation, he attended OTS and received his commission in August 1982. He entered the School of Engineering, Air Force Institute of Technology in September 1982.

> Permanent address: 3600 Lexington Avenue
> Port Arthur, Texas 77640

SECURITY CLASSIFICATION OF THIS PAGE

REPORT DOCUMENTATION PAGE

1a. REPORT SECURITY CLASSIFICATION	1b. RESTRICTIVE MARKINGS
UNCLASSIFIED	

2a. SECURITY CLASSIFICATION AUTHORITY	3. DISTRIBUTION/AVAILABILITY OF REPORT
	Approved for public release, distri-
2b. DECLASSIFICATION/DOWNGRADING SCHEDULE	bution unlimited

4. PERFORMING ORGANIZATION REPORT NUMBER(S)	5. MONITORING ORGANIZATION REPORT NUMBER(S)
AFIT/GE/EE/83D-28	

6a. NAME OF PERFORMING ORGANIZATION	6b. OFFICE SYMBOL (If applicable)	7a. NAME OF MONITORING ORGANIZATION
Air Force Institute of Technology	AFIT/EN	

6c. ADDRESS (City, State and ZIP Code)	7b. ADDRESS (City, State and ZIP Code)
Wright-Patterson AFB, OH 45433	

8a. NAME OF FUNDING/SPONSORING ORGANIZATION	8b. OFFICE SYMBOL (If applicable)	9. PROCUREMENT INSTRUMENT IDENTIFICATION NUMBER
Air Force Weapons Lab	AFWL/RNAA	

8c. ADDRESS (City, State and ZIP Code)	10. SOURCE OF FUNDING NOS.			
Kirtland AFB, NM 87117	PROGRAM ELEMENT NO.	PROJECT NO.	TASK NO.	WORK UNIT NO.

11. TITLE (Include Security Classification)
See Box 19

12. PERSONAL AUTHOR(S)
Mary P. Jeffrey, 1Lt USAF   James L. Hebert, 2Lt USAF

13a. TYPE OF REPORT	13b. TIME COVERED	14. DATE OF REPORT (Yr., Mo., Day)	15. PAGE COUNT
	FROM _____ TO _____	December 1983	122

16. SUPPLEMENTARY NOTATION

Approved for public release; IAW AFR 190-17

Approved for public release: IAW AFR 190-17.
LYNN E. WOLAVER
Dean for Research and Professional Development
Air Force Institute of Technology (ATC)
Wright-Patterson AFB OH

17.	COSATI CODES		18. SUBJECT TERMS (Continue on reverse if necessary and identify by block number)	
FIELD	GROUP	SUB. GR.	Pulse Generator	Explosive Generator
10	02		Electric Generator	Magnetocumulative Generator

19. ABSTRACT (Continue on reverse if necessary and identify by block number)

Title: Computer Modeling and Experimental Valdiation of Losses in
          a Strip Geometry Explosive Magnetic Flux Compression
          Generator

Advisors: Major Timothy L. Skvarenina, AFIT/EN
          Dr. Robert E. Reinovsky, AFWL/RNAA

20. DISTRIBUTION/AVAILABILITY OF ABSTRACT	21. ABSTRACT SECURITY CLASSIFICATION
UNCLASSIFIED/UNLIMITED ☒ SAME AS RPT. ☒ DTIC USERS ☐	UNCLASSIFIED

22a. NAME OF RESPONSIBLE INDIVIDUAL	22b. TELEPHONE NUMBER (Include Area Code)	22c. OFFICE SYMBOL
Mary P. Jeffrey, 1Lt, USAF	513-255-5533	AFIT/EN

DD FORM 1473, 83 APR   EDITION OF 1 JAN 73 IS OBSOLETE.

A computer program to predict the performance of a strip geometry explosive magnetic flux compression generator (MCG) was developed and validated.

The program contains five separate models of the MCG, two theoretical and three empirically based. The first model is a theoretical lossless flux conserved model. The second model accounts for resistive losses due to plate resistance and a flux diffusion equivalent resistance. The first empirical model models the remaining losses as a slipping loss. The second empirical model adjusts the flux conserved model with an additional time varying inductance. The final empirical model is a simple flux trapping efficiency model.

Actual MCG experiments were conducted using the Air Force Weapons Laboratory's strip MCG. The data from these experiments was used to validate the computer program. Input currents varied from 294.0 KA to 1100.0 KA with resulting output currents of 2210.0 KA to 10261.0 KA and current amplification factors between 6.29 and 15.75.